Studies on Stress Granules in *Aspergillus oryzae*

(麹菌 *Aspergillus oryzae* におけるストレス顆粒に関する研究)

by

Hsiang-Ting Huang

A dissertation submitted to the

Graduate School of Agricultural and Life Sciences,

Faculty of Agriculture,

The University of Tokyo

in partial fulfillment of the requirements for the degree of

DOCTOR OF PHILOSOPHY

in

Biotechnology

March, 2014

Table of content

General Introduction 1

Objective 20

Chapter 1. Cytoplasmic mRNP granules in *A. oryzae* 21

Introduction 22

Results 24

1. Stress-induced formation of stress granules 24
2. Colocalization of stress granules with processing bodies (P-bodies) upon heat stress 27
3. *Aopub1* disruptant has defects in the conidia formation and displays more severe growth retardation in stress conditions 29

Discussion 31

Chapter 2. Identification of AoSO as a novel stress granule component upon heat stress in *A. oryzae* 56

Introduction 57

Results 58

1. Colocalization of AoSO with stress granules in response to heat stress 58
2. AoSO affects the formation and localization of stress granules 59

Discussion 61

Chapter 3. Participation of autophagy in the clearance of stress granules under sustained heat stress 71

Introduction 72

Results 74

1. Colocalization of autophagosome and stress granules in cells subjected to heat stress 74

2. Heat stress induces the degradation of stress granule components 75

3. Participation of autophagy in the degradation of stress granule component under sustained heat stress 75

Discussion 77

Chapter 4. Post-translational modifications of stress granule component AoPab1 in response to heat stress 86

Introduction 87

Results 89

1. AoPab1 is subjected to extensive post-translational modifications 89

2. Identification of post-translational modifications in AoPab1 in response to heat stress 89

3. *In silico* prediction of AoPab1 phosphorylation sites 91

Discussion 93

Conclusion and Perspectives 109

Materials and Methods 116

Appendixes 135

Appendix I. Strain list 136

Appendix II. Plasmid list 138

Appendix III. Primer list 139

Appendix IV. Medium compositions 141

Appendix V. Buffers and solutions 143

References 151

Acknowledgements 186

Abstract 190

Abbreviations

A.A.	Amino acid
amyB	*amylaseB*
APS	Ammonium persulfate
ATG	Autophagy-related
ATM	Ataxia-telangiectasia mutated
BPB	Bromophenolblue
CaMK-II	Calcium/calmodulin-dependent protein kinase type II
CDC2	Cell division cycle protein 2
CDK5	Cyclin-dependent kinase 5
CHAPS	3-[(3-cholamidopropyl)dimethylammonio]-1-propanesulfonate
CKI	Casein kinase I
CKII	Casein kinase II
CMA	Chaperone-mediated autophagy
DNA	Deoxyribonucleic acid
DNAPK	DNA-dependent protein kinase
DTT	Dithiothreitol
EDTA	Ethylenediaminetetraacetic acid
EGFP	Enhanced green fluorescent protein
EGFR	Epidermal growth factor receptor
ER	Endoplasmic reticulum
eIF	Eukaryotic translation initiation factor
eRF	Eukaryotic translation release factor
HSP	Heat shock protein
HSR	Heat-shock response
INSR	Insulin receptor kinase
IVC	Intravacuolar compartment
MAPK	Mitogen-activated protein kinase
MKK-2	Mitogen-activated protein kinase kinase-2
mRNA	Messenger ribonucleic acid
mRNP	Messenger ribonucleoprotein
O-GlcNAc	O-linked-N-acetylglucosamine
ORF	Open reading frame
PABP	Poly(A)-binding protein
PAGE	Polyacrylamide gel electrophoresis
P-body	mRNA processing body
PCR	Polymerase chain reaction

PEG	Polyethylene Glycol
PKA	Protein kinase A
PKB	Protein kinase B
PKC	Protein kinase C
PKG	Protein kinase G
PMSF	phenylmethylsulfonyl fluoride
PTM	Post-translational modification
Pub1	Poly(A/U)-binding protein 1
S6K	Ribosomal S6 kinase
SCC	Saline-sodium citrate
SDS	Sodium dodecyl sulfate
SRC	Src tyrosine kinase
TEMED	N, N, N', N'-tetramethylethylenediamine
TFA	Trifluoroacetic acid
TORC1	Target of rapamycin complex 1
UPS	Ubiquitin-proteasome system
UTR	Untranslated region

General Introduction

1. Environmental stress response

Microorganisms are constantly challenged by ever-changing growth conditions in their environment, including nutrient fluctuations, osmotic imbalance, and nonoptimal temperatures. The ability to sense environmental stimuli, including stress, activate signal transduction, and mount appropriate acute and adaptive responses is crucial for eukaryotic cell survival (Figure 0-1). Adaptation requires physiological and metabolic changes, including cell cycle arrest, metabolic reprogramming, altered cell wall and membrane dynamics, and is ultimately achieved through the regulation of gene expression (Verghese *et al*., 2012). Traditionally, transcriptional regulation has been regarded as the major determinant of gene expression. However, accumulating evidence indicates that posttranscriptional modulation of mRNA stability and translation plays a key role in the control of gene expression and provides greater plasticity, allowing cells to immediately adjust protein synthesis in response to changes in the environment (Figure 0-1) (Holcik and Sonenberg, 2005). Recent studies have demonstrated that one aspect of this modulation involves the remodeling of mRNAs translated from polysomes into non-translating messenger ribonucleoproteins (mRNPs), which accumulate in discrete cytoplasmic foci known as stress granules and processing bodies (P-bodies) (Eulalio *et al*., 2007; Parker and Sheth, 2007; Anderson and Kedersha, 2009a; Anderson and Kedersha, 2009b; Buchan and Parker, 2009; Erickson and Lykke-Andersen, 2011; Decker and Parker, 2012).

2. Stress granules

Environmental stress response mechanisms in eukaryotic cells are characterized by global translational inhibition, which inhibits protein synthesis to conserve anabolic energy and also involves the reconfiguration of gene expression to effectively manage stress conditions. Global translational arrest is initiated by the

activation of several stress-responsive serine/threonine kinases, including general control non-derepressible-2 (GCN2), dsRNA-dependent protein kinase R (PKR), heme-regulated inhibitor kinase (HRI), and PKR-like ER kinase (PERK), which phosphorylate the translation initiation factor eIF2α (Wek *et al*., 2006). eIF2α is a subunit of eIF2 (together with eIF2β and eIF2γ), which is part of a ternary complex, consisting of eIF2, GTP, and methionyl-initiator tRNA (Met-tRNAi ^{Met}), that delivers initiator tRNA to the 40S ribosome (Figure 0-2) (Klann and Dever, 2004; Holcik and Sonenberg, 2005; Jackson *et al*., 2010). During translation initiation, GTP is hydrolyzed to GDP, generating eIF2-GDP, which needs to be recharged to eIF2-GTP by a guanine nucleotide exchange factor following each round of initiation. Phosphorylation of eIF2 by eIF2α kinases inhibits the formation of eIF2-GTP, thereby reducing the level of the ternary complex, which ultimately limits translation initiation (Holcik and Sonenberg, 2005). The stalled preinitiation complexes, together with their associated mRNAs, are routed into stress granules. However, a subset of mRNAs required for cell survival under stress conditions are not delivered to stress granules but stabilized and preferentially translated in the cytoplasm (Harding *et al*., 2000; Anderson and Kedersha, 2002; Lu *et al*., 2006; Powley *et al*., 2009). As stress granules are formed in response to stress, they are generally not observable under normal growth. Although the composition of stress granules is dynamic and dependent on the type of stress and cell species, they typically contain 40S ribosomal subunits, translation initiation factors (eIF4G, eIF4E, eIF4A, eIF4B, eIF3, and eIF2), and proteins involved in the regulation of mRNA function (Table 0-1) (Buchan and Parker; 2009; Buchan *et al*., 2011). The function of stress granules is not fully understood; however, they have been implicated in the posttranscriptional regulation processes, such as mRNA translational repression and storage, and cellular signal transduction (Arimoto *et al*., 2008; Buchan and Parker, 2009; Takahara and Maeda,

2012).

3. P-bodies

Eukaryotic mRNA degradation is generally initiated by the deadenylation of poly(A) tails, which triggers either decapping and 5’ to 3’ exonucleolysis or exosome-dependent 3’ to 5’ degradation (Figure 0-3) (Wilusz *et al*., 2001; Parker and Song, 2004; Garneau *et al*., 2007; Parker, 2012). As the inhibition of translation initiation increases the rate of deadenylation and decapping (Muhlrad *et al*., 1995; Muckenthaler *et al*., 1997; LaGrandeur and Parker, 1999; Schwartz and Parker, 1999), the rate of mRNA degradation and translation initiation are often inversely related (Coller and Parker, 2005; Decker and Parker, 2012). The cellular components involved in mRNA decapping and degradation, such as decapping enzyme complex Dcp1p/Dcp2p, the activators of decapping and/or repressors of translation Dhh1p/RCK/p54, Lsm1-7p complex, Edc3p, Pat1p and the 5’ to 3’ exonuclease Xrn1p, often accumulate in P-bodies as core components (Table 0-1) (Sheth and Parker, 2003; Franks and Lykke-Andersen, 2008; Nissan *et al*., 2010). In addition, proteins functioning in different posttranscriptional processes, including microRNA (miRNA)-mediated silencing, AU-rich element (ARE)-mRNA decay, mRNA surveillance (nonsense-mediated decay, NMD), and mRNA storage, have also been reported to localize in P-bodies under certain conditions (Brengues *et al*., 2005; Eulalio *et al*., 2007; Franks and Lykke-Andersen, 2008).

4. Autophagy

Cellular homeostasis requires a balance between anabolism and catabolism. In eukaryotic cells, the two major mechanisms for intracellular degradation are the ubiquitin-proteasome system (UPS) and autophagy/lysosomal degradation.

The major pathway of selective protein degradation in eukaryotic cells uses ubiquitin as a marker that targets cytosolic and nuclear proteins for rapid proteolysis (Pickart, 2001). Ubiquitin is a 76-amino-acid polypeptide that is highly conserved in all eukaryotes. Proteins are marked for degradation by the attachment of ubiquitin to the amino group of the side chain of a lysine residue. Additional ubiquitins are then added to form a multiubiquitin chain that serve as recognition motifs for delivery to and degradation by a large multisubunit protease complex, 26S proteasomes. The UPS is involved in rapidly eliminating single proteins to regulate many cellular processes, including cell division, signal transduction and gene expression.

Autophagy is a conserved and tightly regulated process in eukaryotic cells for the bulk degradation of cytoplasmic components, including entire organelles in the vacuole or lysosome (Reggiori and Klionsky, 2013). Autophagy is responsible mainly for the degradation of long-lived proteins and entire organelles, and thereby maintains intracellular homeostasis and contributes to many normal physiological processes. The defective in autophagy has found in a variety of human diseases (Huang and Klionsky, 2007; Murrow and Debnath, 2013). This pathway is also stimulated by multiple forms of cellular stress, including nutrient or growth factor deprivation, hypoxia, reactive oxygen species, DNA damage, protein aggregates, damaged organelles, or intracellular pathogens (Kroemer *et al*., 2010). Intensive studies in the last few years have shown that autophagy in filamentous fungi is not only involved in nutrient homeostasis but also in other cellular processes such as differentiation, pathogenicity, and secondary metabolite production, as a consequence of adaptation to diverse fungal lifestyles (Pollack *et al*., 2009; Khan *et al*., 2012; Voigt and Pöggeler, 2013). Autophagy-defective mutant, *Aoatg8* disruptant, has shown grave influences on morphogenesis and morphology in *A. oryzae*, including reduced numbers of aerial hyphae, disrupted conidiation, and delayed germination (Kikuma *et al*., 2006; Kikuma

and Kitamoto, 2011).

There are three principal routes of autophagic degradation, which differ mainly in the means of cargo delivery to the vacoule: macroautophagy, microautophagy, and chaperone-mediated autophagy (CMA) (Figure 0-4) (Huang and Klionsky, 2007; Kaushik and Cuervo, 2012). Both microautophagy and macroautophagy include nonselective and selective processes (Reggiori and Klionsky, 2013). In the process of microautophagy, cytoplasm or organelles are directly engulfed by vacuole membrane invaginations and scissions to produce intravacuolar vesicles that are subsequently degraded (Kunz *et al*. 2004; Uttenweiler and Mayer 2008), whereas the morphological hallmark of macroautophagy is the sequestration of the targeted cargo within *de novo* cytosolic double-membrane vesicles that subsequently fuse with the vacuole (Reggiori and Klionsky, 2013). These vesicles are called autophagosomes in nonselective macroautophagy, and are given different names in selective macroautophagy. In the selective degradation of mitochondria and peroxisomes in mitophagy and pexophagy, these vesicles are termed mitophagosome and pexophagosome, respectively (Manjithaya *et al*., 2010; Feng *et al*., 2013). Unlike micro- and macroautophagy, CMA does not involve a similar type of membrane rearrangement. CMA involves the translocation of unfolded proteins with containing the KFERQ, CMA recognition motif that is recognized by the LAMP2A (lysosome-associated membrane protein 2A) receptor, on the lysosome. This process requires a molecular chaperone, Hsc70, both in the cytosol and within the lysosome lumen (Kaushik and Cuervo, 2012).

In the model organism *S. cerevisiae*, the process of autophagosome biogenesis is divided into induction, nucleation, expansion, fusion and breakdown phases (Figure 0-5) (Rubinsztein *et al*. 2012), which are sequentially involved and regulated by autophagy-related (*ATG*) genes. Genetic analysis of yeasts have identified 36 *ATG*

genes, of which 17 are core ATG proteins required for all autophagy-related pathways and 19 are ATG proteins specifically involved in selective autophagy or the induction of specific autophagy-related pathways in certain condition (Table 0-2) (Kraft *et al*., 2010; Inoue and Klionsky 2010; Mizushima *et al*., 2011).

5. Aspergilli

The taxonomic classification of filamentous fungi Aspergilli identifies the fungi in the genus *Aspergillus*, family Trichocomaceae, order Eurotiales, phylum Ascomycota and within the kingdom of Fungi. This genus was first described in 1729 by the Italian biologist Pier Antonio Micheli (1679-1736) and named after the morphological structure of the conidiophore, the structure which bears asexual spores looks like an aspergillum (from the Latin *aspergere*, "to scatter"), a device used for sprinkling holy water during a liturgical service (Bennett, 2009). *Aspergillus* species are one of the most common groups of molds found in a variety of ecological niches. Almost 200 species have been identified and all grouped together because they form similar asexual reproductive structures. Species of *Aspergillus* have received great attention for their important roles in medically and economically. Several species are well known fungal pathogens threatening to human and animal health and causing dramatic agricultural losses. On the other hand, for the capacity to produce high levels of secondary metabolites and secreted enzymes, several *Aspergillus* species, in particular *Aspergillus niger* and *Aspergillus oryzae*, are commercially important in industrial applications. Today, many commercial proteins are produced by Aspergilli (Fleißner and Petra Dersch, 2010).

6. *A. oryzae*

A. oryzae is a fungus widely used as Koji in traditional Japanese fermentation

industries, including sake, soy sauce, and miso. Koji is a culture prepared by growing koji mold on cooked grains and/ or soybeans in a warm, humid place. Koji serves as a source of enzymes that break down natural plant starch and proteins into simpler compounds when it is used in making fermented foods. This style of fermentation is thought to have originated 3000-2000 years ago in China (Machida *et al*., 2008). For the long history of extensive use of *A. oryzae* in food fermentation industries, *A. oryzae* has been given to as Generally Recognized as Safe (GRAS) by the Food and Drug Administration (FDA) in the United States (Tailor and Richardson, 1979; Abe *et al*., 2006). The safety of this organism is also supported by World Health Organization (WHO) (FAO_WHO, 1987).

In comparison to other eukaryotic expression systems, such as yeast, algae, or insect cells, filamentous fungi possess the exceptional advantage of an unbeatable secretion capacity. Among filamentous fungi, *A. oryzae* is known to have a prominent potential for the secretory production of various enzymes (Machida *et al*., 2005; Kobayashi *et al*., 2007; Machida *et al*., 2008), and being manipulated genetically for heterologous protein production. *A. oryzae* was used for the first example of commercial production of heterologous enzyme in 1988 (Christensen *et al*., 1988). Recent advances in genomic technologies have facilitated biotechnological application of *A. oryzae* as a protein production host. The genome project of *A. oryzae* was completed and the whole genome sequence is available (Machida *et al*., 2005). In addition, several novel genetic engineering strategies have been developed in recent years to improve the expression and secretion of recombinant proteins in *A. oryzae* (Fleißner and Petra Dersch, 2010).

Although *A. oryzae* offers significant advantages for biotechnological application as an expression system for protein production, heterologous protein production yields are lower in *A. oryzae* than those of homologous proteins. Limitations in

production, stability, and secretion of heterologous proteins remain often unknown due to the complexity of filamentous fungi. Therefore, a deeper understanding of the physiology and the metabolism of *A. oryzae* and ongoing development of novel genetic engineering tools are required to develop efficient large-scale protein production for industrial applications.

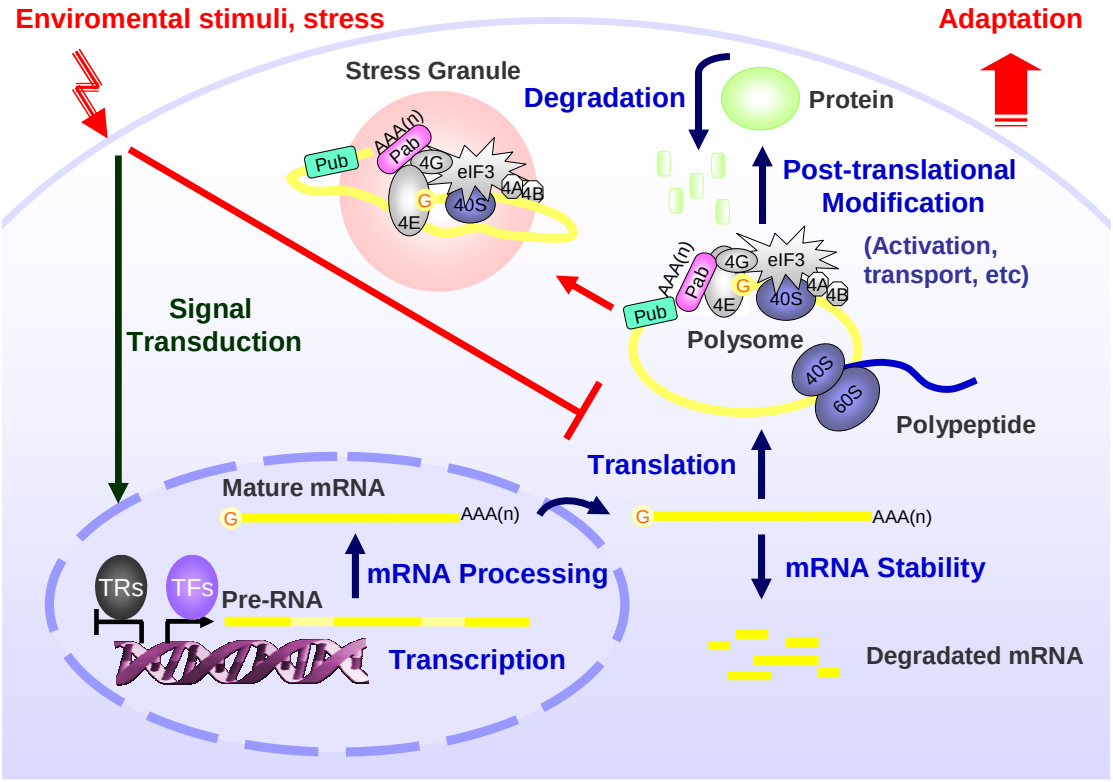

Figure 0-1. Gene regulation in eukaryotes.

The expression of biologically active protein in eukaryotic cells is controlled at multiple points during the process of gene expression, including chromatin remodeling, transcriptional initiation, processing and modification of mRNA transcripts, transport of mRNA into cytoplasm, stability/decay of mRNA transcripts, initiation and elongation of mRNA translation, posttranslational modification, and intracellular transport and degradation of the expressed protein. When cells are encountered unfavorable growth conditions, global translational inhibition occurs and leads to the formation of stress granules. TFs: transcription factors; TRs: transcription repressors.

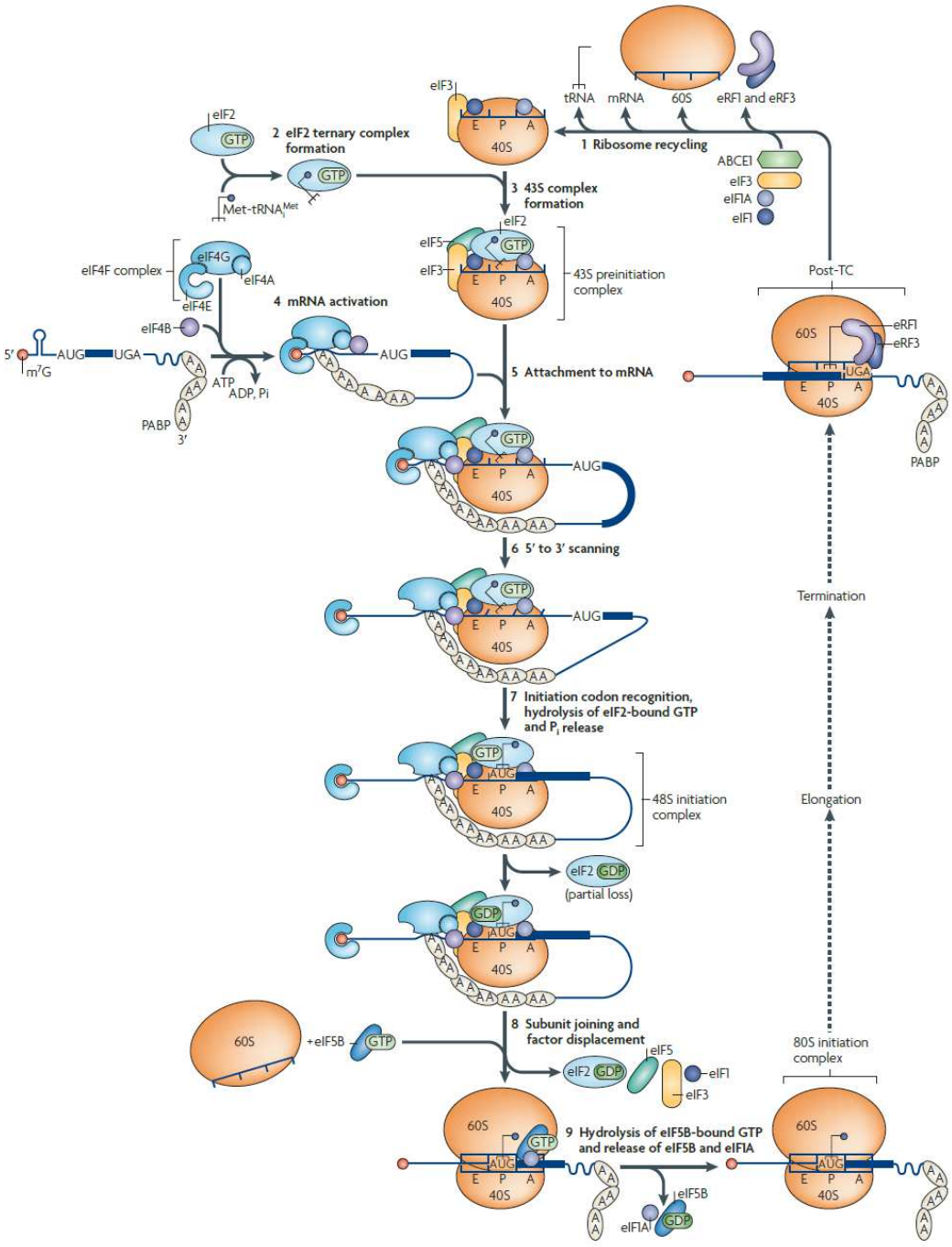

(Jackson *et al.*, Nat Rev Mol Cell Biol, 11: 113-127, 2010)

Figure 0-2. Model of the canonical pathway of eukaryotic translation initiation.

The canonical pathway of eukaryotic translation initiation is divided into eight stages (2-9). These stages follow the recycling of post-termination complexes (post-TCs; **1**) to yield separated 40S and 60S ribosomal subunits, and result in the formation of an 80S ribosomal initiation complex, in which Met-tRNA$^{Met}_{i}$ is base paired with the initiation codon in the ribosomal P-site and which is competent to start the translation elongation stage. These stages are: eukaryotic initiation factor 2 (eIF2)-GTP-Met-Met-tRNA$^{Met}_{i}$ ternary complex formation (**2**); formation of a 43S preinitiation complex comprising a 40S subunit, eIF1, eIF1A, eIF3, eIF2-GTP- Met-tRNA$^{Met}_{i}$ and probably eIF5 (**3**); mRNA activation, during which the mRNA cap-proximal region is unwound in an ATP-dependent manner by eIF4F with eIF4B (**4**); attachment of the 43S complex to this mRNA region (**5**); scanning of the 5' UTR in a 5' to 3' direction by 43S complexes (**6**); recognition of the initiation codon and 48S initiation complex formation, which switches the scanning complex to a 'closed' conformation and leads to displacement of eIF1 to allow eIF5-mediated hydrolysis of eIF2-bound GTP and Pi release (**7**); joining of 60S subunits to 48S complexes and concomitant displacement of eIF2-GDP and other factors (eIF1, eIF3, eIF4B, eIF4F and eIF5) mediated by eIF5B (**8**); and GTP hydrolysis by eIF5B and release of eIF1A and GDP-bound eIF5B from assembled elongationcompetent 80S ribosomes (**9**). Translation is a cyclical process, in which termination follows elongation and leads to recycling (**1**), which generates separated ribosomal subunits. The model omits potential 'closed loop' interactions involving poly(A)-binding protein (PABP), eukaryotic release factor 3 (eRF3) and eIF4F during recycling, and the recycling of eIF2-GDP by eIF2B. Whether eRF3 is still present on ribosomes at the recycling stage is unknown.

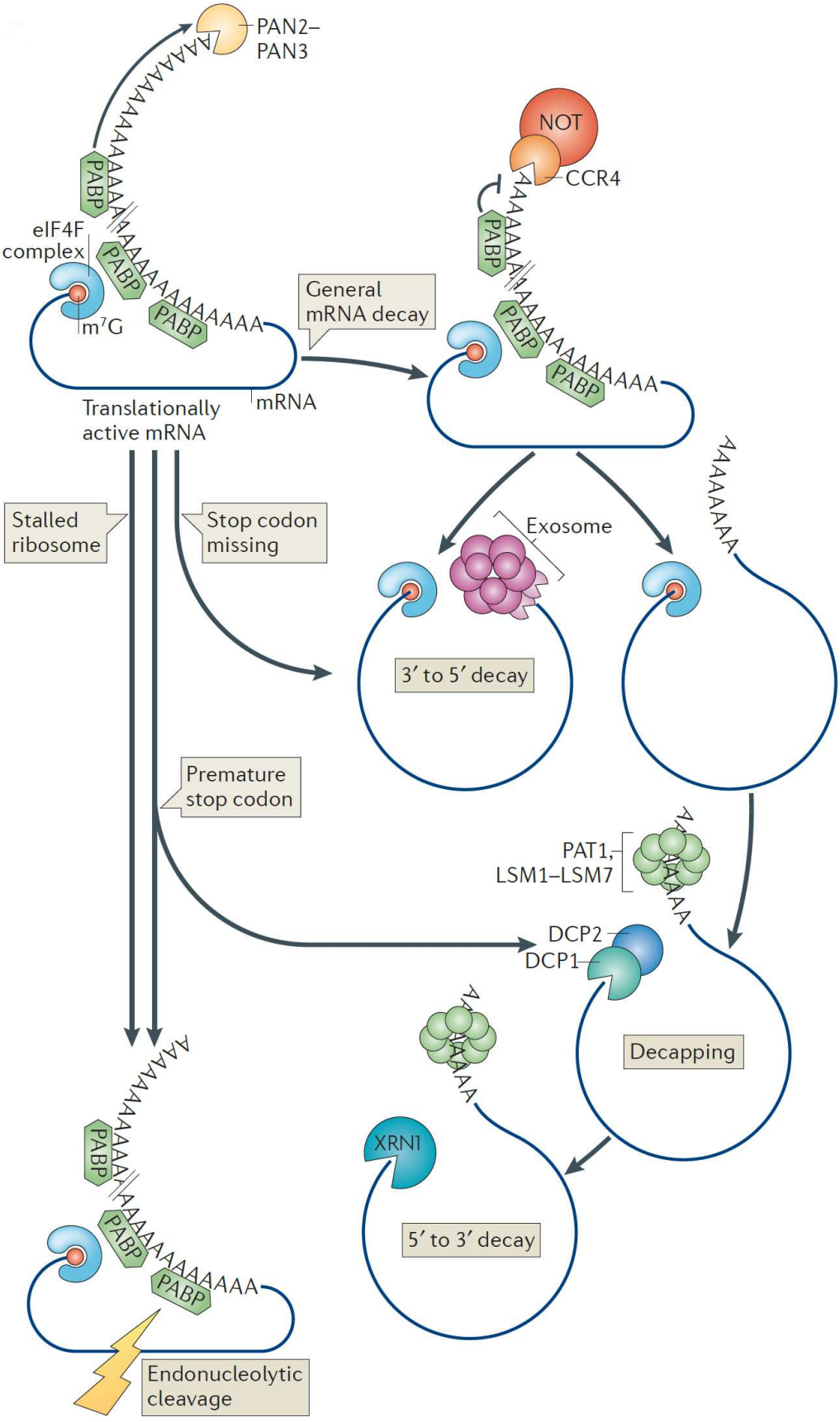

(Norbury, Nat Rev Mol Cell Biol, 14: 643-653, 2013)

Figure 0-3. mRNAs degradation in eukaryotes.

For simplicity, translation initiation factors other than the eIF4F complex (which includes the cap-binding protein eIF4E) and poly(A)-binding protein (PABP) are not shown. Initial trimming of the poly(A) tail is carried out by the poly(A) nuclease 2 (PAN2)-PAN3 deadenylase and is stimulated by PABP. General mRNA decay proceeds via further deadenylation by the CCR4-NOT complex, which is inhibited by PABP but may be stimulated in an mRNA-specific manner by trans-acting proteins bound to regulatory elements in the 3′ untranslated region (3′ UTR). Once the residual poly(A) tail is eroded to around 12 or fewer nucleotides, PABP can no longer bind, and decay proceeds either by further 3’ to 5’ exonucleolysis carried out by the exosome complex or, more frequently, by recruitment of the PAT1-LSM1-LSM7 complex, which stimulates decapping by decapping protein 1 (DCP1)-DCP2 and subsequent 5’ to 3’ exonucleolysis by the exoribonuclease XRN1. The absence of a translation stop codon short-circuits the general decay pathway by stimulating exosome-mediated 3’ to 5’ decay (non-stop decay), whereas stalled ribosomes trigger endonucleolytic mRNA cleavage (no-go decay). The presence of a premature stop codon also leads to endonucleolytic cleavage as well as deadenylation and decapping (nonsense-mediated decay; NMD). However, in *S. cerevisiae*, the NMD pathway instead involves deadenylation-independent decapping (not shown).

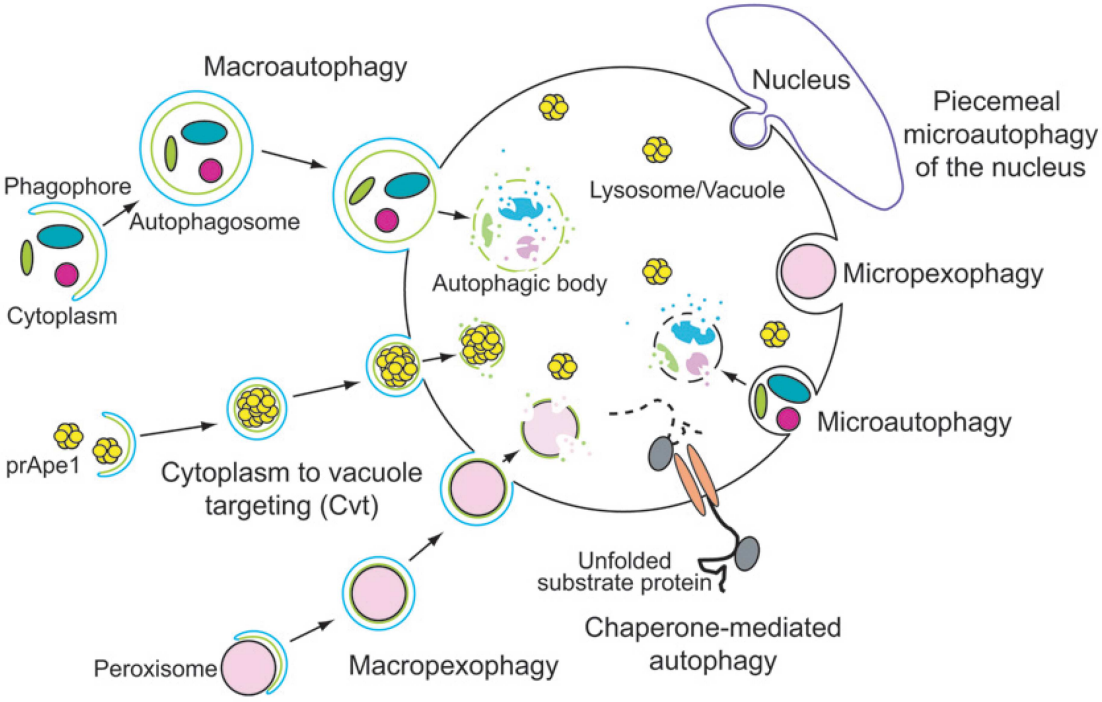

(Huang and Klionsky. Cell Cycle 6: 1837-1849, 2007)

Figure 0-4. Schematic diagram of autophagy-related pathways.

Three fundamentally different modes of autophagy are macroautophagy, microautophagy, and chaperone-mediated autophagy (CMA). And both macroautophagy and microautophagy include nonselective and selective processes. The biosynthetic delivery of the resident hydrolase amino-peptidase I into the yeast vacuole is mediated through the cytoplasm to vacuole targeting pathway, a type of specific autophagy. prApe1, precursor aminopeptidase I.

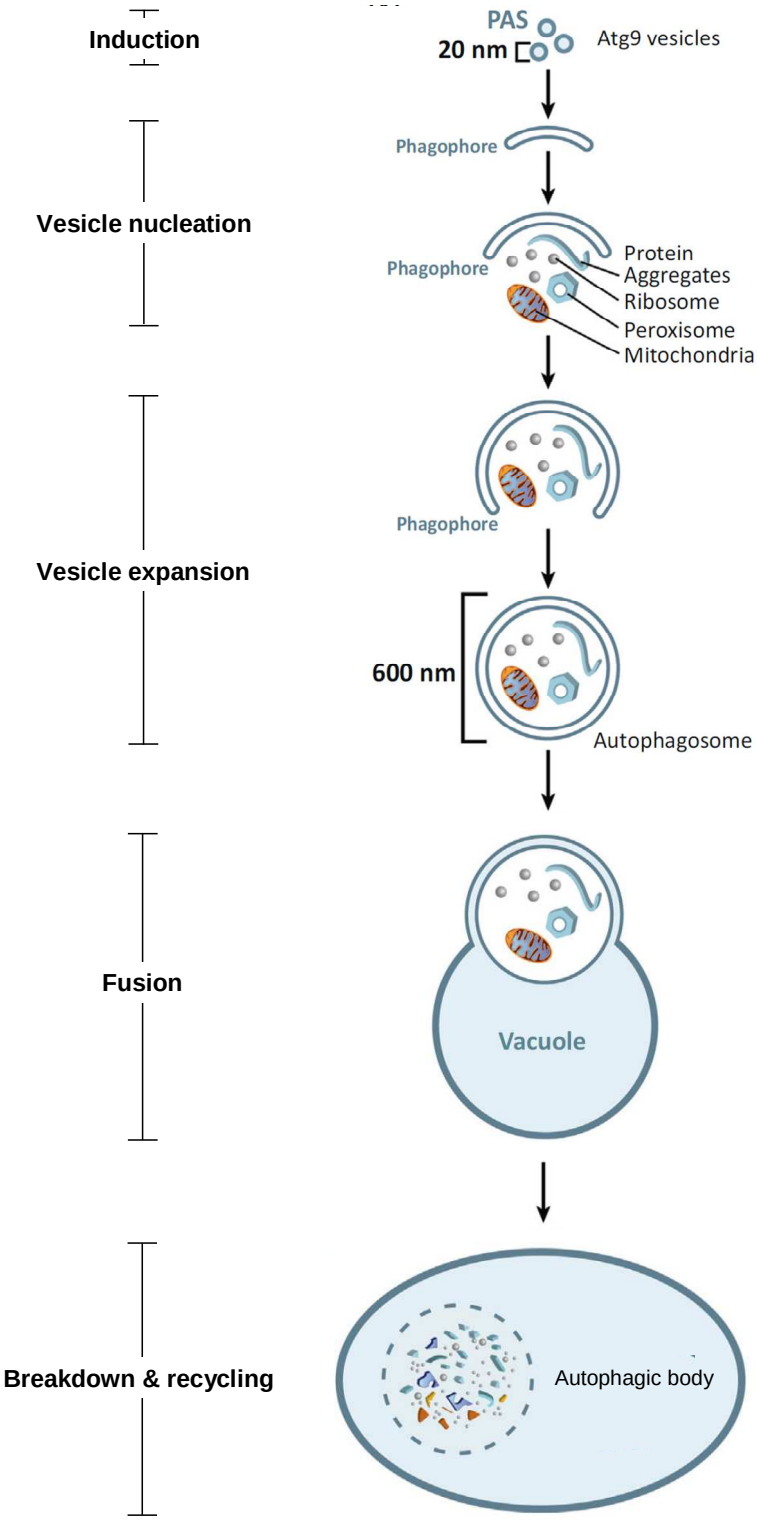

(Stanley *et al*., Trend Cell Biol, 2013, in press)

Figure 0-5. Five sequential steps of autophagy based on findings in *S. cerevisiae*.

After induction of autophagy, an initial sequestering phagophore is assembled at the

phagophore assembly site (PAS). PAS is located next to vacuole. Expansion and curvature of the phagophore lead to the engulfment of the cytoplasmic cargo into the double-membraned autophagosome. Fusion of the autophagosomal outer membrane with the vacuolar membrane results in the release of the autophagic body, which is surrounded by the inner autophagosomal membrane. Autophagic bodies and the sequestered cargo are broken down by hydrolytic enzymes. Finally, the breakdown products are exported into the cytoplasm for re-use.

Table 0-1. Protein components of stress granules and P-bodies

Name	Function	References
Components found predominantly in P-bodies		
Ccr4/Pop2/Not complex	Deadenylase	Sheth and Parker 2003; Cougot et al. 2004
Dcp1	Decapping enzyme subunit	Sheth and Parker 2003; Cougot et al. 2004
Dcp2	Decapping enzyme	Sheth and Parker 2003; Cougot et al. 2004
Edc1 and 2	Decapping activators	Neef and Thiele 2009
Edc3	Decapping activator	Kshirsagar and Parker 2004; Fenger-Gron et al. 2005
eIF4E-T	Translation repressor	Andrei et al. 2005; Ferraiuolo et al. 2005
eRF1 and eRF3	Translation termination	Buchan et al. 2008
GW182	miRNA function	Eystathioy et al. 2003
Hedls/Ge-1	Decapping activator	Fenger-Gron et al. 2005; Yu et al. 2005
Lsm1-7 complex	Decapping activator	Ingelfinger et al. 2002; Sheth and Parker 2003
Pat1/PatL1	Translation repressor/ decapping activator	Sheth and Parker 2003; Scheller et al. 2007
Upf1-3	Nonsense-mediated decay	Sheth and Parker 2006; Durand et al. 2007
Components found predominantly in stress granules		
40S ribosomal subunit	Translation	Kedersha et al. 2002; Grousl et al. 2009
Ataxin-2/Pbp1	Translation/mRNA processing	Nonhoff et al. 2007; Buchan et al. 2008
DDX3/Ded1	RNA helicase	Chalupnikova et al. 2008; Lai et al. 2008; Hilliker et al. 2011
eIF2α	Translation initiation	Kedersha et al. 2002; Kimball et al. 2003
eIF3	Translation initiation	Kedersha et al. 2002; Grousl et al. 2009
eIF4A	Translation initiation	Low et al. 2005; Buchan et al. 2011
eIF4B	Translation initiation	Low et al. 2005; Buchan et al. 2011
eIF4G	Translation initiation	Kedersha et al. 2005; Hoyle et al. 2007
FMRP	Translation, repression/ miRNA function	Mazroui et al. 2002; Kim et al. 2006
G3BP	Scaffolding protein, endoribonuclease	Tourriere et al. 2001
Pabp	polyA-binding protein	Kedersha et al. 1999; Hoyle et al. 2007
RACK1	Signaling scaffold protein	Arimoto et al. 2008
TIA-1/TIAR/Pub1/Ngr1	Translation repression/ mRNA stability	Kedersha et al. 1999; Buchan et al. 2008
Components found in both P-bodies and stress granules		
Agonaute proteins	miRNA function	Sen and Blau 2005; Leung et al. 2006
Dhh1/Rck/p54/	Translation repressor/ decapping activator	Sheth and Parker 2003; Wilczynska et al. 2005
eIF4E	Translation initiation	Andrei et al. 2005; Ferraiuolo et al. 2005; Hoyle et al. 2007
FAST	Fas activated serine/ threonine phosphoprotein	Kedersha et al. 2005
Rap55/Scd6	Translation repressor	Yang et al. 2006; Teixeira and Parker 2007
Xrn1	5′ to 3′ exonuclease	Sheth and Parker 2003; Kedersha et al. 200

(Decker and Parker R, Cold Spring Harb Perspect Biol. 4: a012286, 2012)

Table 0-2. Thirty-six *atg* genes have been identified in yeasts.

The 17 core *ATG* genes and 19 specific *ATG* genes involved in the induction of autophagy and selective autophagy, respectively.

17 core ATG proteins
Atg1p
Atg2p
Atg3p
Atg4p
Atg5p
Atg6p
Atg7p
Atg8p
Atg9p
Atg10p
Atg12p
Atg13p
Atg14p
Atg15p
Atg16p
Atg18p
Atg22p

19 specific ATG proteins			
Autophagy induction	Cvt Pathway	Pexophagy	Mitophagy
Atg17p	Atg19p	Atg25p	Atg32p
Atg29p	Atg21p	Atg26p	Atg33p
Atg31p	Atg23p	Atg28p	
	Atg27p	Atg30p	
	Atg34p	Atg35p	
		Atg36p	
	Atg11p, Atg20p, Atg24p		

Objective

On December 4, 2013 Japanese cuisine, "Washoku", was added to UNESCO's Intangible Cultural Heritage. *A. oryzae* is the most important strain in traditional Japanese fermentation industries to make sake, soy sauce, *miso*, *mirin*, and rice vinegar. All of these consist of the fundamental flavoring of traditional Japanese foods. Furthermore, for the enormous secretion capacity, *A. oryzae* has prominent potential for the biotechnological application as a protein production host. During the manufacture of fermented food or protein production using *A. oryzae*, if cells experience stress (e.g. nonoptimal ambient temperature), cells will rapidly stall protein synthesis and stop growth, resulting reduced quality of products and yield. In recent years, an emerging role of cytoplasmic mRNP granules such as stress granules in the posttranscriptional regulation of gene expression during stress gives rise to extensive studies in yeast and mammalian cells. However, related researches are deficient in filametous fugi. P-bodies have been described in *Candida albicans* and *Aspergillus nidulans* (Morozov *et al*., 2010; Jung and Kim, 2011), but stress granules have not yet to be defined. Advance in basic research and applied science is important for understanding and preservation of Japanese culture. Therefore, in this study, stress granules were studied in *A. oryzae.*

Chapter 1

Cytoplasmic mRNP granules in *A. oryzae*

Introduction

Stress granules are cytoplasmic mRNP granules conserved in eukaryotes and have been studied extensively in yeast and mammalian cells. However, the existence and function of stress granules in filamentous fungi, including *A. oryzae*, have not yet to be defined. Additionally, P-bodies are another type of mRNP granules in eukaryotic cytoplasm involved in translation repression and mRNA degradation. Although stress granules and P-bodies are compositionally and morphologically distinct entities, evidence suggests that they are spatially and functionally linked. For these reason, the aim of chapter 1 was to investigate the formation of stress granules in *A. oryzae* cells exposed to various stresses and the relative localizations of stress granules and P-bodies.

To monitor stress granules by fluorescence microscopy, a stress granule marker protein fused with EGFP is necessary. To date a number of factors have been identified as core components of stress granules in mammalian cells and yeasts (Table 0-1). In *S. cerevisiae*, the poly(A)-binding protein (PABP), Pab1p, has been reported to be one of the most reliable and easily visualized components of stress granules (Buchan *et al*., 2010).

PABP is an abundant cytoplasmic protein in eukaryotes that binds the poly(A) tail of mRNA to regulate multiple aspects of mRNA processing, translation and degradation. PABP simultaneously binds to the mRNA 3’ poly(A) tail and interacts with the translation factor eIF4G, part of the cap-binding complex eIF4F (eIF4E, eIF4G and eIF4A), bringing the ends of the mRNA into functional proximity (Figure 0-2) (Klann and Dever, 2004; Holcik and Sonenberg, 2005; Jackson *et al*., 2010). This ‘closed-loop’ conformation enhances translation initiation by increasing ribosomal recruitment while also protecting the mRNA from deadenylation, decapping and degradation (Fabian *et al*., 2010; Livingstone *et al*., 2010). PABP also has other roles

in post-transcriptional regulation, both positively and negatively regulating mRNA-specific translation and mRNA stability (Brook *et al*., 2009; Burgess and Gray, 2010). All of the PABPs have the same domain structure consisting of four conserved RNA binding domains (RRM1-4) followed by a linker region and a C-terminal MLLE (mademoiselle) domain named after its conserved and essential signature motif KITGMLLE (Brook *et al*., 2009; Burgess and Gray, 2010; Kozlov *et al*., 2010). The MLLE domain binds to proteins that contain a 12-15-amino acid motif, termed PAM2 (Albrecht and Lengauer, 2004; Kozlov *et al*., 2001). The motif is found in proteins associated with mRNA deadenylation [transducer of erbB-2 protein 1/2 (Tob1/2) and PABP-dependent poly(A) nuclease subunit 3 (PAN3)] (Ikematsu *et al*. 1999; Okochi *et al*., 2005; Uchida *et al*., 2004), eukaryotic translation release factor 3 (eRF3) (Hoshino *et al*., 1999), P-bodies (Ataxin-2 and GW182) (Ciosk *et al*., 2004; Fabian *et al*., 2009), Poly(A)-interacting protein 1/2 (Paip1/2) (Khaleghpour *et al*., 2001; Roy *et al*., 2002), and protein deubiquitination [ubiquitin-specific protease 10 (USP10)] (Lim *et al*., 2006). MLLE domains are found in all eukaryotic cytoplasmic PABPs and uniquely in two other proteins as follows: a ubiquitin ligase UBR5 (also known as HYD, EDD, or Rat100) and a distant PABP homolog RRM4 in filamentous fungi (Deo *et al*., 2001; König *et al*., 2009).

Results

1. Stress-induced formation of stress granules

1.1 Homolog of the poly(A)-binding protein in *A. oryzae*

A homolog of the *S. cerevisiae PAB1* gene was found in the *A. oryzae* genome database (DOGAN; http://www.bio.nite.go.jp/dogan/Top) and designated as *Aopab1* (AO090003000927). *Aopab1* locates on the chromosome 2 and consists of 2424 nucleotides (with two introns in the C-terminal region) encoding a putative protein with 765 amino acids and a predicted molecular mass of 83.0 kDa. The deduced amino acid sequence of AoPab1 is composed of two parts, an N-terminal portion that contains four RNA recognition motifs (RRMs) and a C-terminal portion that contains a less-conserved linker region and a conserved C-terminal MLLE domain, typical for all PABPs (Figure 1-1A). A conserved KITGMLLE motif is also found in the MLLE domain of AoPab1 (Figure 1-1B).

A phylogenetic tree was obtained using a sequence alignment of the predicted protein sequence of AoPab1 with homologs in other filamentous fungi, yeast, plant, human and fly revealed high similarities between the different species (Figure 1-2). The identity to other Aspergilli varies between 79 % and 100 %.

Based on these analyses, AoPab1 was chosen to be used as a stress granule marker in *A. oryzae*.

1.2 Formation of stress granules in response to stress

1.2.1 Ectopic expression of AoPab1-EGFP as a marker of stress granules

To monitor stress granules by fluorescence microscopy using AoPab1-EGFP as a stress granule marker, *Aopab1* gene was cloned using the genomic DNA of *A. oryzae* wild-type strain RIB40 as a template and the entire region of *Aopab1* gene was confirmed by determining the nucleotide sequence. An AoPab1-EGFP expressing

plasmid pgDPaPab1E and a control plasmid expressing EGFP alone were constructed using the MultiSite Gateway system (Invitrogen, Carlsbad, CA, USA) (Figure 1-3).

Global translational arrest is a common environmental stress response in eukaryotes (Sonenberg and Hinnebusch, 2009), and the inhibition of translation initiation leads to the formation of stress granules. Therefore, as the first step in characterizing stress granules in *A. oryzae*, several external stimuli were used to assess the induction of stress granules in cells (Figures 1-4, 1-5, and 1-6). Under normal growth conditions, AoPab1-EGFP was dispersed throughout the cytoplasm (Figure 1-4A). Exposing cells to heat stress (45°C, 10 min) led to an induction of stress granules, as judged by the accumulation of AoPab1-EGFP as cytoplasmic foci (Figure 1-4A). No accumulation of EGFP was observed in the negative control strain expressing EGFP alone (Figure 1-4B). Similarly, stress granules were observed after cells were exposed to cold stress (4°C, 30 min), glucose deprivation (10 min), ER stress (10 mM DTT, 60 min), osmotic stress (1.2 M sorbitol, 30 min), and oxidative stress (2 mM H_2O_2, 30 min) (Figures 1-5 and 1-6). In response to glucose deprivation, the accumulation of AoPab1-EGFP appeared to be short lived, as no accumulation was observed after 30 min in the majority of cells (data not shown). Small foci of AoPab1-EGFP were formed when the culture medium was replaced with medium containing 2 mM H_2O_2, and continued to increase in size by fusing together to form one large aggregate (Figure 1-6). Of the examined stresses by medium replacement, osmotic stress might be the most severe to cells, as accumulation of AoPab1-EGFP was observed less than 1 min after exposure to 1.2 M sorbitol, and a large aggregate of AoPab1-EGFP was formed shortly thereafter.

1.2.2 Ectopic expression of AoPub1-EGFP as a marker of stress granules

To ensure that these observations were not unique to AoPab1, I also examined

the Poly(A/U)-binding protein AoPub1 (AO090001000353), which is another well-known component of stress granules (Buchan *et al*., 2008), under stress conditions. *Aopub1* gene was cloned using the genomic DNA of wild-type strain RIB40 as a template and the entire region of *Aopub1* gene was confirmed by determining the nucleotide sequence. An AoPub1-EGFP expressing plasmid pgDPaPub1E (Figure 1-7) was constructed and introduced into strain NSRKu70-1-1A. Similar results were consistently observed when cells expressing AoPub1-EGFP were exposed to heat stress (45°C, 10 min), glucose deprivation (10 min), ER stress (10 mM DTT, 60 min), oxidative stress (2 mM H_2O_2 , 30 min), and osmotic stress (1.2 M sorbitol, 30 min) (Figure 1-8).

1.2.3 Endogenous expression of AoPab1-EGFP as a marker of stress granules

Several components of stress granules contain glutamine and asparagine (Q/N)-rich prion-like domains, which have a strong tendency to self-aggregate, and are implicated in the assembly of these mRNP granules (Gilks *et al*., 2004; Yao *et al*., 2007; Reijns *et al*., 2008). It has been reported that RRM1 domain and Q/G/P-rich region mediate self-association of Pab1p (Yao *et al*., 2007). To exclude the possibility that observed accumulation of stress granule marker proteins were artificial effects due to overexpression of their components, EGFP was targeted to the genomic locus of *Aopab1*. To express AoPab1-EGFP under control of the endogenous promoter, DNA fragment containing 3' terminal 1.5 kb of *Aopab1* (stop codon was removed), *egfp*, *adeA* gene, and 1.5 kb of 3'-flanking regions of *Aopab1* was generated using fusion PCR and ligated into pCR4Blunt-TOPO vector, generating plasmid pTPab1EaA (Figure 1-9). The targeting DNA fragment was amplified using plasmid pTPab1EaA as a template and introduced into an *adeA* mutant. Transformants were confirmed by Southern blotting analysis (Figure 1-10). Subcellular localization of

AoPab1-EGFP expressed under control of the endogenous promoter showed similar results to those of *amyB* promoters in cells exposed to heat stress (45°C, 10 min), cold stress (4°C, 30 min), and glucose deprivation (10 min) (Figure 1-11).

These results indicated that ectopic expression of AoPab1-EGFP is a reliable marker to analyze stress granules in *A. oryzae*.

2. Colocalization of stress granules with P-bodies upon heat stress

2.1 Ectopic expression of AoDcp2-EGFP or AoEdc3-EGFP as a marker of P-bodies

In eukaryotic cells, non-translating mRNAs also accumulate in P-bodies, which contain a conserved core of proteins involved in translational repression and mRNA degradation. Although stress granules and P-bodies are compositionally and morphologically distinct entities, evidence suggests they are spatially and functionally linked (Kedersha *et al*., 2005; Wilczynska *et al*., 2005; Brengues and Parker, 2007; Hoyle *et al*., 2007; Buchan *et al*., 2008; Mollet *et al*., 2008; Grousl *et al*., 2009). To avoid any observation specific to a certain protein, two proteins were chosen for the markers of P-bodies. Dcp2p is the catalytic subunit of a decapping enzyme that cleaves the 5'cap of mRNA (van Dijk *et al*., 2002; She *et al*., 2006), and its activity is accelerated by Edc3p. Dcp2p and Edc3p are frequently found as a distinct component of P-bodies in *S. cerevisiae* (Buchan *et al*., 2010). The homologs of *S. cerevisiae DCP2* and *EDC3* were found in the *A. oryzae* genome database, and designated as *Aodcp2* (AO090120000363) and *Aoedc3* (AO090120000481), respectively. To monitor P-bodies in *A. oryzae*, *Aodcp2* and *Aoedc3* were cloned using the genomic DNA of wild-type strain RIB40 as a template and the entire region of genes were confirmed by determining the nucleotide sequence. Expressing plasmids of AoDcp2-EGFP and AoEdc3-EGFP (Figure 1-12) were constructed and introduced

into strain NS4 individually.

In unstressed cells, AoDcp2-EGFP and AoEdc3-EGFP expressed under control of the *amyB* promoter were detected as discrete bright dots in the cytoplasm, in which it also showed a faint diffuse distribution (Figures 1-13 and 1-14). In *S. cerevisiae*, stress conditions such as glucose and nitrogen depletion, osmotic stress, and UV irradiation lead to an increase in the number of P-bodies (Teixeira *et al*., 2005; Nilsson and Sunnerhagen, 2011). Here, I confirmed that P-bodies were increased in size and number when *A. oryzae* cells expressing AoDcp2-EGFP or AoEdc3-EGFP were exposed to heat stress, low temperature, and carbon deprivation (Figures 1-13 and 1-14).

2.2 Endogenous expression of AoDcp2-EGFP as a marker of P-bodies

As stress granules, several components of P-bodies also contain glutamine and asparagine (Q/N)-rich prion-like domains to mediate the assembly of these mRNP granules (Reijns *et al*., 2008). The Yjef-N domain of Edc3p acts as a scaffold and cross-binding domain, and is required for the formation of P-bodies (Decker *et al*., 2007). In addition, Dcp2p also possesses a conserved Q/N-rich domain (Decker *et al*., 2007). To avoid mislocalization due to overexpression, AoDcp2-EGFP was expressed under control of the endogenous promoter. The same strategy was used to target EGFP at the genomic locus of *Aodcp2* as that for *Aopab1*. DNA fragment containing 3' terminal 1.5 kb of *Aodcp2* (stop codon was removed), EGFP, *adeA* gene, and 1.5 kb of 3'-flanking regions of *Aodcp2* was generated using fusion PCR and ligated into pCR4Blunt-TOPO vector, generating plasmid pTDcp2EaA (Figure 1-15). The targeting DNA fragment was amplified using plasmid pTDcp2EaA as a template and introduced into an *adeA* mutant. Transformants were confirmed by Southern blotting analysis (Figure 1-16). Subcellular localization of AoDcp2-EGFP expressed under

control of the endogenous promoter showed similar results to those of *amyB* promoter in cells exposed to heat stress (45°C, 10 min), cold stress (4°C, 30 min), and glucose deprivation (10 min) (Figure 1-17).

2.3 Colocalization of stress granules with P-bodies in cells subjected to heat stress

To determine the relative localizations of stress granules and P-bodies, AoPab1-mDsRed expressing plasmid pgCPaPab1DR (Figure 1-18A) was constructed and introduced into AoDcp2-EGFP expressing strain. The generating strain co-expressing AoDcp2-EGFP and AoPab1-mDsRed was examined after being exposed to 45°C for 10 min. Under heat stress, AoPab1-mDsRed cytoplasmic foci were colocalized with P-bodies labeled with AoDcp2-EGFP (Figure 1-18B).

3. *Aopub1* disruptant has defects in the conidia formation and displays more severe growth retardation in stress conditions

The ability to form stress granules is correlated with the survival of cells exposed to stress (Buchan and Parker, 2009). The C-terminal regions of TIA-1 and TIAR (mammalian homologs of AoPub1) and their orthologs contain a glutamine/asparagine (Q/N)-rich prion-like domain, which have a strong tendency to self-aggregate and promote stress granule formation (Kedersha *et al*., 1999; Kedersha *et al*., 2000; Michelitsch and Weissman, 2000; Gilks *et al*., 2004). To investigate whether the formation of stress granules influences cell survival against stress, a DNA fragment containing the 1.3 kb of 5'-flanking region of *Aopub1*, *pyrG* marker, and 1.5 kb of 3'-flanking region of *Aopub1* was amplified using plasmid pgdPub1 (Figure 1-19A) as a template, and was introduced into a *pyrG* null mutant. Disruption of *Aopub1* was confirmed by Southern blotting (Figure 1-19B). *Aopub1* disruptant was cultured on PD plates containing 10 mM DTT, 2 mM H_2O_2, or 1.2 M sorbitol to

examine the sensitivity to these three types of stress conditions. The induction of stress granules was confirmed in the AoPub1-EGFP expressing strain under each of the stress conditions previously (Figure 1-8). The phenotype of the *Aopub1* disruptant was characterized by a slower growth rate compared to wild-type cells, and a severe impairment in the formation of conidia (Figure 1-20A). The growth retardation of the *Aopub1* disruptant was more severe under all examined stress conditions (Figure 1-20B). Colony sizes of *Aopub1* disruptant compared with those of wild-type strain were reduced by 16.5%, 21.1%, 24.7%, and 33.2% in the control, 10 mM DTT, 2 mM H_2O_2, and 1.2 M sorbitol conditions, respectively.

Discussion

Stress granules are conserved in *A. oryzae*

Stress granules are widely observed in eukaryotes; however, prior to the present study, these mRNP granules had not yet been defined in filamentous fungi. I used EGFP-fused AoPab1 or AoPub1 as a stress granule marker, and observed that AoPab1 and AoPub1 accumulated as cytoplasmic foci at the hyphal tip of cells exposed to various stresses (Figures 1-4, 1-5, 1-6, 1-8, and 1-11). This finding indicates that the formation of stress granules is a general phenomenon in response to external stress, and suggests that stress-induced reprogramming of mRNAs to enter stress granules occurs in *A. oryzae*.

It is noteworthy that in mammalian and yeast cells, numerous stress granules are distributed throughout the cytoplasm following exposure to stress; however, only a few stress granules that were located predominately at the hyphal tip were found in *A. oryzae* (Figures 1-4, 1-5, 1-6, 1-8, and 1-11). Although the underlying reason for this observation is not yet clear, the polarized localization of stress granules suggests a spatial specificity of the posttranscriptional regulation of gene expression in *A. oryzae*. It is well known that filamentous fungi have a highly polarized cell structure, in which secretory vesicles, cytoskeletal elements, and related components are concentrated at the hyphal tip as a well-organized cluster that determines hyphal growth and polarity (Harris *et al*., 2005; Steinberg, 2007). The localization of ribosomes at the hyphal tip supports the idea that mRNA translation actively occurs in this region (Howard, 1981). Based on these findings, I speculate that asymmetrical localization of mRNA at the hyphal tip results in the spatially restricted formation of stress granules or that mRNAs at the hyphal tip are preferentially routed into stress granules as an acute response to stress.

Stress granules and P-bodies are spatially and functionally linked

The core component of stress granules, AoPab1-mDsRed, was colocalized with P-bodies labeled with AoDcp2-EGFP (Figure 1-18B). The spatial relation of stress granules and P-bodies is also seen in mammalian cells and *S. cerevisiae* (Kedersha *et al*., 2005; Hoyle *et al*., 2007; Buchan *et al*., 2008; Grousl *et al*., 2009). Moreover, Fluorescence Recovery After Photobleaching (FRAP) studies have revealed that certain P-bodies and stress granules components shuttle (Kedersha *et al*., 2005; Mollet *et al*., 2008), and some of these proteins are components of both P-bodies and stress granules, suggesting that there is crosstalk between P-bodies and stress granules (Table 0-1).

C-terminal of PABP contains a conserved MLLE domain, which binds to PAM2 motif. Generally, proteins containing PAM2 motifs are over-represented in P-bodies, such as Tob (Ikematsu *et al*., 1999; Okochi *et al*., 2005), PAN3 (Uchida *et al*., 2004), Ataxin-2 (Ciosk *et al*., 2004), and GW182 (Fabian *et al*., 2009). Tob1 and Tob2 are members of the anti-proliferative (APRO) protein family (Mauxion *et al*., 2009). Tob1 contains a single C-terminal PAM2 motif, and Tob2 contains two PAM2 motifs, and both bind to MLLE domain. The N-termini of Tob1 and Tob2 contain a conserved APRO domain that binds to the Ccr4-Not-Caf1 deadenylase complex. Ccr4-Not-Caf1 and Pan3-Pan2 are two major deadenylation complexes which are enriched in P-bodies (Figure 0-3) (Parker, 2012; Norbury, 2013). Human poly(A) binding protein PABPC1 also binds to the PAN2-PAN3 deadenylase complex via the PAM2 motif of PAN3 to stimulate poly(A)-specific nuclease activity (Uchida *et al*., 2004; Funakoshi, *et al*., 2007; Siddiqui *et al*., 2007). Ataxin-2 and GW182 are both found in P-bodies and share common structural elements. Both contain glutamine-rich stretches, which may promote their association with P-bodies (Kozlov *et al*., 2010). Reducing the expression of Ataxin-2 in mammalian cells using siRNAs impairs the formation of

stress granules (Nonhoff *et al*., 2007). Enhancement and suppression of Ataxin-2 expression in human cells lead to decrease and increase in the levels of PABP, respectively, without affecting the levels of PABP mRNA (Nonhoff *et al*., 2007). GW182 is a marker protein of P-bodies (also known as GW bodies), which binds to a core component of the RNA-induced silencing complex (RISC), argonaute 2 (Ago2) (Eulalio *et al*., 2007). GW182 decreases the association of PABP with silenced miRNA targets, thereby facilitating translational repression and deadenylation (Zekri *et al*., 2013). These observations together suggest that colocalization of stress granules and P-bodies in *A. oryzae* (Figure 1-18B) may be mediated through protein-protein interaction of AoPab1 and several protein components of P-bodies.

The stress-induced formation of stress granules, in which mRNAs are not degraded, but maintained in a nontranslating state, is thought to make mRNAs available for rapid reinitiation when cells recover from stress. In agreement with this speculation, stress-induced stabilization of liable mRNAs has been reported (Laroia *et al*., 1999; Bollig *et al*., 2002; Takahashi *et al*., 2011), suggesting that certain components of the mRNA degradation pathway are impaired in response to stress. This finding may explain why the number and size of P-bodies were increased coordinately in *A. oryzae* cells under stress (Figures 1-13, 1-14, and 1-17).

Taken together, these observations indicate that although stress granules and P-bodies are distinct strutures, they are functionally interconnected through the interaction of their components.

Aopub1 disruptant has defects in the conidia formation and displays more severe growth retardation in stress conditions

The formation of stress granules in response to stress is widely observed in eukaryotes. The physiological role of the assembly of mRNAs into these large

aggregate-like assemblies remains unclear; however, this evolutionarily conserved response suggests that stress granules serve important functions in eukaryotes. Although relatively little is known about the mechanisms regulating the formation of stress granules, their assembly seems to be mediated through a self-assembly process that involves the Q/N-rich prion-like domains of a number of protein components associated with stress granules, including TIA-1, a mammalian homolog of AoPub1 (Kedersha *et al*., 1999; Gilks *et al*., 2004; Decker and Parker, 2012). As Pab1p is an essential protein in *S. cerevisiae* and is not required for stress granule formation (Swisher and Parker, 2010), I investigated whether deletion of the *Aopub1* gene confers cellular sensitivity to stress. The *Aopub1* disruptant displayed a slower growth rate compared to wild-type cells, and the growth retardation was more severe when cells were cultured under stress conditions, which included ER, oxidative, and osmotic stresses (Figure 1-20). I have tried to analyze the stress granule formation in the *Aopub1* deletion mutant. However, I could not transform *Aopub1* deletion mutant with the plasmid expressing AoPab1-EGFP because no protoplasts were generated by treatment of the cell-wall digestive enzyme. Although I lack of direct evidence that the formation of stress granules was impaired in the *Aopub1* disruptant, a Δ*pub1* strain of *S. cerevisiae* displays a dramatic decrease in the average number of stress granules, as judged by Pab1p localization (Buchan *et al*., 2008; Shah *et al*., 2013). The data presented here suggest that the integrity of stress granules is important for the survival of *A. oryzae* cells exposed to stress.

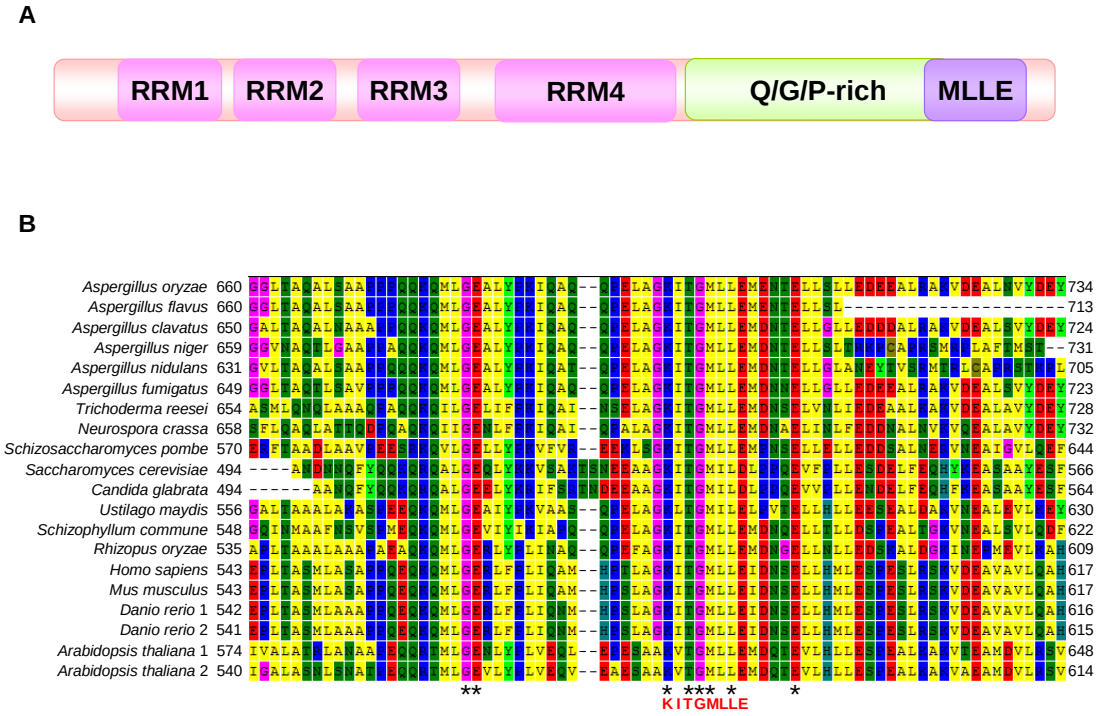

Figure 1-1. Sequence conservation of AoPab1.

(A) Schematic representation of the domain arrangement of AoPab1. AoPab1 has the same domain structure to its homologs in other species, consisting of four conserved RNA-binding domains (RRM1-4) followed by a linker region and a C-terminal MLLE (mademoiselle) domain. (B) Sequence alignment of the MLLE domains in PABP proteins.

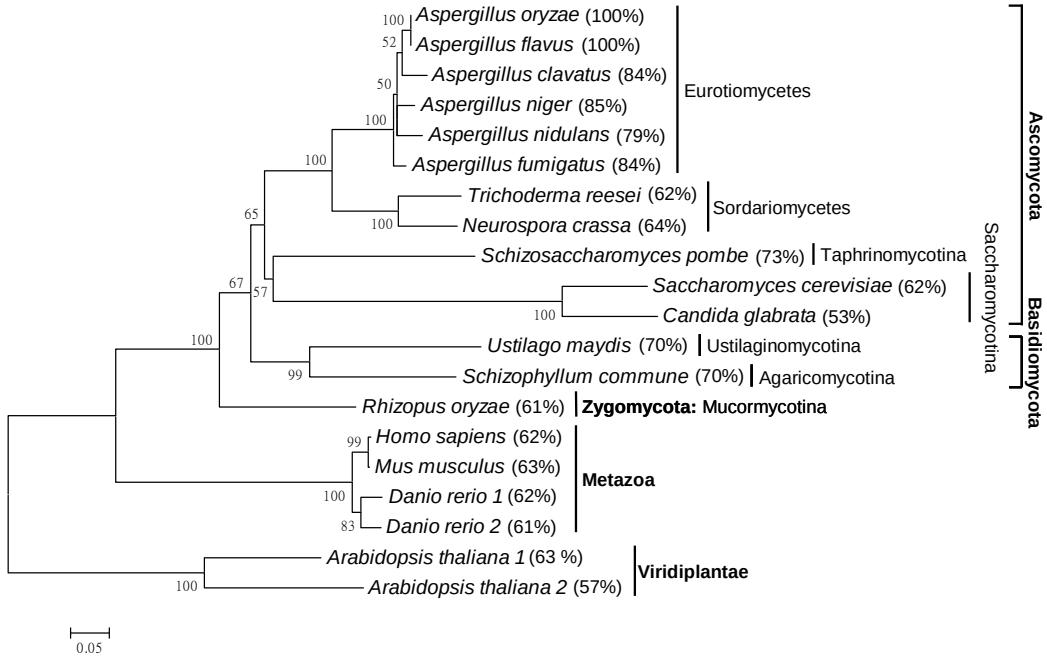

Figure 1-2. Phylogenetic comparison of AoPab1 among different organisms. Accession numbers for sequences are: *Aspergillus oryzae* (XP_001820045.1), *Aspergillus flavus* (XP_002374401), *Aspergillus clavatus* (XP_001269718.1), *Aspergillus niger* (XP_001388739.1), *Aspergillus nidulans* (XP_661604.1), *Aspergillus fumigatus* (XP_750167.1), *Trichoderma reesei* (EGR47358.1), *Neurospora crassa* (EAA31189.1), *Schizosaccharomyces pombe* (NP_593377.1), *Saccharomyces cerevisiae* (NP_011092.1), *Candida glabrata* (XP_449280.1), *Ustilago maydis* (XP_759641.1), *Schizophyllum commune* (XP_003031361.1), *Rhizopus oryzae* (EIE84000.1), *Homo sapiens* (P11940.2), *Mus musculus* (NP_032800.2), *Danio rerio* isoforms 1 and 2 (NP_001026846.1, NP_957176.1), *Arabidopsis thaliana* isoforms 1 and 2 (P42731.1, Q9FXA2). The phylogenetic tree was inferred using the Neighbor-Joining method (Saitou and Nei, 1987). The bootstrap consensus tree inferred from 1000 replicates is taken to represent the evolutionary history of the taxa analyzed (Felsenstein, 1985). The tree is drawn to scale, with branch lengths in the same units as those of the evolutionary distances

used to infer the phylogenetic tree. The evolutionary distances were computed using the JTT matrix-based method (Jones *et al.*, 1992) and are in the units of the number of amino acid substitutions per site. The rate variation among sites was modeled with a gamma distribution (shape parameter = 1). The analysis involved 20 amino acid sequences. All positions containing gaps and missing data were eliminated. There were a total of 452 positions in the final dataset. Protein identities to *A. oryzae* AoPab1 are given in parentheses.

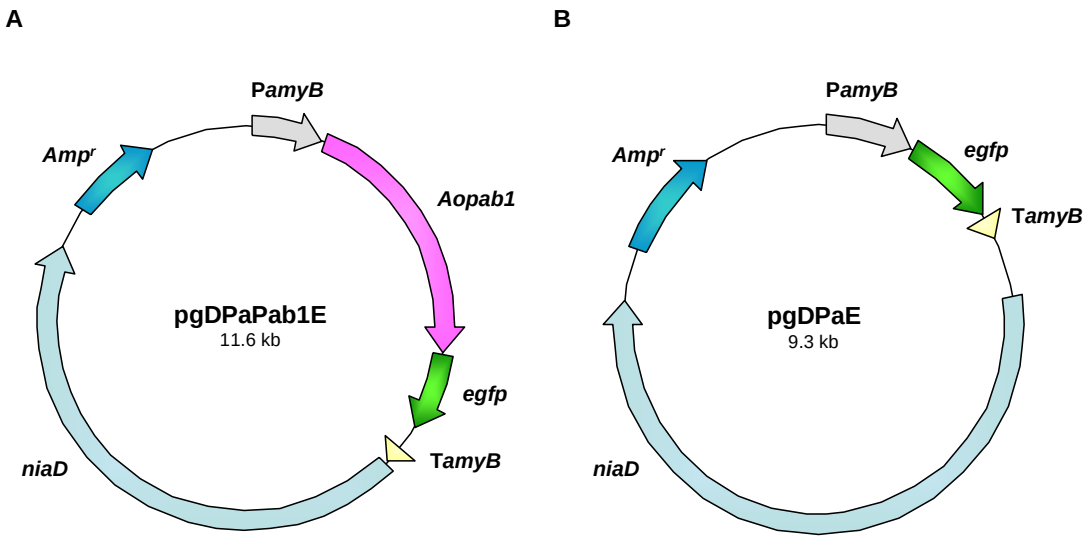

Figure 1-3. Plasmid construction for the ectopic expression of AoPab1-EGFP (A) and EGFP alone (B).

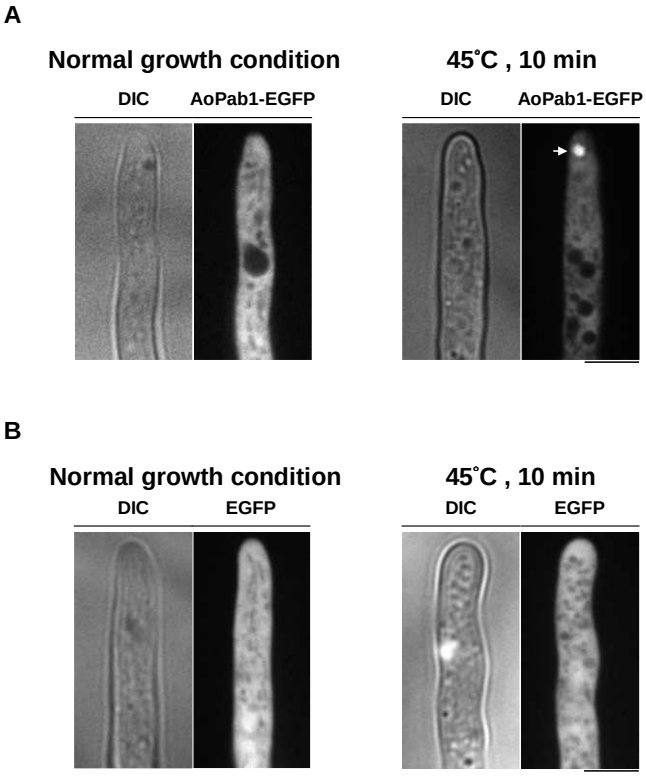

Figure 1-4. Formation of stress granules in response to heat stress.

Approximately 10^4 conidia of cells expressing AoPab1-EGFP under control of the *amyB* promoter were grown in CD+Met medium at 30°C for 18 h before being exposed to various types of stress. (A) Subcellular localization of AoPab1-EGFP. Accumulation of AoPab1-EGFP (indicated by the arrow) was induced when cells were exposed to 45°C for 10 min. (B) Subcellular localization of EGFP. Accumulation of EGFP was not observed in cells exposed to heat stress. Scale bars = 5 μm

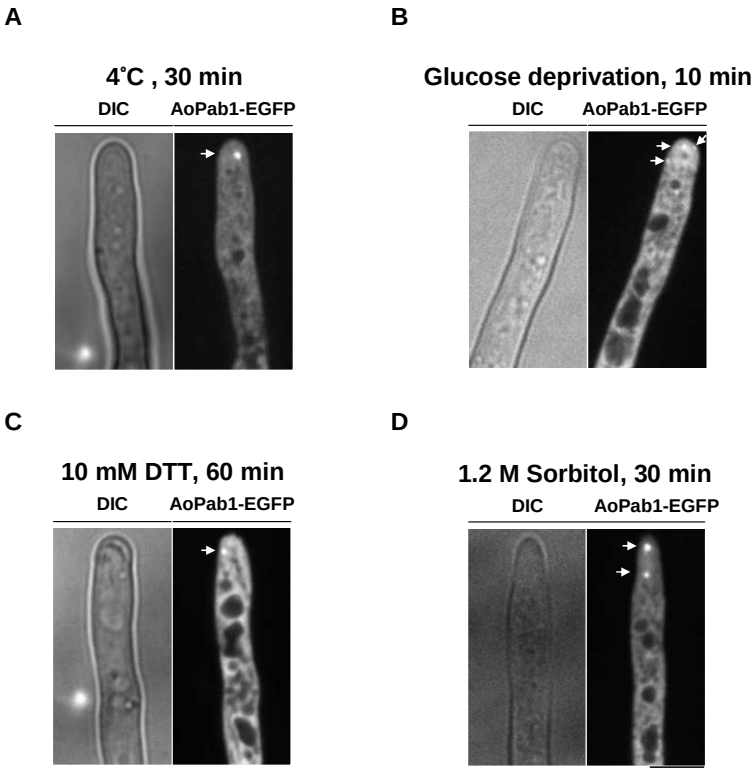

Figure 1-5. Formation of stress granules in response to various stress conditions. Approximately 10^4 conidia of cells expressing AoPab1-EGFP under control of the *amyB* promoter were grown in CD+Met medium at 30°C for 18 h before being exposed to various types of stress and the subcellular localization of AoPab1-EGFP was observed. Accumulation of AoPab1-EGFP (indicated by the arrows) was induced in cells treated with cold stress (4°C, 30 min) (A), glucose deprivation (10 min) (B), ER stress (10 mM DTT, 60 min) (C), and osmotic stress (1.2 M sorbitol, 30 min) (D). Scale bar = 5 μm.

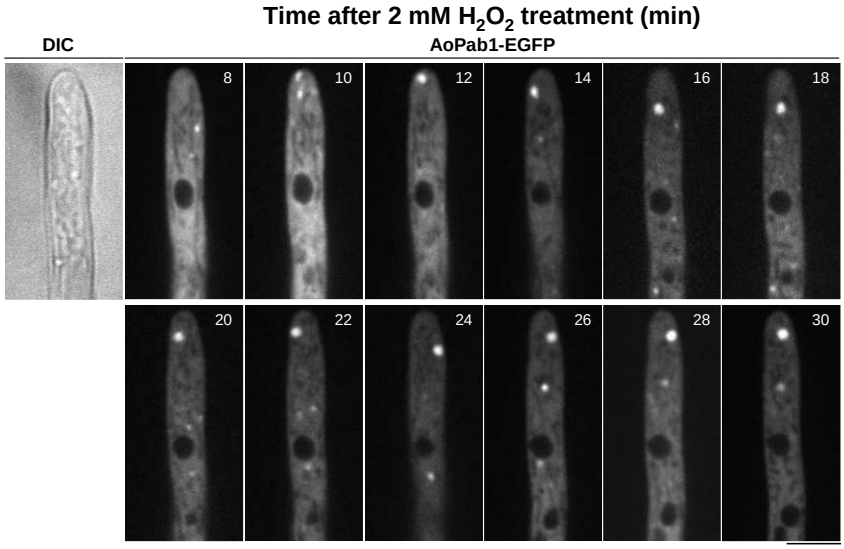

Figure 1-6. Time-lapse observation of stress granule formation upon oxidative stress.

Approximately 10^4 conidia of cells expressing AoPab1-EGFP under control of the *amyB* promoter were grown in CD+Met medium at 30°C for 18 h before being exposed to oxidative stress (2 mM H_2O_2). Accumulation of AoPab1-EGFP in cells was observed in a time-lapse manner. Scale bar = 5 μm.

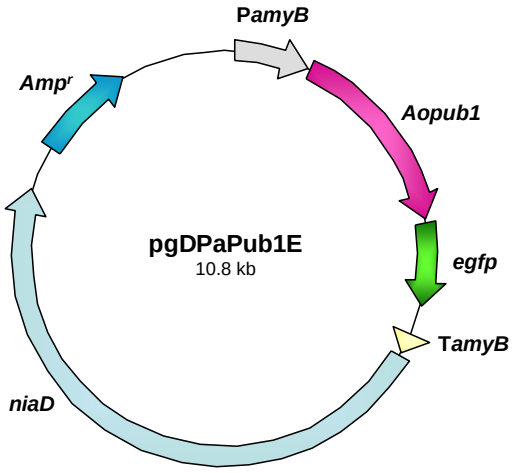

Figure 1-7. Plasmid construction for the ectopic expression of AoPub1-EGFP.

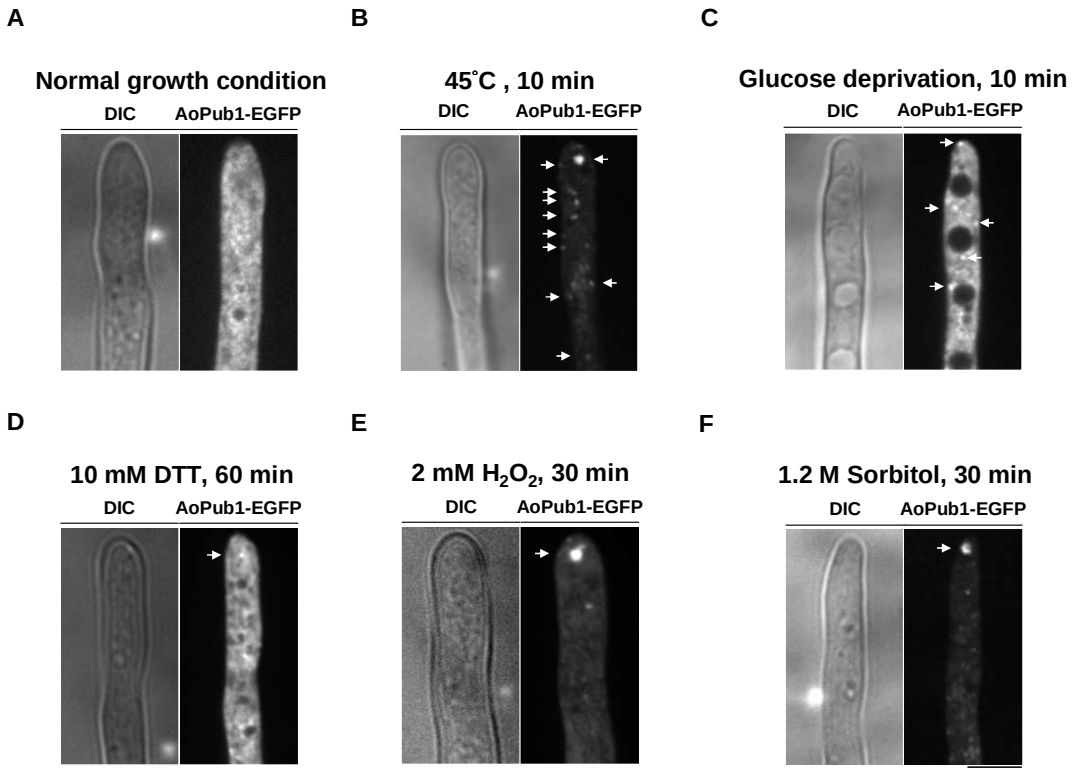

Figure 1-8. Formation of stress granules in cells expressing AoPub1-EGFP as a marker.

Approximately 10^4 conidia of cells expressing AoPub1-EGFP under control of the *amyB* promoter were grown in CD+Met medium at 30°C for 18 h before being exposed to various types of stress and the subcellular localization of AoPub1-EGFP was observed. Under normal growth conditions, AoPub1-EGFP was dispersed throughout the cytoplasm (A). Accumulation of AoPub1-EGFP (indicated by the arrows) was induced in cells treated with heat stress (45°C, 10 min) (B), glucose deprivation (10 min) (C), ER stress (10 mM DTT, 60 min) (D), oxidative stress (2 mM H_2O_2, 30 min) (E), and osmotic stress (1.2 M sorbitol, 30 min) (F). Scale bar = 5 μm.

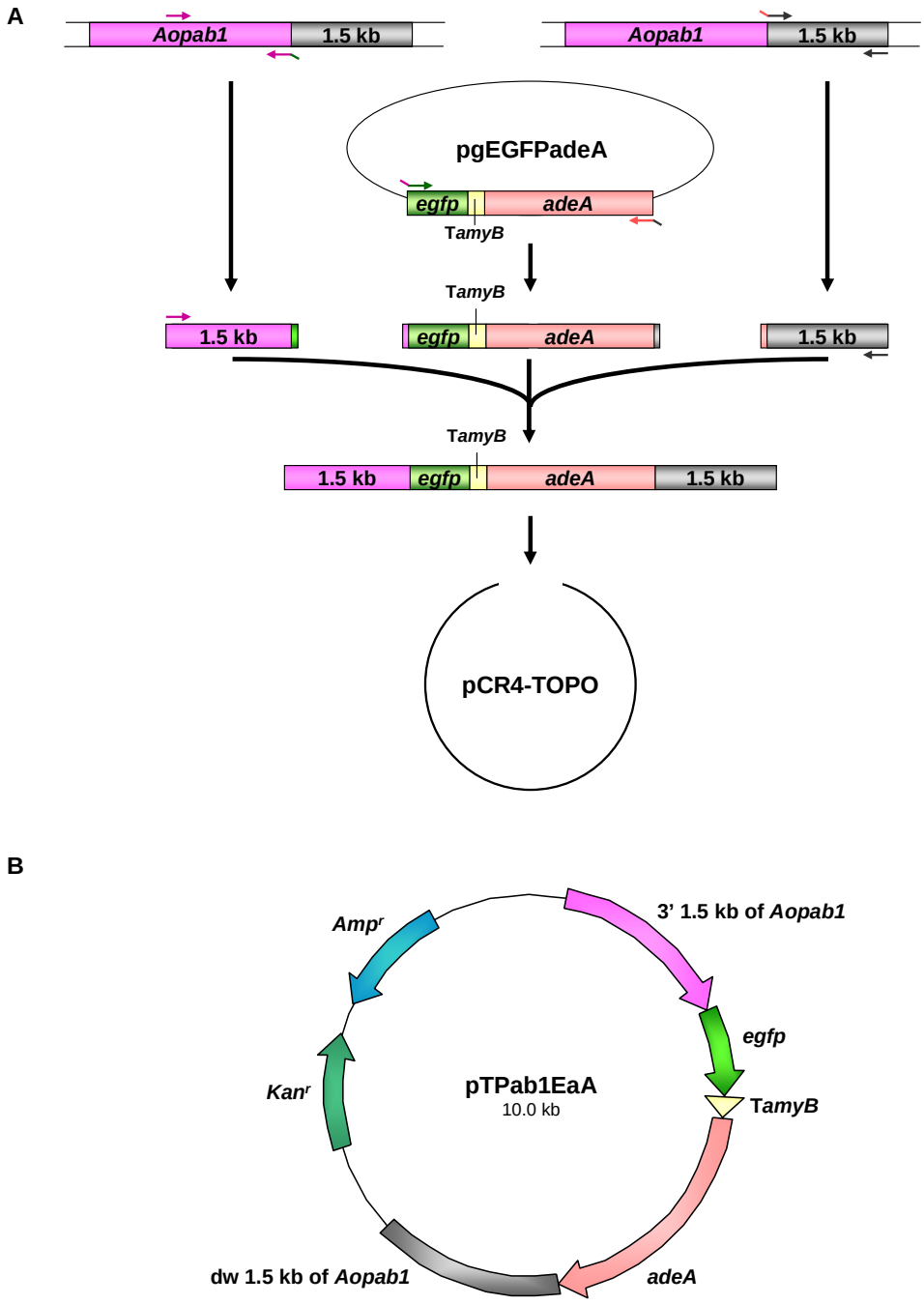

Figure 1-9. Plasmid construction for targeting *egfp* gene at *Aopab1* genomic locus. (A) Strategy for generation of targeting DNA fragment using fusion PCR. The resulting DNA fragment was ligated into TOPO vector, generating plasmid pTPab1EaA (B).

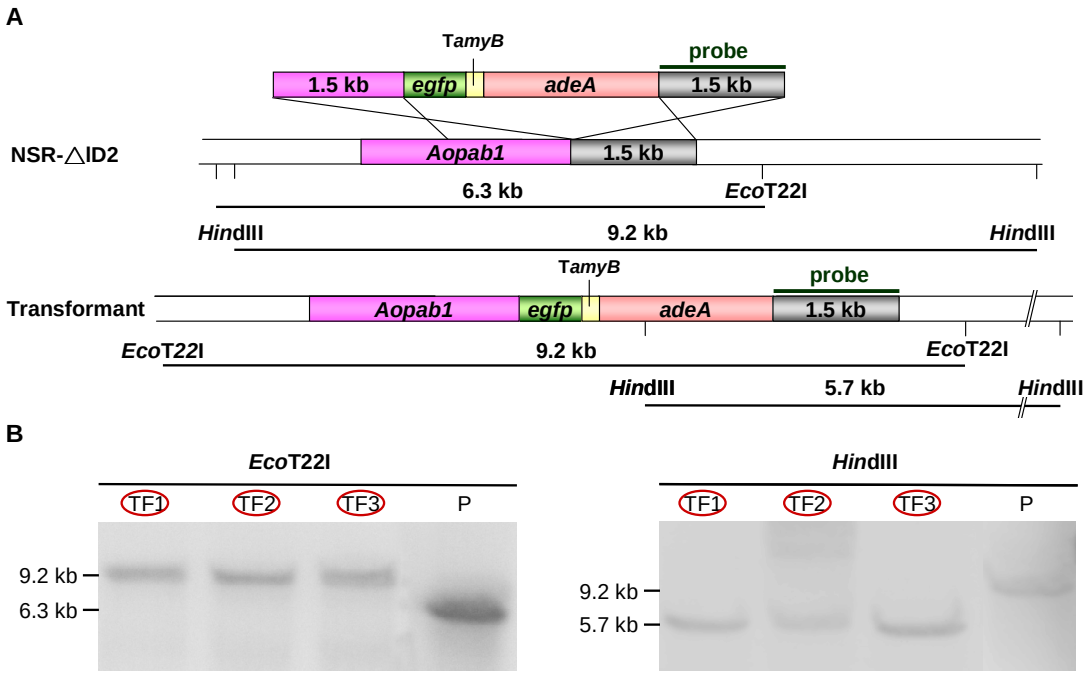

Figure 1-10 *Egfp* gene was tagged at *Aopab1* locus and confirmed by Southern blotting analysis.

(A) The schematic diagram of predicted sizes of DNA fragments in the parent strain and transformants digested with the *Eco*T22I and *Hin*dIII, and the result was shown in (B).

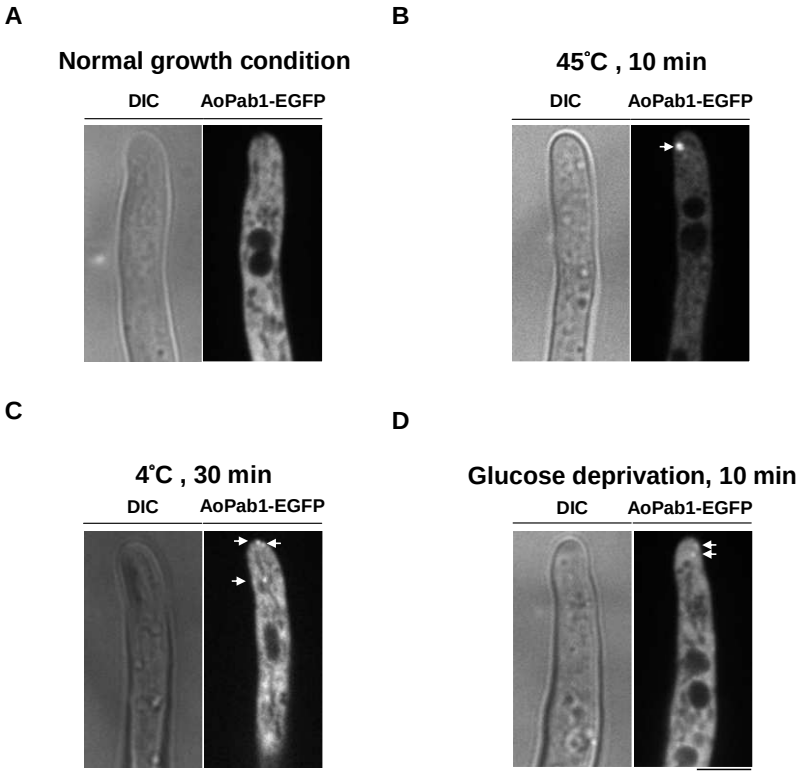

Figure 1-11. Formation of stress granules in cells expressing AoPab1-EGFP under control of the endogenous promoter.

Approximately 10^4 conidia of cells expressing AoPab1-EGFP under control of the endogenous promoter were grown in CD+Met medium at 30°C for 18 h before being exposed to various types of stress and the subcellular localization of AoPab1-EGFP was observed. Under normal growth conditions, AoPab1-EGFP was dispersed throughout the cytoplasm (A). Accumulation of AoPab1-EGFP (indicated by the arrows) was induced in cells treated with heat stress (45°C, 10 min) (B), cold stress (4°C, 30 min) (C), and glucose deprivation (10 min) (D). Scale bar = 5 μm.

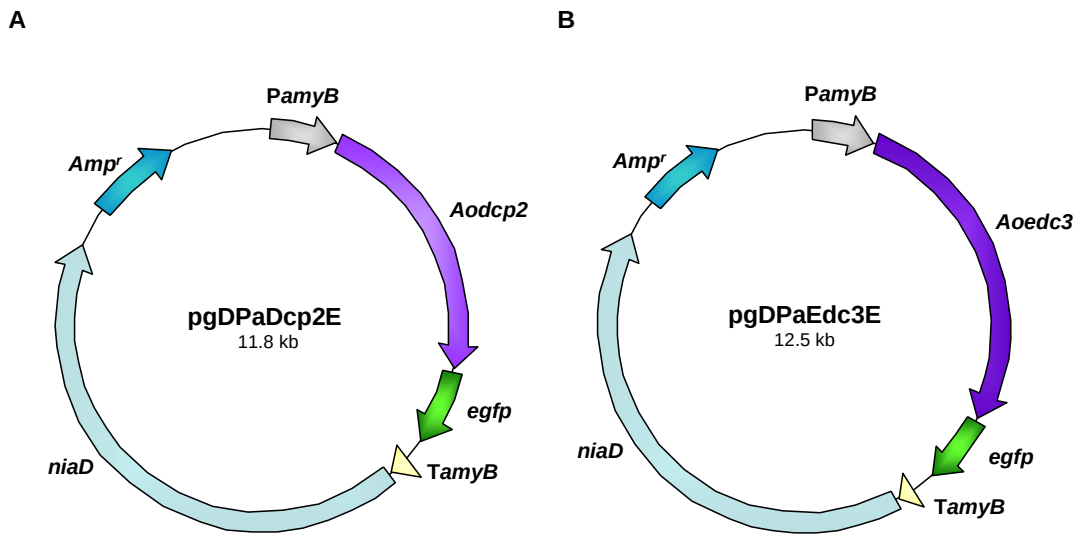

Figure 1-12. Plasmid construction for the ectopic expression of makers of P-bodies.

(A) AoDcp2-EGFP expressing plasmid. (B)AoEdc3-EGFP expressing plasmid.

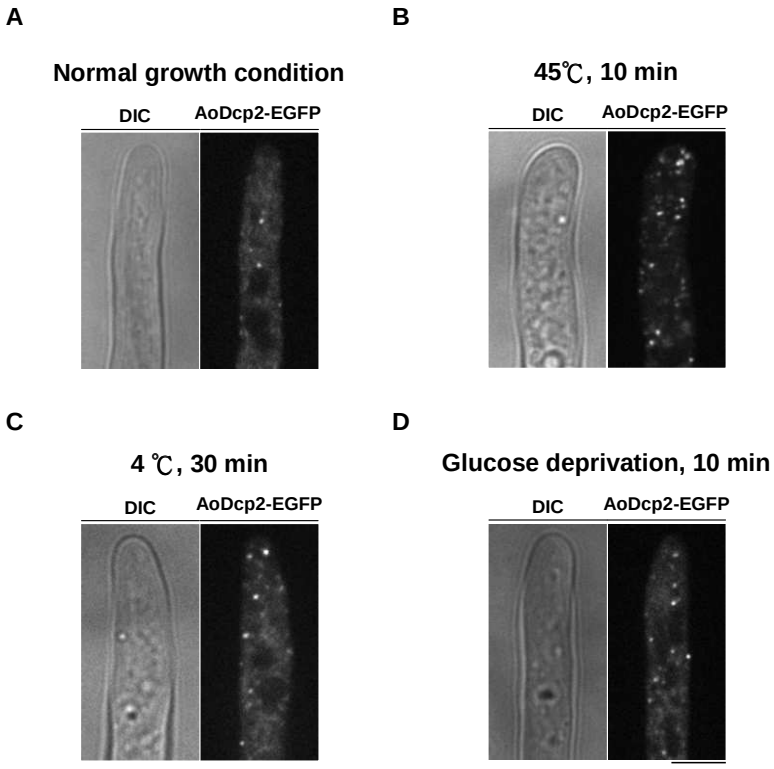

Figure 1-13. Formation of P-bodies in cells expressing AoDcp2-EGFP as a marker.

Approximately 10^4 conidia of cells expressing AoDcp2-EGFP under control of the *amyB* promoter were grown in CD+Met medium at 30°C for 18 h before being exposed to various types of stress and the subcellular localization of AoDcp2-EGFP was observed. AoDcp2-EGFP was detected as discrete bright dots in the cytoplasm in unstressed cells (A), and increased in size and number when cells expressing AoDcp2-EGFP were exposed to heat stress (45°C, 10 min) (B), low temperature (4°C, 30 min) (C), and glucose deprivation (10 min) (D). Scale bar = 5 μm.

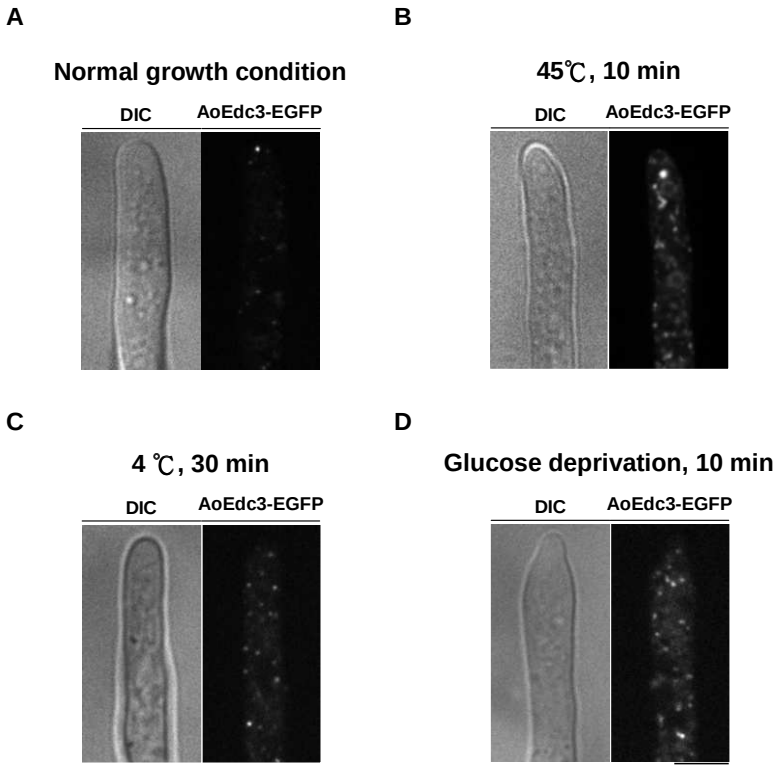

Figure 1-14. Formation of P-bodies in cells expressing AoEdc3-EGFP as a marker.

Approximately 10^4 conidia of cells expressing AoEdc3-EGFP under control of the *amyB* promoter were grown in CD+Met medium at 30°C for 18 h before being exposed to various types of stress and the subcellular localization of AoEdc3-EGFP was observed. AoEdc3-EGFP was detected as discrete bright dots in the cytoplasm in unstressed cells (A), and increased in size and number when cells expressing AoEdc3-EGFP were exposed to heat stress (45°C, 10 min) (B), low temperature (4°C, 30 min) (C), and glucose deprivation (10 min) (D). Scale bar = 5 μm.

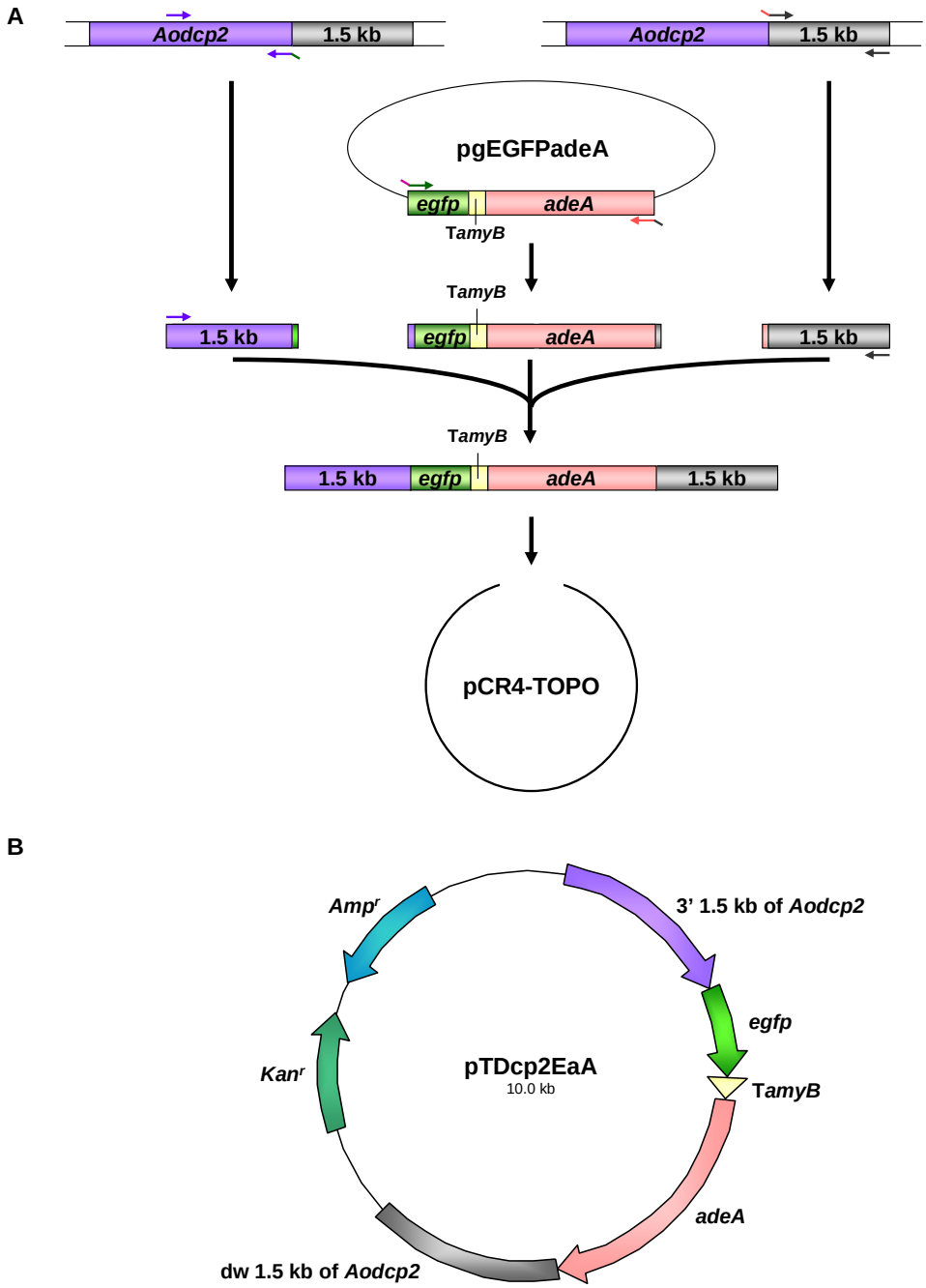

Figure 1-15. Plasmid construction for targeting *egfp* gene at *Aodcp2* genomic locus. (A) Strategy for generation of targeting DNA fragment using fusion PCR. The resulting DNA fragment was ligated into TOPO vector, generating plasmid pTDcp2EaA (B).

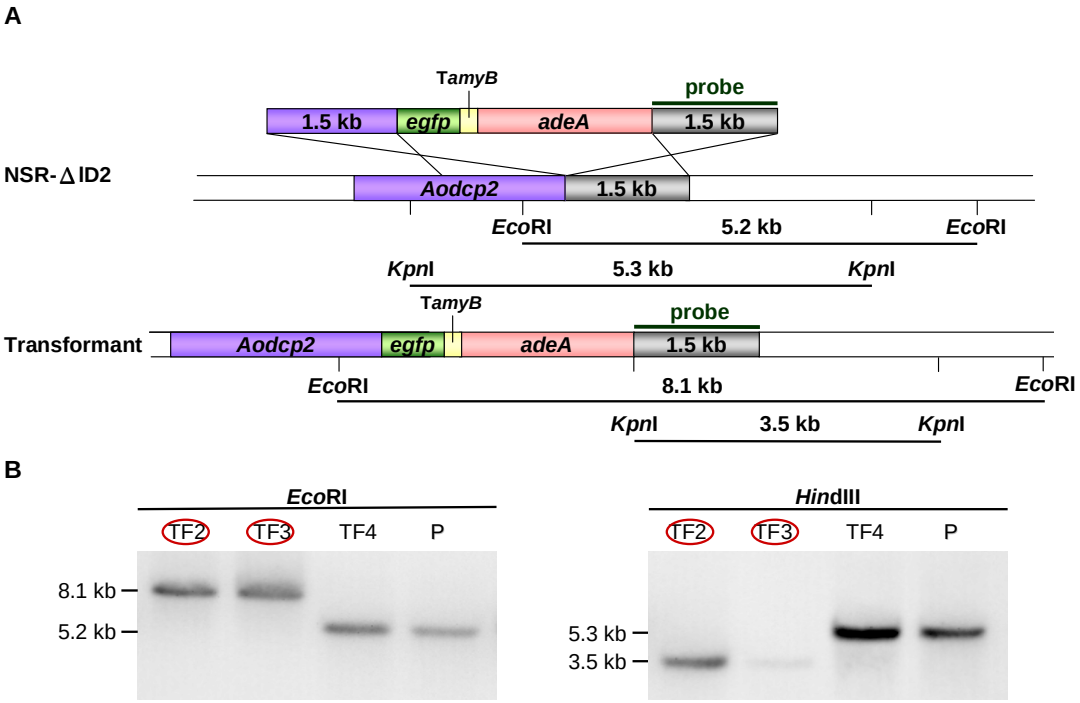

Figure 1-16 *Egfp* gene was tagged at *Aodcp2* locus and confirmed by Southern blot analysis.

(A) The schematic diagram of predicted sizes of DNA fragments in the parent strain and transformants digested with the *Eco*RI and *Hin*dIII, and the result was shown in (B).

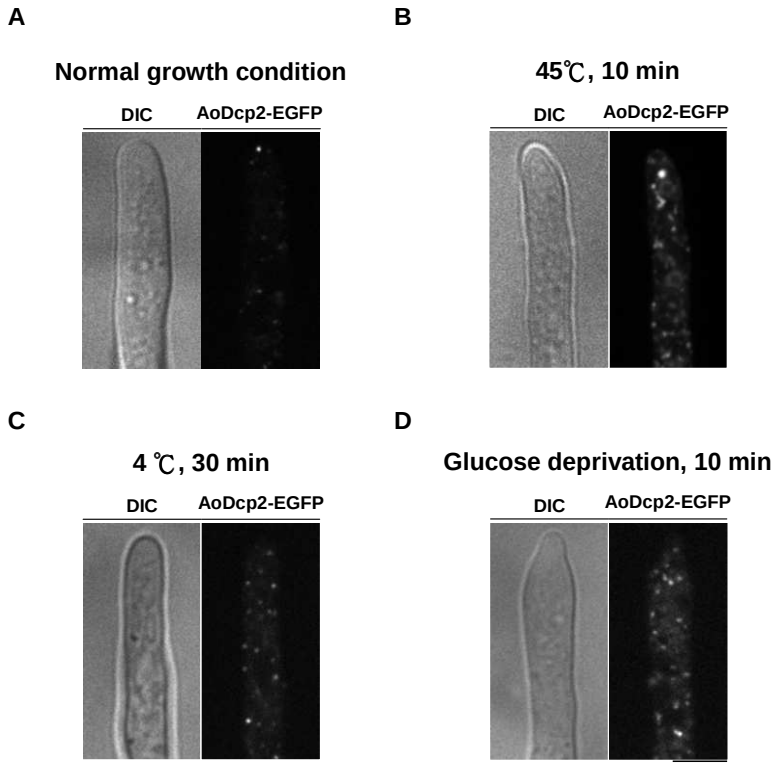

Figure 1-17. Formation of P-bodies in cells expressing AoDcp2-EGFP under control of the endogenous promoter.

Approximately 10^4 conidia of cells expressing AoDcp2-EGFP under control of the endogenous promoter were grown in CD+Met medium at 30°C for 18 h before being exposed to various types of stress and the subcellular localization of AoDcp2-EGFP was observed. AoDcp2-EGFP was detected as discrete bright dots in the cytoplasm in unstressed cells (A), and increased in size and number when cells expressing AoDcp2-EGFP were exposed to heat stress (45°C, 10 min) (B), low temperature (4°C, 30 min) (C), and glucose deprivation (10 min) (D). Scale bar = 5 μm.

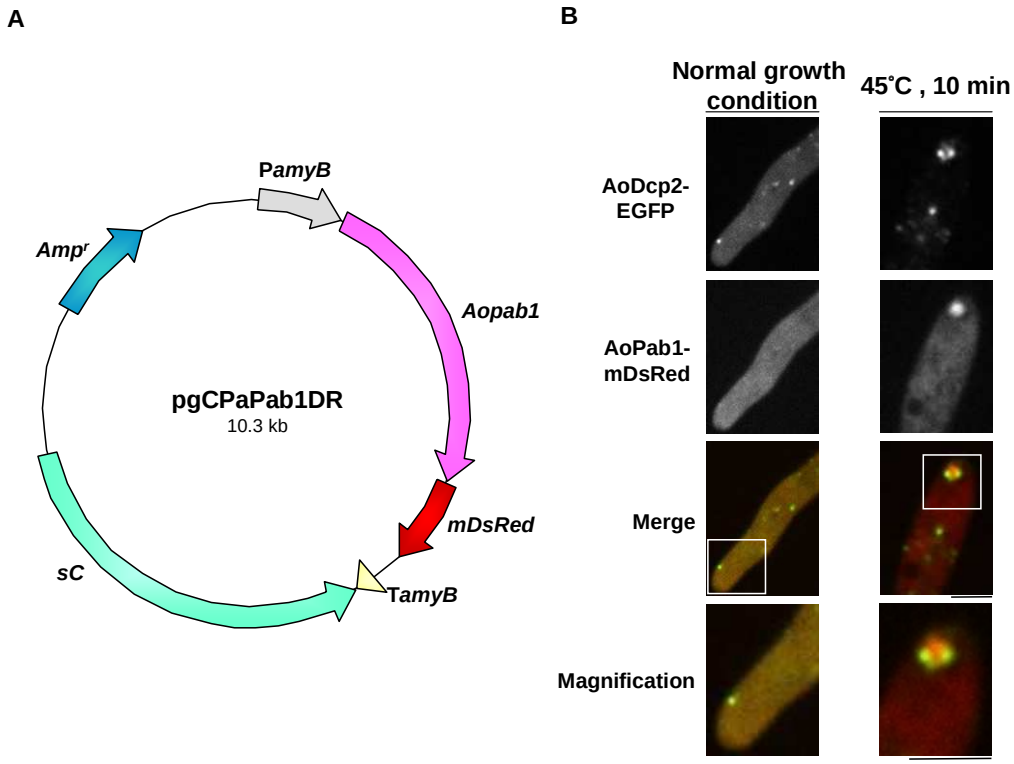

Figure 1-18. Colocalizations of P-bodies and stress granules in response to heat stress.

(A) Plasmid construction for the ectopic expression of AoPab1-mDsRed. (B) Subcellular localization of AoDcp2-EGFP and AoPab1-mDsRed. AoDcp2-EGFP and AoPab1-mDsRed were used as markers of P-bodies and stress granules, respectively. Approximately 10^4 conidia of cells co-expressing AoDcp2-EGFP and AoPab1-mDsRed were grown in CD medium at 30°C for 18 h before being exposed to 45°C for 10 min. The lowest panels show magnified images of the apical region of the cell (within the boxed area in the above image). Scale bars = 5 μm.

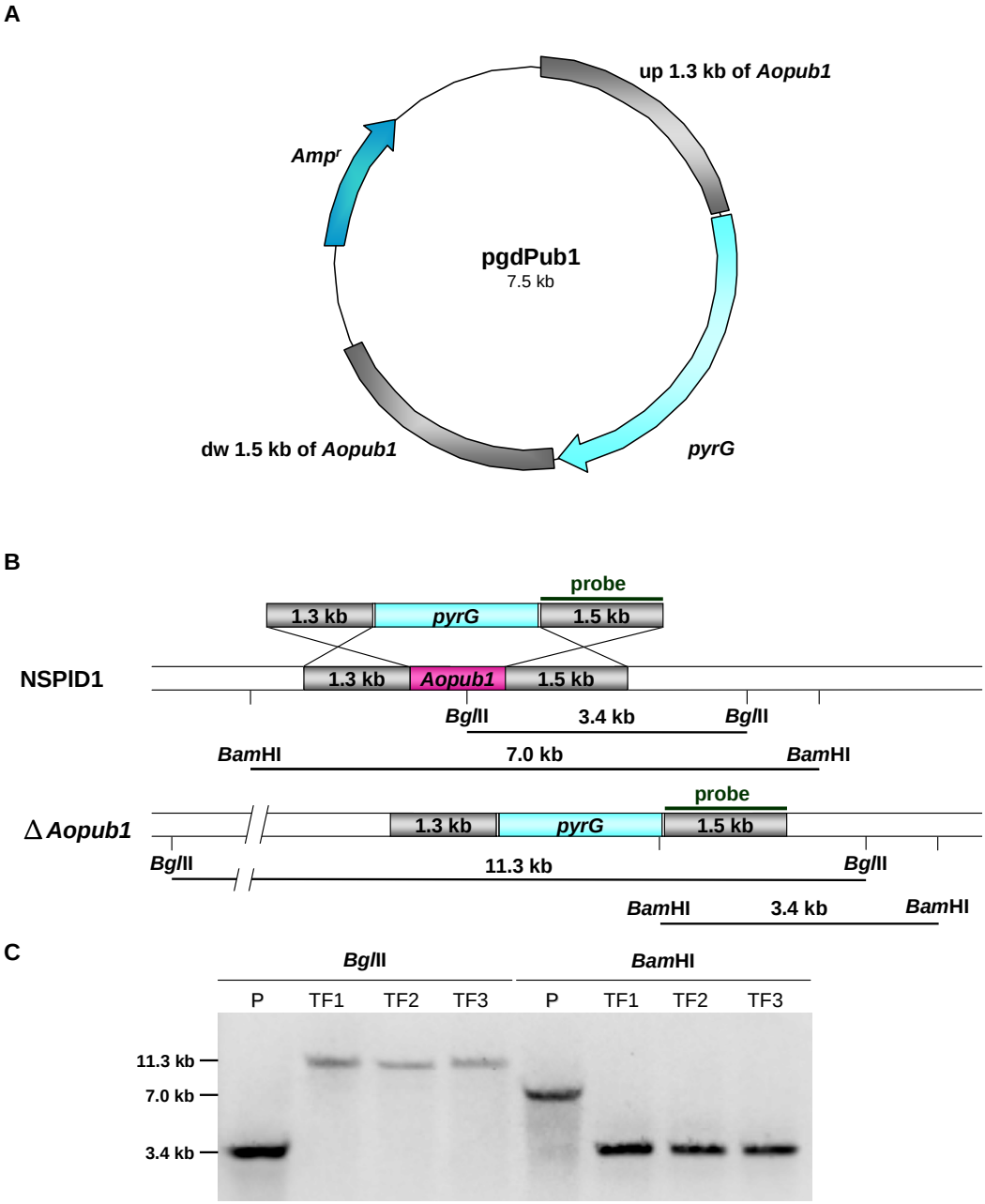

Figure 1-19. *Aopub1* gene was disrupted and confirmed by Southern blotting analysis.

(A) Plasmid construction for the expression of *Aopub1* disrupting cassette. (B) The schematic diagram of predicted sizes of DNA fragments in parent strain and transformants digested with the *Bgl*II and *Bam*HI, and the result was shown in (C).

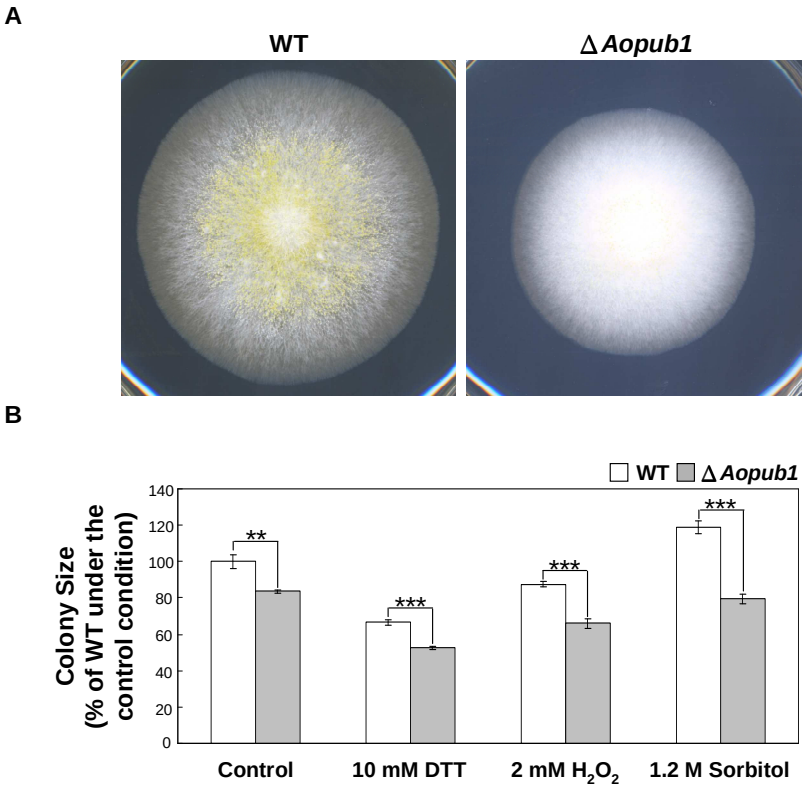

Figure 1-20. *Aopub1* disruptant showed defects in the conidia formation and more severe growth retardation in stress conditions. (A) Approximately 10^3 conidia of wild-type and *Aopub1* disruptant cells were spotted onto PD plates, and cultured at 30°C for 4 days. (B) Approximately 10^3 conidia of wild-type and *Aopub1* disruptant cells were spotted onto PD plates with or without 10 mM DTT, 2 mM H_2O_2, or 1.2 M sorbitol, and cultured at 30°C for 4 days. Colony diameters were compared to those of the wild-type strain under the control condition, which was set to 100%. Data represent the mean ± S.D. of three biological replicates. The asterisk denotes a statistically significant difference, as judged by the Student's t-test with $P < 0.01$ (**) and $P < 0.001$ (***).

Chapter 2

Identification of AoSO as a novel stress granule component upon heat stress in *A. oryzae*

Introduction

The mycelia of filamentous fungi consist of a network of interconnected hyphae, which are compartmentalized by septa. Septa contain a central pore that allows the movement of cytoplasm and organelles between adjacent hyphae for direct communication and coordination (Shepherd *et al*., 1993; Markham, 1994; Jedd and Pieuchot, 2012). However, mycelia with cytoplasmic continuity are susceptible to catastrophic failure due to cytoplasmic loss when individual hyphae are injured. Fungi defend against such loss by the rapid occlusion of septal pores in response to hyphal damage and stressful environmental conditions (Aylmore *et al*., 1984; Markham, 1994; van Peer *et al*., 2009). The *Neurospora crassa* SO (SOFT) protein, and its *Sordaria macrospora* homolog, Pro40, were shown to be essential for hyphal fusion (Fleißner *et al*., 2005; Fleißner and Glass, 2007; Fleißner *et al*., 2009) and sexual development (Engh *et al*., 2007), respectively. Subcellular localization studies reveals that SO is evenly distributed throughout the cytoplasm under normal growth conditions, but accumulates at the septal pore in injured, aging, and dying hyphae (Fleißner and Glass, 2007). It has been shown in our laboratory previously that an *A. oryzae* homolog of SO, AoSO, accumulates at the septal pore when cells are exposed to various stresses (Maruyama *et al*., 2010). The stress-induced accumulation behavior of AoSO is similar to the components of stress granules. Therefore, the aim of chapter 2 was to investigate whether AoSO interacts with stress granules in *A. oryzae*.

Results

1 Colocalization of AoSO with stress granules in response to heat stress

To investigate the possibility that AoSO protein is involved in the function of stress granules, AoPab1-mDsRed expressing plasmid pgCPaPab1DR (Figure 1-18A) was introduced into AoSO-EGFP expressing strain. The generated strain co-expressing AoSO-EGFP and AoPab1-mDsRed was used to examine the cellular localizations of AoSO and stress granules in cells exposed to heat stress (Figure 2-1A). The functionality of AoSO-EGFP was previously confirmed by demonstrating that expression of the fusion protein complemented the phenotypes of Δ*Aoso* strain (Maruyama *et al*., 2010). Under normal growth conditions, AoSO-EGFP was evenly distributed throughout the cytoplasm, but accumulated at the septal pore after cells were exposed to heat stress, as previously reported (Maruyama *et al*., 2010). However, AoPab1-mDsRed did not accumulate at the septal pore in cells exposed to heat stress (Figure 2-1A) or any other of the examined stress conditions (cold stress, glucose deprivation, and ER, osmotic and oxidative stresses; data not shown). In cells exposed to heat stress, AoSO-EGFP also accumulated as cytoplasmic foci, which colocalized with stress granules labeled with AoPab1-mDsRed at the hyphal tip (Figure 2-1A).

To further determine the physical association of AoSO with the stress granule component AoPab1, AoPab1-3HA expressing plasmid was constructed (Figure 2-2A) and introduced into AoSO-EGFP expressing strain. The generated strain co-expressing AoSO-EGFP and AoPab1-3HA was confirmed by immunoblotting (Figure 2-2B) and used in co-immunoprecipitation experiments. AoPab1-3HA was immunoprecipitated using anti-HA magnetic beads. The interaction between AoSO-EGFP and AoPab1-3HA was confirmed by co-immunoprecipitation. This association is not mediated via the EGFP portion as no association was detected in the negative control strain co-expressing EGFP and AoPab1-3HA.

To clarify if the aggregation of AoSO requires the presence of non-translating mRNAs, cycloheximide, which blocks translational elongation and traps mRNAs in polysomes, was used to deplete the pool of non-translating mRNAs (Kedersha *et al*., 2000; Buchan *et al*., 2008; Grousl *et al*., 2009) (Figure 2-1A and 2-1B). The strain co-expressing AoSO-EGFP and AoPab1-mDsRed was treated with 200 μg/ml cycloheximide for 30 min before being exposed to heat stress. The formation of stress granules labeled with AoPab1-mDsRed was sensitive to the cycloheximide treatment, confirming that they are typical mRNP granules, as previously reported (Kedersha *et al*., 2000; Buchan *et al*., 2008; Grousl *et al*., 2009). In addition, the heat stress-induced formation of cytoplasmic AoSO foci at the hyphal tip was greatly impaired by cycloheximide (Figure 2-1A and 2-1B), suggesting that cytoplasmic AoSO foci require a pool of free mRNAs for their aggregation. However, cycloheximide did not affect the accumulation of AoSO at the septal pore. Overall, these results suggest that AoSO is a novel component of mRNP granules in the filamentous fungus *A. oryzae*.

2 AoSO affects the formation and localization of stress granules

To gain a better understanding of the role of AoSO in stress granules, the effect of *Aoso* deletion on stress granule formation was examined. AoPab1-EGFP expressing plasmid pgDPaPab1E (Figure 1-3A) was introduced into *Aoso*-deletion strain and confirmed using Suthern blotting analysis (figure 2-4). The formation of stress granules in response to heat stress was observed in the *Aoso*-deletion strain (Figure 2-5A). However, compared to 100% formation of stress granules in wild-type cells exposed to heat stress, the heat stress-induced formation of stress granules in the *Aoso*-deletion strain was decreased to 87.7 ± 1.34 % (hyphae=50; n=7; $p < 0.005$) (Figure 2-5B). No obvious change in the size of stress granules was observed in the

Aoso-deletion strain. The movement of stress granules labeled with AoPab1-EGFP in stressed cells was monitored by live-cell imaging, which revealed that in contrast to other types of stress where the stress granules were highly dynamic (please refer to http://www.plosone.org/article/info%3Adoi%2F10.1371%2Fjournal.pone.0072209#s5 for the Supplementary Video S2), the heat stress-induced stress granules were nearly stationary (refer to the previous link for the Supplementary Video S3). By taking advantage of this feature, the effect of *Aoso* deletion on stress granules was further evaluated by measuring the distance between the hyphal tip and stress granules. The distribution of the largest stress granules labeled with AoPab1-EGFP was less concentrated and more distant from the hyphal tip in the *Aoso*-deletion strain (Figure 2-5C). Additionally, I observed that in a small portion of hyphae, heat stress-induced stress granules were more dynamic in the *Aoso*-deletion strain (refer to the previous link for the Supplementary Video S4). However, the motility of heat-stress induced stress granules in the *Aoso*-deletion strain was different from that of all the other stress conditions examined in this study with a long distance movement, but moved around in a confined region (refer to the previous link for the Supplementary Videos S2 and S4). I have examined the growth test of the *Aoso* deletion strain on PD plates containing 10 mM DTT, 2 mM H_2O_2, or 1.2 M sorbitol; however, no growth difference between wild-type and the *Aoso* deletion strain was observed (Figure 2-6). Taken together, the results indicated that AoSO is not absolutely necessary for the formation of stress granules, but AoSO influences the formation and localization of stress granules in cells exposed to heat stress.

Discussion

AoSO is a component of stress granules

Deletion of the *so* gene in *N. crassa* results in a pleiotropic phenotype characterized by a lack of hyphal anastomoses, reduced aerial hyphae, slower growth rate, altered conidiation pattern, and female sterility (Fleißner *et al*., 2005). Mutation of the conserved WW domain in SO, which is predicted to mediate protein-protein interactions, does not affect SO localization to the septal pore; however, the phenotypic defects of the *so* disruptant are not fully complemented (Fleißner and Glass, 2007). Clearly, SO is a multi-function protein, and a plugging of the septal pore is not sufficient to explain the multiple phenotypic defects observed in the *so*-deletion strain. The molecular function of the SO protein remains largely unknown. Localization analyses have revealed that the *N. crassa* SO homolog *S. macrospora* Pro40 partially associates with Woronin bodies (Engh *et al*., 2007), and that *N. crassa* SO contributes to the sealing efficiency of pores plugged by Woronin bodies after hyphal injury (Fleißner and Glass, 2007). Additionally, cell-cell signaling and tropic growth of *N. crassa* germlings involve the unusual subcellular dynamics of SO and the MAP kinase (MAK-2), which are recruited to the plasma membrane of cell tips of interacting germlings in an oscillating and alternating manner (Fleißner *et al*., 2009). In the present study, we found that AoSO accumulates not only at the septal pore, but also at the hyphal tip, in cells exposed to heat stress. In addition, cytoplasmic AoSO foci colocalized with AoPab1-mDsRed-labeled stress granules at the hyphal tip and were sensitive to cycloheximide treatment (Figure 2-2), suggesting that cytoplasmic AoSO foci are mRNP granules, and that AoSO therefore may participate in the posttranscriptional regulation of mRNA in response to heat stress. The physical association between AoSO-EGFP and AoPab1-3HA was further confirmed by co-immunoprecipitation (Figure 2-4); however, this association was not induced or

increased after cells were exposed to heat stress. An inconsistence between the results of co-immunoprecipitation and colocalization analysis may be explained by the different culture conditions (DPY complete medium in submerged culture and CD+Met minimal medium in stationary culture). Orthologs of the *so* gene have only been identified in the genomes of Pezizomycotina species (Fleißner *et al*., 2005), therefore AoSO is presumed to be a novel component of stress granules specific to Pezizomycotina. The effect of *Aoso* deletion on the function of stress granules revealed that AoSO is not indispensable for stress granule formation; however, the formation and localization of stress granules were influenced in the absence of AoSO (Figure 2-5).

Protein-protein interaction has been implicated in the assembly of mRNP granules, including stress granules. One mechanism of assembly is mediated through the glutamine/asparagine (Q/N)-rich prion-like domain, which has a strong tendency to self-aggregate and is found in many components of mRNP granules (Kedersha *et al*., 1999; Kedersha *et al*., 2000; Michelitsch and Weissman, 2000; Gilks *et al*., 2004). Moreover, the long, intrinsically disordered domains identified in septal pore-associated (SPA) proteins show an inherent tendency to aggregate (Lai *et al*., 2012). The N-terminal domain of AoSO is also predicted to be disordered (Figure 2-7), suggesting that it has the potential to form aggregates of mRNP granules, although *N. crassa* SO, which contains a disordered domain that is enriched in glutamine, fails to form aggregates *in vitro* (Lai *et al*., 2012). In consistence with this property, deletion of *Aoso* resulted in a 12.3 ± 1.34 % reduction in the number of tip cells displaying stress granules labeled with AoPab1-EGFP under the heat stress condition. Additionally, I also observed that in a small portion of hyphae, heat stress-induced stress granules were more dynamic in the *Aoso*-deletion strain. It remains unclear how AoSO influences the localization and motility of stress granules. As mentioned in the

Chapter 1, the vast majority of proteins that bind to PABP through its MLLE domain contain a PAM2 motif; however, PAM2 domain is not found in AoSO. The interaction of PAPB and PAM2 motif containing proteins is mediated through highly-structural recognition. It may not be surprising considering that highly disordered AoSO takes a different way to interact with AoPab1. AoSO contains a conserved WW domain, as well as a proline-rich domain predicted to mediate protein-protein interactions. The localization and dynamics of stress granules may be indirectly influenced through protein-protein interactions of AoSO with other proteins.

Present findings, in addition to the known functions of AoSO and its homologs in hyphal fusion, sexual reproduction, and septal plugging (Fleißner *et al*., 2005; Engh *et al*., 2007; Maruyama *et al*., 2010), raise the possibility that AoSO participates in the posttranscriptional regulation of mRNA in response to heat stress. However, the localization of mRNAs in AoSO cytoplasmic foci remains to be conclusively demonstrated.

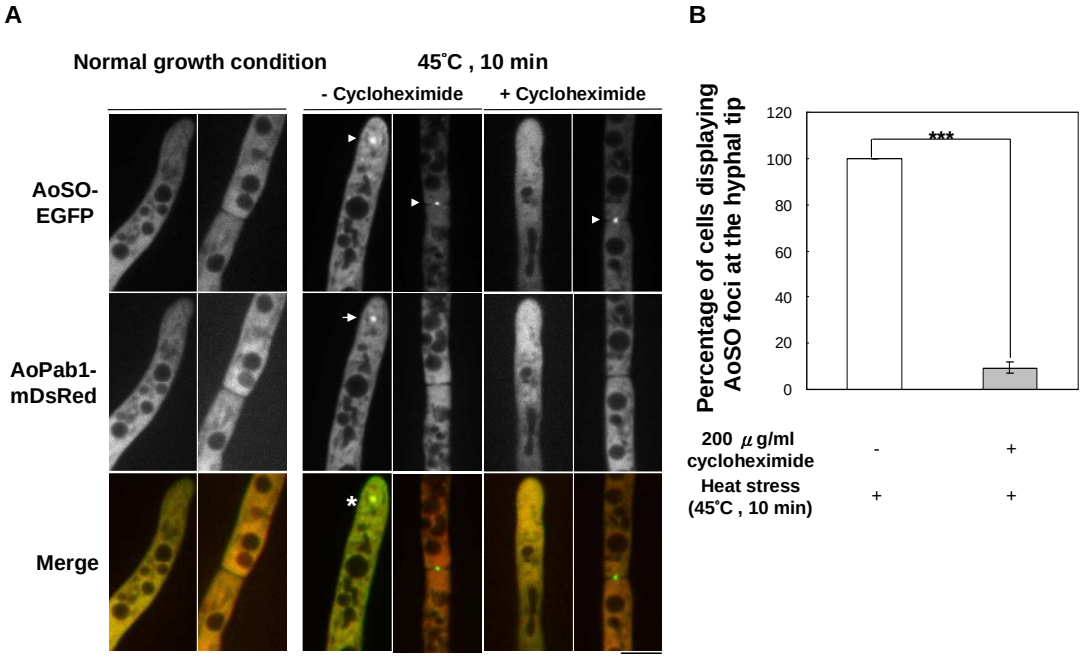

Figure 2-1. Subcellular localizations of AoSO-EGFP and AoPab1-mDsRed in response to heat stress.

(A) A wild-type strain co-expressing AoSO-EGFP and AoPab1-mDsRed was used to examine the relative localizations of AoSO and stress granules under normal growth conditions and heat stress. Approximately 10^4 conidia of cells were grown in CD medium at 30°C for 18 h before being exposed to 45°C for 10 min. Arrowheads indicate AoSO foci, and arrows indicate stress granules. Colocalization of a stress granule and an AoSO cytoplasmic focus is indicated by the asterisk. The effect of cycloheximide on the formation of mRNP granules was examined by pre-treating cells with 200 μg/ml cycloheximide for 30 min before being exposed to heat stress. Scale bar = 5 μm. (B) Effect of cycloheximide on the formation of AoSO cytoplasmic foci at the hyphal tip. Cells were incubated with CD medium containing 200 μg/ml cycloheximide for 30 min before being exposed to heat stress. The percentage of cells displaying AoSO cytoplasmic foci at the hyphal tip was determined. Error bars represent the standard error. ***P < 0.0001. The presented data are from three independent experiments, each with n = 50.

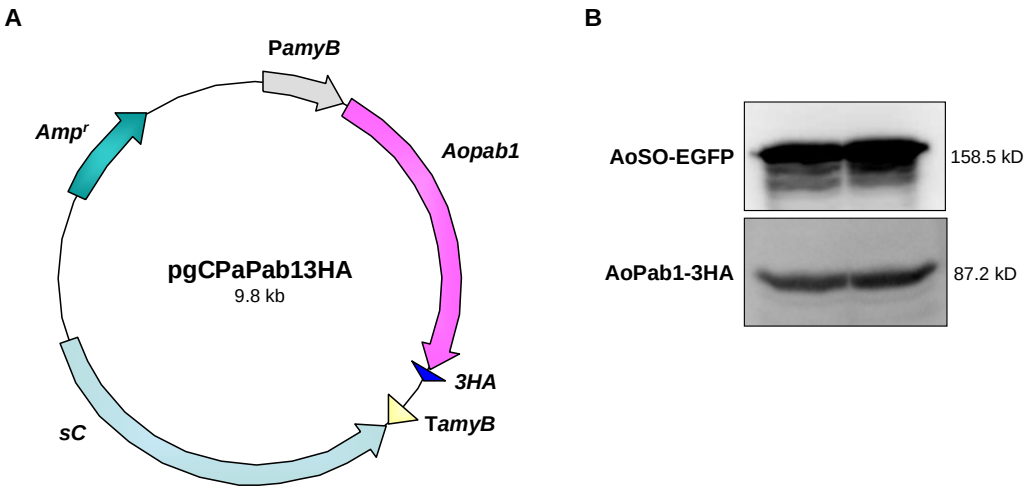

Figure 2-2. Construction of strains co-expressing AoPab1-3HA with AoSO-EGFP.

(A) Plasmid pgCPaPab13HA was introduced into strains expressing AoSO-EGFP (B) Co-expression of AoSO-EGFP and AoPab1-3HA was confirmed by Western blotting.

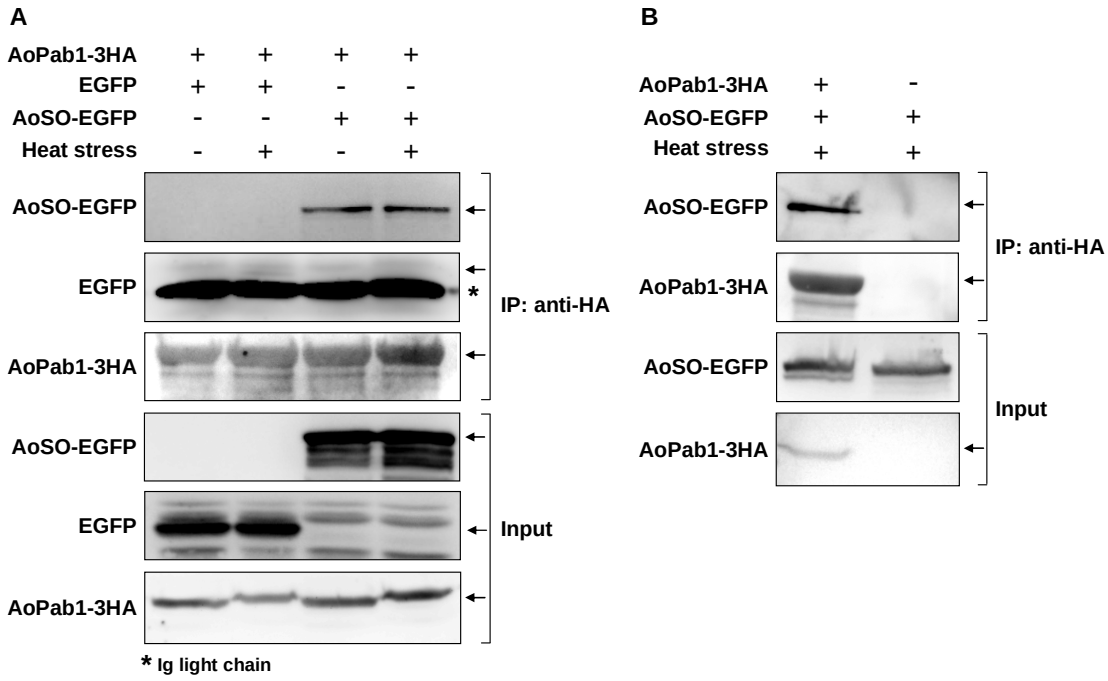

Figure 2-3. Co-immunoprecipitation of AoSO-EGFP and AoPab1-3HA.

(A) Approximately 10^7 conidia of cells expressing AoSO-EGFP and AoPab1-3HA or EGFP and AoPab1-3HA were inoculated in 20 ml DPY medium, and cultured at 30°C for 10 h before being exposed to heat stress. Mycelia were harvested and proteins were extracted for immunoprecipitation using anti-HA-tag mAb-Magnetic Agarose beads. (B) A strain expressing AoSO-EGFP alone was used as a negative control (right lane).

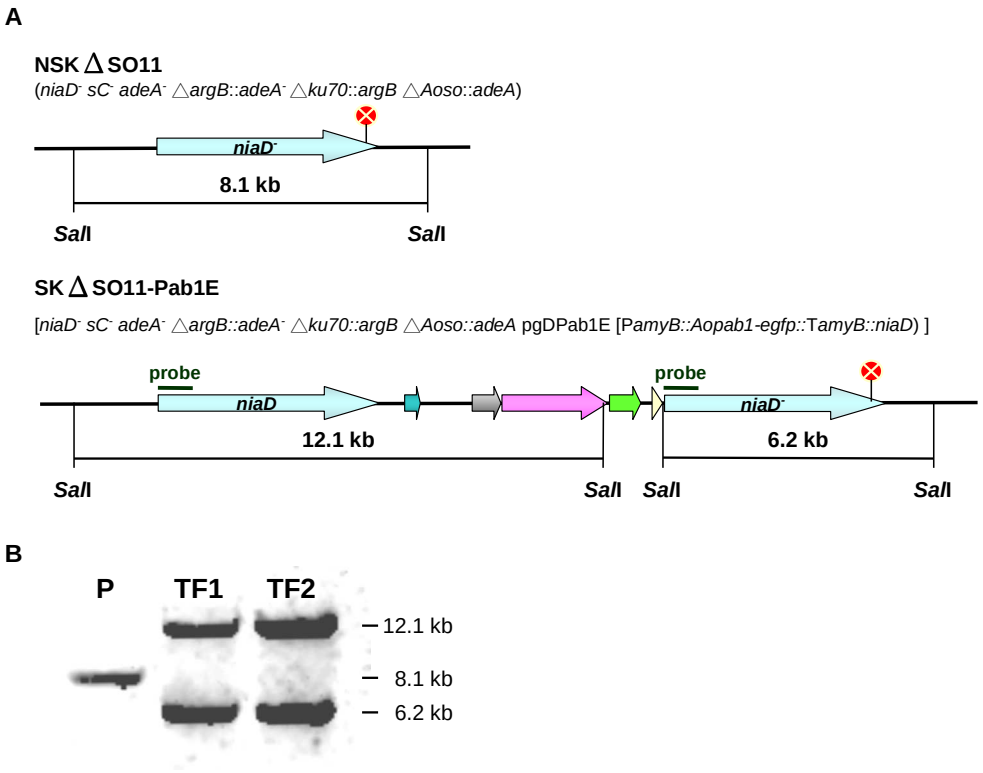

Figure 2-4. *Aopab1-egfp* was introduced into *Aoso*-deleted strain and confirmed by Southern blot analysis.

(A) The schematic diagram of predicted sizes of DNA fragments in parent strain and transformants digested with the *Sal*I, and the result of Southern bolt analysis is shown in (B).

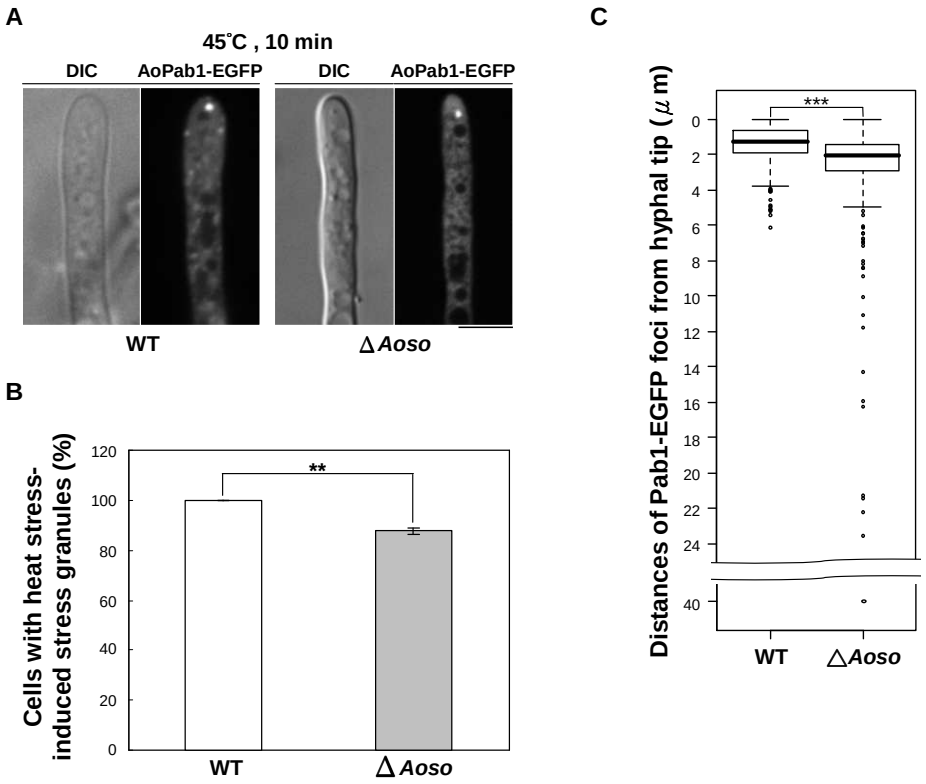

Figure 2-5. Effect of *Aoso* deletion on stress granules.

(A) Stress granule formation in wild-type (WT) and *Aoso*-deletion mutant (Δ*Aoso*) cells was detected using AoPab1-EGFP as a marker. Approximately 10^4 conidia of cells expressing AoPab1-EGFP were grown in CD+Met medium at 30°C for 18 h before being exposed to 45°C for 10 min. Scale bar = 5 μm. (B) Effect of *Aoso* deletion on the formation of stress granule. (C) Distribution of stress granule localization. The distance of AoPab1-EGFP foci from the hyphal tip is displayed using a box plot where the top and bottom of the box represent limits of the upper and lower quartiles, with the median being indicated by the horizontal line within the box. The whiskers show the highest and lowest reading within 1.5 times the interquartile range. The outliers are indicated by dots. The data were derived from three independent experiments with a total of 260 measurements in the WT and Δ*Aoso* strains, respectively. **P < 0.01; ***P < 0.001.

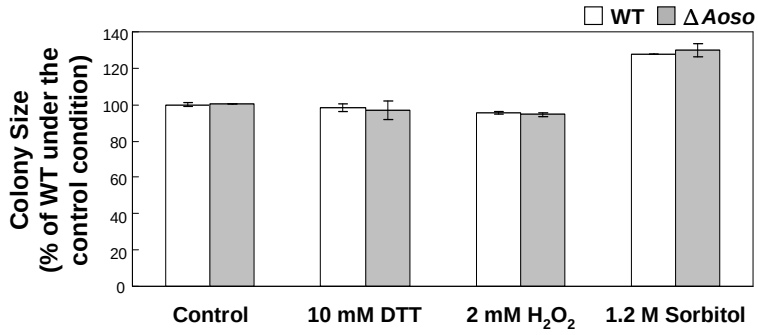

Figure 2-6. *Aoso* disruptant showed no growth defects in stress conditions. Approximately 10^3 conidia of wild-type and *Aoso* disruptant cells were spotted onto PD plates with or without 10 mM DTT, 2 mM H_2O_2, or 1.2 M sorbitol, and cultured at 30°C for 4 days. Colony diameters were compared to those of the wild-type strain under the control condition, which was set to 100%. Data represent the mean ± S.D. of three biological replicates.

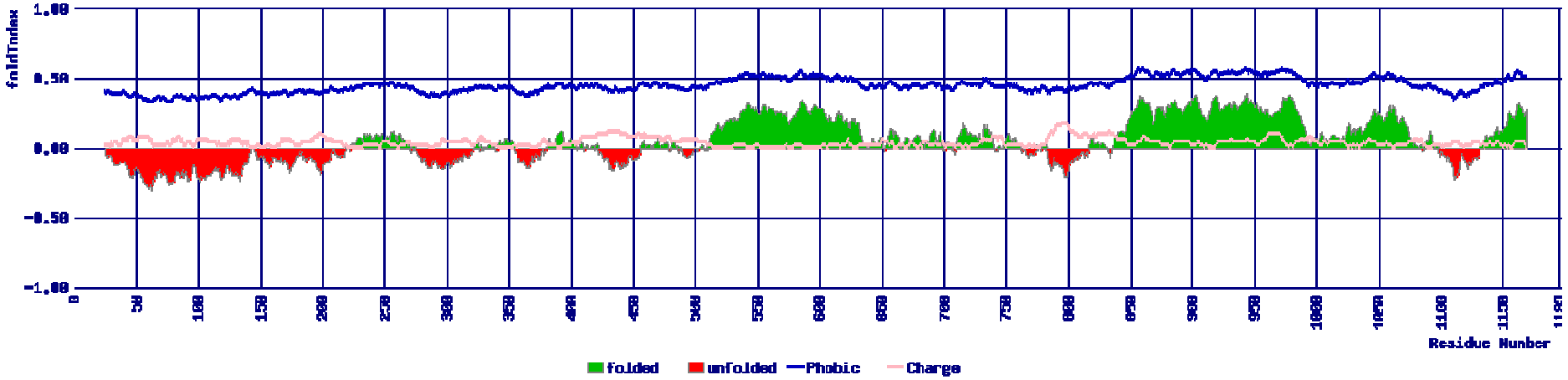

Figure 2-7. Disorder prediction of AoSO.

The primary sequences of AoSO were analyzed for natively ordered structure. The x axis corresponds to amino acid sequence displayed from N-terminus to C-terminus (left to right) of AoSO. The y axis indicates the predicted probability of disorder. The regions below the horizontal midline, filled in with red, are predicted to be natively unfolded based upon primary sequence information alone. The regions above the horizontal midline, filled in with green, are predicted to be natively folded, based upon primary sequence.

Chapter 3

Participation of autophagy in the clearance of stress granules under sustained heat stress

Introduction

Heat stress is a fundamental challenge for all microbes. The prominent physiological impact of heat stress is proteotoxicity: ambient temperature destabilizes cellular proteins (Zhang and Calderwood, 2011; Morano *et al*., 2012; Velichko *et al*., 2013; Verghese *et al*., 2012). Lethality could be the result from misfolding and the subsequent loss of function of one or more essential proteins. Alternatively, the accumulation of a significant number of misfolded polypeptides could have secondary consequences, such as an impairment of normal protein degradation by the ubiquitin-proteasome system (UPS) or the formation of toxic protein aggregates. The heat-shock response (HSR) is an ancient and highly conserved molecular response to disruptions of protein homeostasis that results in the repression of the protein biosynthetic capacity and transcriptional induction of a battery of cytoprotective genes encoding the heat shock proteins (HSPs) (Morano *et al*., 2012; Verghese *et al*., 2012; Velichko *et al*., 2013). Many HSPs function as molecular chaperones to protect thermally damaged proteins from aggregation, unfold aggregated proteins, and refold damaged proteins or target them for efficient degradation through proteasome or chaperone-mediated autophagy (CMA) (Kaushik and Cuervo, 2012; Saibil, 2013). In addition to HSR, to counteract the harmful effects from damaged proteins, intracellular degradation systems are invoked during stress. The two major mechanisms for intracellular degradation are the ubiquitin-proteasome system (UPS) and autophagy/lysosomal proteolysis. Autophagy is a conserved and tightly regulated process in eukaryotic cells for the bulk degradation of cytoplasmic components in the vacuole or lysosome to maintain cellular homeostasis (Reggiori and Klionsky, 2013). This pathway constitutes a major protective mechanism that allows cells to survive in response to multiple stressors (Swanlund *et al*., 2008; Kroemer *et al*., 2010; Zhang and Calderwood, 2011).

The formation of stress granules in response to stress for temporary storage of mRNAs is a conserved phenomenon in eukaryotes. However, little is known about the fate of stress granules. Through intensive microscopy analyses of stress granules in the preceding Chapters, it is interesting to find that under normal growth condition, vacuoles are usually not observed at the healthy hyphal tip in *A. oryzae*. When cells are exposed to stress, stress granules were often found to dock with vacuole-like structures at the hyphal tip (e.g. Figure 2-5A). Increased hyphal vacuolation has also been observed in nutrient-starved *A. oryzae* mycelia (Pollack *et al*., 2008). These observations suggest an increase in degradation/recycling activities in these regions of the mycelium during stress. As both autophagy pathway and stress granule formation are considered as an adaptive response when cells are exposed to stress, it raises a possibility that under sustained stress condition, where stress granule-associated mRNPs unable to return to translation, stress granules might be eliminated by autophagy to maintain cellular homeostasis. Therefore, the aim of Chapter 3 was to clarify whether under sustained heat stress, stress granules were degraded by autophagy.

Results

1. Colocalization of autophagosome and stress granules in cells subjected to heat stress

Stress granules were often found to dock with vacuole-like structures at the hyphal tip during stress (e.g. Figure 2-5A). Autophagy/lysosomal pathway is one of the two major systems for intracellular protein degradation in eukaryotes, and is known to be induced by various stress conditions (Swanlund *et al*., 2008; Kroemer *et al*., 2010; Zhang and Calderwood, 2011). These observations suggest a possibility that under sustained stress condition, stress granules are eliminated by autophagy to maintain cellular homeostasis and survival. To clarify it, EGFP-tagged marker protein was used to monitor autophagy by fluorescence microscopy. The ubiquitin-like protein Atg8p is conjugated to phosphatidylethanolamine and recruited to nascent autophagosomes, thus building part of the autophagosomal membrane (Shpilka *et al*., 2011; Stanley *et al*., 2013). Previously in our laboratory, a homolog of the *S. cerevisiae ATG8*, *Aoatg8*, was isolated and used as a specific marker of autophagy (Kikuma *et al*., 2006). Although nutrient depletion is the most potent known physiological inducer of autophagy, a variety of stress stimuli have been known to induce autophagy, including nutrient stress, ER stress, hypoxia, redox stress, mitochondrial damage, and heat stress (Swanlund *et al*., 2008; Kroemer *et al*., 2010; Zhang and Calderwood, 2011). Therefore, firstly several external stimuli were used to assess the induction of autophagy in cells expressing EGFP-AoAtg8 under control of the endogenous promoter (Figure 3-1). Under normal growth conditions, EGFP-AoAtg8 was detected as bright dots in the cytoplasm (Figure 3-1A), which are considered as phagophore-assembly site (PAS)-like structures of autophagosome nucleation. Exposing cells to heat stress, ER stress, and oxidative stress led to an induction of number and size of EGFP-AoAtg8 foci (Figure 3-1B, C, and D). Some of these foci

were found in the vicinity of vacuole-like structures.

To determine the relative localizations of EGFP-AoAtg8 and stress granules, AoPab1-mDsRed expressing plasmid pgCPaPab1DR (Figure 1-18A) was introduced into EGFP-AoAtg8 expressing strain. The generated strain co-expressing EGFP-AoAtg8 and AoPab1-mDsRed was examined after being exposed to 45°C for 10 min. EGFP-AoAtg8 cytoplasmic foci were colocalized with stress granules labeled with AoPab1-mDsRed (Figure 3-2) in cells exposed to heat stress. Since autophagy is a pathway for intracellular protein degradation, colocalization of stress granules with autophagy suggests that autophagy may be involved in the degradation of stress granules under sustained stress.

2. Heat stress induces the degradation of stress granule components

The protein degradative process is typically accelerated by environmental stresses. To investigate whether heat stress induces degradation of stress granule components, cells co-expressing AoPab1-3HA and AoSO-EGFP were exposed to heat stress for 0, 10, 30, and 60 min. The relative protein amounts of AoPab1-3HA and AoSO-EGFP were analyzed by immunoblotting. The levels of AoPab1-3HA in cells exposed to heat stress for different times revealed that AoPab1-3HA were decreased in a time-dependent manner, while the levels of α-tubulin were not changed (Figure 3-3). Additionally, AoSO-EGFP, another stress granule component identified in the Chapter 2, was also decreased in cell exposed to heat stress in a similar pattern (Figure 3-3). These results give a possibility that under sustained heat stress condition, stress granules were degraded.

3. Participation of autophagy in the degradation of stress granule component under sustained heat stress

To determine whether autophagy is involved in the degradation of stress granule components, an autophagy-defective mutant, *Aoatg8*-deletion strain was used for further analysis. Firstly, AoPab1-EGFP expressing plasmid pgDPaPab1E (Figure 1-3A) was introduced into the *Aoatg8*-deletion strain, and subcelluar localization of AoPab1-EGFP was analyzed (Figure 3-4). Stress granules were induced in the *Aoatg8*-deletion cells exposed to heat stress for 10 min. No significant difference of subcelluar localization of AoPab1-EGFP in wild-type and the *Aoatg8*-deletion cells was observed.

To compare the protein level of AoPab1 with that in Figure 3-1, AoPab1-3HA expressing plasmid pgCPaPab13HA (Figure 2-3A) was introduced into the *Aoatg8*-deletion strain. Protein amounts of AoPab1-3HA in cells exposed to heat stress were analyzed by immunoblotting (Figure 3-5 A and B). ~70% of AoPab1-3HA still remained in cells exposed to heat stress for 60 min. Comparing heat stress-induced degradation kinetics of AoPab1-3HA in the wild-type and *Aoatg8* disruptant cells, reveals that heat stress-induced decrease of AoPab1-3HA was inhibited in the *Aoatg8*-deletion strain (Figure 3-5C).

Discussion

Mutual regulation of TORC1, autophagy, and stress granules

Autophagy is a conserved and tightly regulated process for the bulk degradation of cytoplasmic components in the vacuole or lysosome to maintain cellular homeostasis (Reggiori and Klionsky, 2013). An increase of autophagosome labeled with EGFP-AoAtg8 was observed in cells exposed to heat stress, ER stress, and oxidative stress (Figure 3-1), suggesting an increase in autophagy-mediated degradation/recycling activities during stress. Autophagy is induced through inhibition of target of rapamycin complex 1 (TORC1) as an essential prosurvival pathway by a wide variety of stresses, including heat stress (Swanlund *et al*., 2008; Kroemer *et al*., 2010; Zhang and Calderwood, 2011). TORC1 is a central regulator of cell growth and metabolism in eukaryotes (De Virgilio and Loewith, 2006; Wullschleger *et al*., 2006). Under optimal growth conditions, TORC1 is activated at the vacuolar membrane and promotes protein synthesis and cell growth. On the other hand, TORC1 inhibits autophagy initiation by direct phosphorylation of Atg13p at several serine residues (Alers *et al*., 2012). The hyperphosphorylation prevents its binding to Atg1p and formation of Atg1p-Atg13p-Atg17p complex. In the absence of growth hormones, or during stress or starvation, TORC1 is released from vacuolar membrane and inactivated (Yan *et al*., 2012; Buchan et al., 2013). Inactivated TORC1 suppresses cell growth to reduce energy demand, and trigger autophagosome nucleation and elongation to enable stress adaptation and survival.

Stress granules are originally identified as a structure for post-transcriptional regulation of gene expression by temporary storage of mRNAs in response to stress (refer to the general introduction). Lines of recent evidence indicate that stress granules play a role as subcellular sites that coordinate signaling pathways involved in the stress response by sequestrating signaling molecules into stress granules (Arimoto

et al., 2008; Takahara and Maeda, 2012). The sequestration of TORC1 into stress granules inhibits its activity and protects cells from DNA damage during recovery from heat stress (Takahara and Maeda, 2012). Interestingly, TORC1 signaling also promotes translation initiation in part via eIF4E, eIF4G, and eIF2 (Wullschleger *et al*., 2006). Phosphorylation of eIF2α by the general control non-derepressible-2 (GCN2) results in the global translational arrest, and therefore the formation of stress granules. GCN2 is negatively regulated by TORC1 (Hinnebusch, 2005; Valbuena *et al*., 2012; Rødland *et al*., 2013). Furthermore, inactivation of TORC1 is probably required for activation of GCN2 in response to stress (Rødland *et al*., 2013). Thus, when environmental conditions repress TORC1 signaling, the resulting inhibition of translation initiation promotes stress granule formation, which in turn recruits and further inhibits TORC1 signaling. On the other hand, inactivated TORC1 leads to an activation of autophagy, which further clears stress granules under sustained stress. Observation of stress granules docked with vacuole-like structures (e.g. Figure 2-5A) and the colocalization of stress granules and autophagosomes (Figure 3-2) provide a spatially related support for the mutual interplay of TORC1 activity, autophagy, and stress granules.

Fates of stress granules

The formation of stress granules in response to stress for temporary storage of mRNAs is a conserved phenomenon in eukaryotes. However, little is known about the fate of stress granules. During recovery from stress, stress granules could be disassembled by dissociation of the interactions creating the larger aggregate (Buchan and Parker, 2009). mRNAs inside stress granules are targeted to P-bodies to be degraded (Sheth and Parker, 2003), or re-entry into polysomes to be translated (Brengues *et al*., 2005; Bhattacharyya *et al*., 2006). In the present study, I provided an

additional fate of stress granules under sustained stress. Colocalization of EGFP-AoAtg8 with stress granules suggests a functional interaction of autophagy and stress granules (Figure 3-2). Degradation of stress granule component AoPab1 was observed in cells exposed to heat stress for 60 min using immunoblotting (Figure 3-3), while this heat stress-induced degradation is greatly inhibited in an autophagy-defective mutant, *Aoatg8*-deletion strain (Figure 3-5). This result provides biochemical evidence that under sustained heat stress, stress granules are degraded at least partially through autophagy. More recently, a microscopy-based genetic screen of yeast genes that affected the dynamics of P-bodies and/or stress granules supports my results (Buchan *et al*., 2013). Mutations that disrupt autophagy, including Δ*ATG8*, Δ*ATG11*, Δ*ATG18*, Δ*MON1*, and Δ*MEH1*, give an increase in constitutive stress granules under normal growth condition. Additionally, disruption of *ATG15*, which is a vacuolar lipase that breaks down autophagic vesicles within the vacuole (Teter *et al*., 2001), results in the accumulation of Pab1p-GFP and Edc3p-mCherry in an intravacuolar compartment (IVC). These observations provide another mechanism regulating the clearance of these structures by targeting stress granules to the vacuole through autophagy.

A pathological hallmark of many neurodegenerative diseases such as Alzheimer's disease (AD), Parkinson's disease (PD), Huntington's disease (HD), amyotrophic lateral sclerosis (ALS), and prion diseases is the accumulation of mutant protein aggregates (Jucker and Walker, 2013; Takalo *et al*., 2013). For the narrow proteasome barrel precludes entry of oligomers/aggregates of mutant proteins, autophagy seems to be as the major route for protein aggregates clearance. These disease-related proteins have aggregate-prone prion-like domain as in many factors of stress granules and also P-bodies (Gilks *et al*., 2004; Yao *et al*., 2007; Reijns *et al*., 2008). Dysfunction of autophagy to remove these protein aggregates results in the pathogenesis of

neurodegenerative disorders (Banerjee *et al*., 2010; Nixon, 2013). More interestingly, colocalizations of classic stress granule markers and RNA with protein aggregates are observed in many neurodegenerative diseases (Ginsberg *et al*., 1998; Ito and Suzuki, 2011; Dewey *et al*., 2012; Wolozin, 2012; Li *et al*., 2013). Prolonged physiological stress or mutations in genes coding for stress granule associated proteins (Nonhoff *et al*., 2007; Johnson *et al*., 2009; Bosco *et al*., 2010; Elden *et al*., 2010; Liu-Yesucevitz *et al*., 2010; Ito and Suzuki, 2011; Moreno *et al*., 2012) lead to enhanced stress granule formation, which accelerates the pathophysiology of protein aggregation in neurodegenerative diseases. These observations raise a hypothesis that inappropriate formation or persistence of stress granules, or some related mRNP aggregate, might be related to the pathogenesis in these diseases (Buchan *et al*., 2013; Li *et al*., 2013). Even more, aggregation of these pathological proteins might be proceeded through the stress granule pathway (Wolozin, 2012). Furthermore, a recent study shows that stress granule markers are immunopositive with autophagy markers in neuronal cytoplasmic inclusions (Mori *et al*., 2013). These observations indicate the importance of stress granules and autophagy in the pathogenesis of neurodegenerative diseases. Thus, clearance of stress granules, which are large mRNA-protein aggregate complexes, by autophagy may be crucial for cell viability under sustained stress.

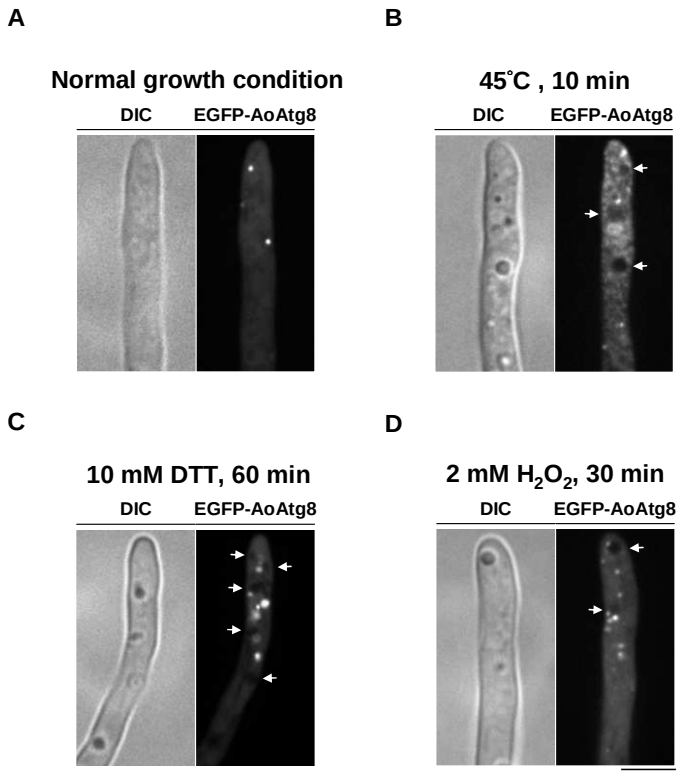

Figure 3-1. Subcellular localization of EGFP-AoAtg8 in cells exposed to heat stress, ER stress, and oxidative stress.

Approximately 10^4 conidia of cells expressing EGFP-AoAtg8 under control of the *amyB* promoter were grown in CD+Met medium at 30°C for 18 h before being exposed to various types of stress and the subcellular localization of EGFP-AoAtg8 was observed in normal growth condition (A), heat stress (45°C, 10 min) (B), ER stress (10 mM DTT, 60 min) (C), and oxidative stress (2 mM H_2O_2, 30 min) (D). White arrows indicate vacuole-like structures. Scale bar = 5 μm.

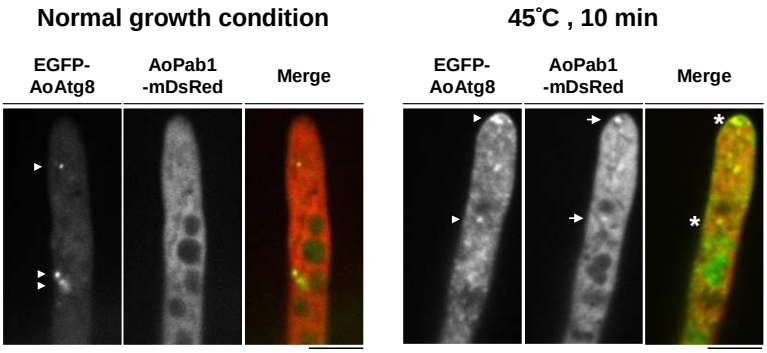

Figure 3-2. Colocalization of EGFP-AoAtg8 with AoPab1-mDsRed in response to heat stress.

EGFP-AoAtg8 and AoPab1-mDsRed were used as markers of autophagosome and stress granules, respectively. Approximately 10^4 conidia of cells were grown in CD medium at 30°C for 18 h before being exposed to 45°C for 10 min. Arrowheads indicate autophagosome, and arrows indicate stress granules. Colocalization of stress granules and autophagosomes are indicated by asterisks. Scale bars = 5 μm.

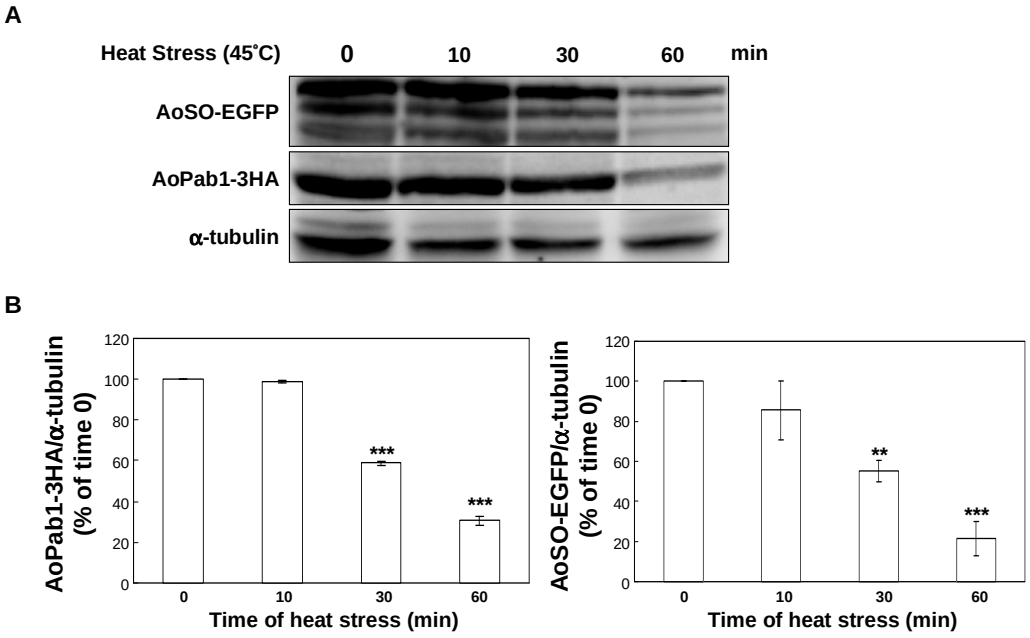

Figure 3-3. Time-dependent decrease of stress granule components AoPab1-3HA and AoSO-EGFP under sustained heat stress.

(A) Cells were exposed to heat stress for 0, 10, 30, or 60 min. The levels of AoPab1-3HA and AoSO-EGFP were detected by immunoblotting. (B) The quantitative results from three independent experiments are shown as means ± standard deviations (SD) compared to time 0. ** p value < 0.01; *** p value < 0.001.

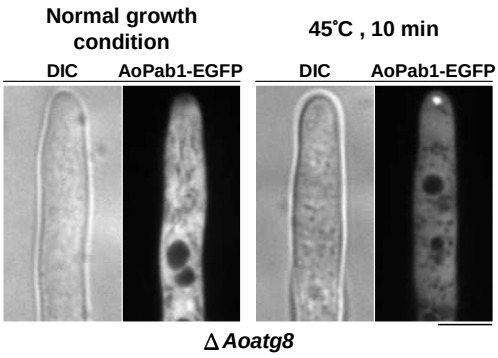

Fig. 3-4. Formation of stress granules in response to heat stress in the autophagy defective mutant.

Heat stress-induced stress granule formation in the *Aoatg8*-deletion mutant (Δ*Aoatg8*) was detected using AoPab1-EGFP as a marker. Mycelia of *Aoatg8*-deletion cells expressing AoPab1-EGFP were collected from the surface of colonies using a toothpick and grown in CD+Met medium at 30°C for 18 h before being exposed to 45°C for 10 min. Scale bar = 5 μm.

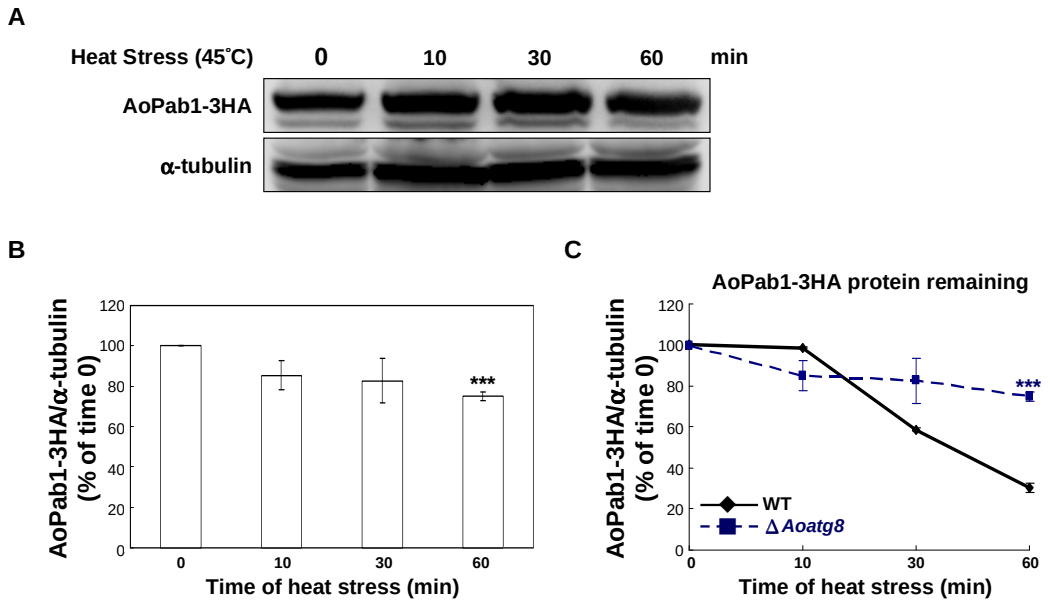

Figure 3-5. Heat stress-induced degradation of stress granule component AoPab1-3HA was inhibited in an autophagy-defective strain.

(A) Cells were exposed to heat stress for 0, 10, 30, or 60 min. The levels of AoPab1-3HA in the *Aoatg8* disruptant cells were detected by immunoblotting. (B) The quantitative results from three independent experiments are shown as means ± standard deviations (SD) compared to time 0. (C) Heat stress-induced degradation kinetics of AoPab1-3HA in the wild-type and *Aoatg8* disruptant cells in sustained heat stress. Intensity of the AoPab1-3HA bands in the wild-type (Figure 3-1A) and *Aoatg8*-deletion cells (Figure 3-5A) were quantified and calculated as a percentage of the intensity of the band at time zero for each treatment. The significance is given at time 60 by comparing the relative AoPab1-3HA levels in the wild-type and *Aoatg8*-deletion cells. *** p value < 0.001.

Chapter 4

Post-translational modifications of stress granule component AoPab1 in response to heat stress

Introduction

The cap-binding complex eIF4F consists of the m^7GTP cap-binding protein eIF4E, the DEAD-box RNA helicase eIF4A and the scaffolding protein eIF4G (Figure 0-2) (Klann and Dever, 2004; Jackson *et al*., 2010). eIF4G also binds to PABP and the 43S component eIF3. Through the interaction of eIF4G and PABP brings the 5′ and 3′ ends of a mRNA in close physical proximity. This ‘closed-loop’ conformation enhanced translation initiation by increasing ribosome recruitment through ATP-dependent helicase activity of eIF4A and also protecting mRNAs from deadenylation, decapping, and degradation (Klann and Dever, 2004; Fabian *et al*., 2010; Jackson *et al*., 2010). The interaction of PABP and eIF4G further increase the poly(A)-binding affinity of PABP and the binding affinity of eIF4E for the 5’ cap structure, resulting in the mutual stabilization of eIF4E and PABP to their respective target regulatory elements (Le *et al*., 1997; Wei *et al*., 1998). The functional interaction between the cap and the poly(A) tail is repressed when cells exposed to stress (Gallie and Tanguay, 1994). Several eIFs have been shown to be phosphorylated or dephosphorylated following environmental stress (Duncan *et al*., 1987; Duncan and Hershey, 1989; Gallie *et al*., 1997). Dephosphorylation of eIF4E following heat stress is concomitant with reduced eIF4F binding to the cap and protein synthesis activity (Duncan *et al*., 1987; Duncan and Hershey, 1989; Lamphear and Panniers , 1990; Lamphear and Panniers , 1991). Post-translational modification (PTM) is crucial for regulating the functions of many eukaryotic proteins. Modulation of protein through PTM provides an appropriate mechanism to ensure coordinated temporospatial and immediate regulation of protein. PABP is present in multiple post-translational modified isoforms in yeast, sea urchin, plant and mammalian cells (Drawbridge *et al*., 1990; Gallie *et al*., 1997; Le *et al*., 2000; Ma *et al*., 2006). Precise PTMs of PABPs have been identified in recent studies. Mammalian PABP has

extensive dynamic PTMs, including lysine acetylation, lysine methylation, arginine methylation and the unusual methylation of aspartic and glutamic acids (Brook *et al*., 2012). Pab1p in *S. cerevisiae* also shows the presence of lysine acetylation, serine phosphorylation, and glutamate methylation (Low *et al*., 2013). The function of these modifications is largely unknown; however, phosphorylation has been implicated in the regulation of its RNA binding and/or protein interactions (Le *et al*., 2000; Brook *et al*., 2012). These observations suggest that post-translational modification of PABP (and its interacting proteins) regulates the functional interaction between the cap and the poly(A) tail and therefore the regulation of gene expression.

PABP is a central regulator of mRNA translation and stability and is a core component of stress granules. In order to coordinate its multi-functions and to rapid response to stress, PABP is considered to be dynamically regulated by PTMs. Although PTMs of PABP have been identified in yeast and mammalian cells (Brook *et al*., 2012; Low *et al*., 2013), PTMs of PABP in response to stress have not been reported. Therefore the aim of Chapter 4 was to identify and map PTMs of AoPab1 in response to heat stress.

Results

1. AoPab1 is subjected to extensive post-translational modifications

To elucidate whether AoPab1 is post-translationally modified, lysates from AoPabl-3HA expressing cells exposed to heat stress for 0, 10 or 30 min were resolved on two-dimensional SDS/PAGE (2D-PAGE) and analyzed using anti-HA antibody. The predicted pI of AoPabl-3HA is 5.45. In unstressed cells, AoPab1-3HA was detected as a continuing band in a range of its predicted pI and reduced pI, indicating multiple PTM forms (Figure 4-1A). In addition to a portion of isoforms of higher pI (basic isoforms), highly acidic isoforms appeared in cells exposed to heat stress for 10 min, and were not observed after exposure of heat stress for 30 min. Exposure to heat stress for 30 min induced a broad distribution of AoPab1 isoforms from pH 3-10 with highly basic species. Basic isoforms appeared after short exposure to heat stress (10 min) and highly basic isoforms appeared later (30 min), suggesting that AoPab1 was modified to become basic in response to heat stress. Furthermore, lysates form cells treated with 2 mM H_2O_2 for 30 min were also resolved on 2D-PAGE and analyzed using anti-HA antibody (Figure 4-1B). The highly basic isoforms of AoPab1 seen in cells exposed to heat stress for 30 min was not observed in cells treated with oxidative stress, suggesting the stress-specific modifications of AoPab1.

2. Identification of post-translational modifications in AoPab1 in response to heat stress

To identify PTMs in AoPabl, AoPabl-3HA was immunoprecipitated from unstressed cells or cells exposed to heat stress for 10 and 30 min, and separated using 10% SDS-PAGE. Coomassie-Blue-stained protein bands of AoPab1-3HA were excised and digested with trypsin. Trypsin-digested peptide mixtures were separated by high-performance liquid chromatography (HPLC) using 75 μm column with flow

rate at 300 nl/min. Profiles of the respective abundances of trypsin-digested peptides are indicated by the HPLC chromatogram in Figure 4-2. Peptides eluted from HPLC column were fragmented by a process called collision-induced dissociation (CID) and MS/MS spectra were acquired for each fragmented peptide. LC-MS/MS analysis of trypsinized peptides resulted in ~60% sequence coverage of AoPab1. PTMs identified in AoPab1 from cells exposed to heat stress for 0, 10, and 30 min are indicated in Figure 4-3, Figure 4-4, and Figure 4-5, respectively. PTMs of AoPab1 in three experimental conditions are summarized in Figure 4-6, which shows that these PTMs distribute throughout all functional domains of AoPab1, with an exception of Q/G/P-rich region. Conserved sites among PABPs are emphasized using red color. A total of 23 PTMs were identified at 21 residues in unstressed cells, including lysine acetylation, lysine methylation, lysine dimethylation, serine phosphorylation, and threonine phosphorylation (Figure 4-3 and Figure 4-6). Compared to PTMs found in AoPab1 from unstressed cells, changes were found at 12 residues in cells exposed to heat stress for 10 min (Figure 4-4 and Figure 4-6). These included dephosphorylation of threonine, demethylation and dedimethylation of lysine, lysine acetylation, lysine methylation, lysine dimethylation, serine phosphorylation, threonine phosphorylation, and a novel lysine trimethylation at Lys^{407} only found in cells exposed to heat stress for 10 min. Compared to PTMs found in AoPab1 in unstressed cells, changes were found at 11 residues in cells exposed to heat stress for 30 min, including dephosphorylation of threonine, demethylation and dedimethylation of lysine, lysine methylation, lysine dimethylation, serine phosphorylation, threonine phosphorylation, and a novel tyrosine phosphorylation at Tyr^{233} only found in cells exposed to heat stress for 30 min (Figure 4-5 and T Figure 4-6). Furthermore, comparing PTMs in AoPab1 from cells exposure to heat stress for 10 min and 30 min revealed that excluding constant modifications appeared in three conditions, the majority of these

residues were modified by different PTMs (17/19), suggesting the dynamic changes in PTMs during the period of heat stress.

One dimethylation was detected at Lys^{215}, which locates in the predicted bipartite nuclear localization signal (NLS) of position 205-219. However, no alteration of this modification was observed in unstressed cells or cells exposed to heat stress. In consistent with this, microscopic analyses in the previous Chapters revealed no localization difference of AoPab1 in nucleus-cytoplasm shuttling after cells were exposed to heat stress (and also other stresses). Furthermore, PABPs are characterized by four conserved RRMs in the N-terminus, to find any link of these PTMs to the primary sequence, distribution of PTMs in four RRMs was compared (Figure 4-7). However, no significant link was found.

A wide variety of stress stimuli, including heat stress, rapidly increase protein modification by O-linked-N-acetylglucosamine (O-GlcNAc) (Zachara et al., 2004). Blocking O-GlcNAc modification, or reducing it, renders cells more sensitive to stress and results in decreased cell survival; and increasing O-GlcNAc levels protects cells. Additionally, O-GlcNAc modification of the translational machinery has reported to be required for stress granule formation (Ohn et al., 2008). However, O-GlcNAc as well as ubiqutin modifications were not detected in AoPab1 in all conditions.

3 *In silico* prediction of AoPab1 phosphorylation sites

The phosphorylation sites were further analyzed as potential phosphorylation sites using an *in silico* method employing neural network predictions for serine, threonine and tyrosin phosphorylation sites in eukaryotic proteins (NetPhos 2.0) (Blom *et al.*, 1999) and predictions of kinase specific eukaryotic protein phosphorylation sites (NetPhosK 1.0) (Blom *et al.*, 2004). The predicted

phosphorylation sites and putative kinases were summarized in Figure 4-8. Putative highly phosphorylatable AoPab1 residues using generic phosphorylation prediction are indicated by red colored letters, which are dispersed throughout the amino acid sequence, with an exception of Q/G/P-rich region, where the phosphorylation potential is remarkably low, suggesting that phosphorylation may not be important for the functional regulation of Q/G/P-rich region. Furthermore, RRM4 has more predicted phosphorylation sites, suggesting that phosphorylation may be important for the regulation of RRM4 activity. The putative kinases predicted using kinase-specific prediction were indicated by blue colored letters at a given site. The prediction score are shown in Table 4-1. Some of phosphorylation sites identified by LC-MS/MS were predicted with the corresponding kinases. Ser^{165}, Thr^{230}, and Thr^{260} are the putative phosphorylation sites of protein kinase C (PKC). Ser^{442} is a putative phosphorylation site of cyclin-dependent kinase CDC2 (cell division cycle protein 2) and casein kinase 2 (CKII). Ser^{476} is a putative phosphorylation site of DNA-dependent protein kinase, ATM (ataxia-telangiectasia mutated) protein kinase, protein kinase A (PKA), and protein kinase G (PKG). Ser^{742} is a putative phosphorylation site of CKII. Among these sites, the phosphorylation at Ser^{165}, Thr^{230}, and Thr^{260}, predicted to be the PKC phosphorylation sites with high potential (Table 4-1), were changed in response to heat stress, suggesting an important role of PKC with its counteracting phosphatase in the regulation of AoPab1 in response to heat stress.

Discussion

1. AoPab1 is dynamically regulated by extensive PTMs

The formation of stress granules in response to stress is accompanied by remodeling mRNAs translated from polysomes into non-translating state and forming dense aggregates with various RNA-binding proteins and traslational regulatory factors. During this process, intensive protein-RNA and/or protein-protein interactions are necessary. PABP is a central regulator of mRNA translation and stability and is a core component of stress granules, and during the formation of stress granules, PTMs may play a role in the rapid regulation of its RNA binding and/or protein interactions in response to sudden changes in the environment.

In 2D-SDS/PAGE and the following immunoblotting, AoPab1 was detected as a continuing band in unstressed cells, indicating that AoPab1 was extensively post-translationally modified under normal growth condition (Figure 4-1A). This result is consistent with PABPs reported in other species (Drawbridge *et al*., 1990; Le *et al*., 2000; Brook *et al*., 2012). PABP is a multifunctional protein that regulates different facets of post-transcriptional gene expression. The complex PTMs may be required for the modulation of its RNA binding and/or protein interactions and contribute to coordinating various functions in different physiological conditions. The dynamic regulation of PABP PTMs during cell cycle is observed in mammalian cells (Brook *et al*., 2012). In *A. oryzae*, the distribution of AoPab1 isoforms was changed in response to heat stress, although no alteration in the isoform state of PABP following heat stress is observed in plant cells (Le *et al*., 2000). These observations suggest that different biological processes/stimuli can regulate PTM status of PABPs. Basic isoforms of AoPab1 appeared after exposure to heat stress for 10 min, and highly basic isoforms appeared only in the prolonged heat stress (Figure 4-1A). These highly basic isoforms were not observed in cells treated with oxidative stress (Figure 4-1B),

suggesting the stress-specific regulation of PTMs in AoPab1.

Reduced pI isoforms of metazoan PABP revealed in 2D-PAGE have been interpreted as indicative of potential phosphorylation (Drawbridge *et al*., 1990; Ma *et al*., 2006). Acidic isoforms of AoPab1 were observed in cells treated with or without heat stress. In agreement with it, phosphorylation was also detected in AoPab1 in LC-MS/MS analyses, although phosphorylation was located at different residues (Figure 4-3, 4-4, 4-5, and Table 4-1). Additionally, highly acidic isoforms of AoPab1 appeared in cells exposed to heat stress for 10 min, but not in unstressed cells or cells exposed to heat stress for 30 min (Figure 4-1A). However, the nature of these highly acidic isoforms and whether they were induced for the acute response to stress, such as stress granule formation, remain to be further confirmed.

2. Identification of PTMs in AoPab1

To identify specific PTMs in response to heat stress, AoPab1 from unstressed cells or cells exposed to heat stress for 10 and 30 min were analyzed using LC-MS/MS. A total of 36 PTMs were identified at 30 residues in three experimental conditions, including lysine acetylation, lysine methylation, lysine dimethylation, lysine trimethylation, and serine, threonine and tyrosine phosphorylation. It should be noted that the LC-MS/MS analyses most likely reflect the overall modification status of AoPab1 in a cell population. Indeed, mammalian PABP is under dynamic regulation of PTM during cell cycle (Brook *et al*., 2012). Furthermore, for trypsinized peptides only resulted in ~60% sequence coverage of AoPab1 in LC-MS/MS analyses, and PTMs in the remaining regions can not be detected in the present study. Finally, LC-MS/MS analyses here were from samples treated without phosphopeptide enrichment. There are some difficulties with the analysis of phosphopeptides. One is the so-called neutral loss phenomenon, whereby the phosphate group is dissociated

from the phosphopeptide, therefore signals from the target phosphopeptides are difficult to detect. Another one is the significant decrease in peptide detection sensitivity due to phosphorylation modification. Consequently, it is often difficult to observe phosphopeptides in protein enzyme digests. Therefore, to achieve higher resolution and accuracy for detection of phosphorylation, phosphopeptide enrichment should be included in sample preparation prior to analysis by mass spectrometry.

Phylogenetic analyses of PABPs in different eukaryotes reveals that after the early gene duplication event each RRM appears to have evolved independently, suggesting that divergences between the four RRMs could impart differences in RNA binding affinities and specificities (Burd *et al*., 1991; Birney *et al*., 1993). An alignment of four RRMs of AoPab1 marked with identified PTMs suggests that PTMs are regulated individually in RRM domains of AoPab1 (Figure 4-7). Notably, trimethylation was identified only in cells exposed to heat stress for 10 min at Lys^{407}, which is located at the intervening region of RRM4, suggesting that the role of trimethylation at Lys^{407} is specific to rapidly regulate RRM4 in response to stress.

3. Methylation and acetylation of lysine

Protein methylation is the second most common posttranslational modification after phosphorylation, mainly at the ε-amine group of lysine and the ϖ or δ guanidine nitrogen of arginine. However, such modification also occurs at other sites in proteins including histidine, glutamate, glutamine, asparagine, D-aspartate/L-isoaspartate, cysteine, and N-terminal and C-terminal residues (Clarke and Tamanoi, 2006).

The most known protein substrates of KMTs are histone proteins. Methylation of histone tails is found at the surface of the nucleosome and is recognized by protein interaction domain species that lead to transcriptional activation or repression (Black *et al*., 2012). Methylation is also found in non-histone proteins (Zhang *et al*., 2012;

Clarke, 2013). In *S. cerevisiae*, with the exception of cytochrome c, all of non-histone proteins modified at lysine residues are involved in translation, including ribosomal proteins, elongation factors, and translational release factors (Clarke, 2013). Interestingly, PABPs are also key regulators in protein translation. LC-MS/MS analyses reveal that AoPab1 is extensively and dynamically modified by lysine methylation (Figures 4-3, 4-4, 4-5, and 4-6). Methylation of PABP is also identified in mammalian cells. Although methylation does not affect the overall charge of protein, it does increase the hydrophobicity and basicity of the lysine residue (Rice *et al*., 2002), resulting in the change of protein-protein and/or protein-nucleic acid interactions. Although the functional significance of lysine methylation in PABPs is still unknown, these observations suggest that lysine methylaton may be important in the regulation of PABPs, and/or the formation of stress granules.

Lysine acetylation has emerged as a major posttranslational modification for histones. In addition to histones, lysine acetylation is now known to occur in over 80 transcription factors, many other nuclear regulators, and various cytoplasmic proteins (Glozak *et al*., 2005), involved in the regulation of different cellular processes, such as transcription, DNA repair, chromatin remodeling, cell cycle, RNA splicing, energy metabolism, endocytosis, cytoskeletal dynamics, apoptosis, nuclear import, protein folding, autophagy, and other cellular signaling (Matthias *et al*., 2008; Yang and Seto, 2008).

Acetyl group neutralizes the charge on lysine residue at physiological pH, thus altering the charge distribution. Acetylation has been implicated in dramatically altering the pI of mammalian PABP (Brook *et al*., 2012). Acetylation of AoPab1 is therefore thought to decrease the interaction with negative charged molecules, and influence its RNA and/or protein interactions.

4. Phosphorylation of serine/threonine/tyrosine

Phosphorylation is a very common posttranslational modification event known to modulate a wide range of biological responses. Beyond the regulation of protein activity, the interrelation of phosphorylation with other posttranslational mechanisms is responsible for the control of diverse signaling pathways, such as a competition of phosphorylation with O-GlcNAc modification at the same residue. The multiple phosphorylated PABP has been reported in yeast, sea urchin, plant and mammalian cells (Drawbridge *et al*., 1990; Gallie *et al*., 1997; Le *et al*., 2000; Ma *et al*., 2006). Kinases responsible for multiple phosphorylation of PABP are unknown; however, treating cells with a specific inhibitor of mitogen-activated protein kinase kinase-2 (MKK-2) reduces the phosphorylation of PABP in mammalian cells (Ma *et al*., 2006). MKK-2 is the upstream regulator of MAPKs and extracellular signal-regulated kinase 1/2 (ERK1/2), which are known to regulate protein synthesis by phosphorylating translational apparatus (Scheper *et al*., 2001; Roux and Blenis, 2004). The ability of PABP to bind poly(A) and eIF4G can be modulated by phosphorylation (Gallie *et al*., 1997; Le *et al*., 2000). Hyperphosphorylated PABP interacts more efficiently with eIF4G than its hypophosphorylated form. The interaction with eIF4G further enhances the binding affinity of PABP to poly(A) (Le *et al*., 1997; Le *et al*., 2000). Phosphorylation was also detected at several residues in AoPab1. Combining LC-MS/MS analyzes and *in silico* prediction of AoPab1 phosphorylation sites, PKC and its counteracting phosphatase are suspected to be involved in the post-translational regulation of AoPab1 in response to heat stress (Figure 4-7, Table 4-1, and Table 4-2). PKC is a serine/threonine kinase conserved among eukaryotes. In mammalian cells, the 11 members of the PKC family are divided into three groups: (1) the conventional PKCs (cPKC-α, -βI, -βII, -γ), which are regulated by calcium and diacylglycerol; (2) the calcium-independent but diacylglycerol-dependent novel PKCs

(nPKC-δ, -ε, -η, -θ); (3) the atypical PKCs (aPKC-ζ, -ι/λ), which are unresponsive to diacylglycerol and calcium and, in contrast to the cPKCs and nPKCs, do not respond to phorbol esters (for reviews, see Newton, 1997; Mochly-Rosen *et al*., 2012). The PKC-μ is distinctive from the other PKCs and shows features characteristic of the Ca^{2+}-calmodulin-dependent protein kinase family (Newton, 1997; Mochly-Rosen *et al*., 2012). In contrast to the mammalian PKC superfamily, Pkc1p is the only protein of this family in *S. cerevisiae*, functioning mainly in cell wall integrity (CWI) pathway, and also in polarity establishment, cell-cycle control, regulation of oligosaccharyl transferase, and control of chitin synthase distribution (Levin, 2011). PKCs have been indentified and characterized in *Aspergillus* species, including *A. niger*, *A. nidulans*, and *A. oryzae* (Morawetz *et al*., 1996; Mizutani *et al*., 2004; Herrmann *et al*., 2006). Apart from CWI pathway, PKCs also play other roles in filamentous fungi. Our laboratory has previously shown the role of PKC in the multimerization and proper localization of Woronin body protein in *A. oryzaze* (Juvvadi *et al*., 2007). In *A. nidulans*, PKC is involved in the suppression of apoptosis and in polarity establishment under heat stress (Katayama *et al*., 2012). As shown in the Chapter 2, heat stress induces the rapid occlusion of septal pores by localization of AoSO. It is known that *S. macrospora* Pro40, the AoSO homolog, partially associates with Woronin bodies, and *N. crassa* SO contributes to the sealing efficiency of pores plugged by Woronin bodies after hyphal injury (Engh et al., 2007; Fleißner and Glass, 2007). Collectively, these observations support that PKC is implicated in the heat stress response in *A. oryzaze*. However, whether AoPab1 is phosphorylated by PKC and how PKC regulates its function in response to heat stress remains to be elucidated.

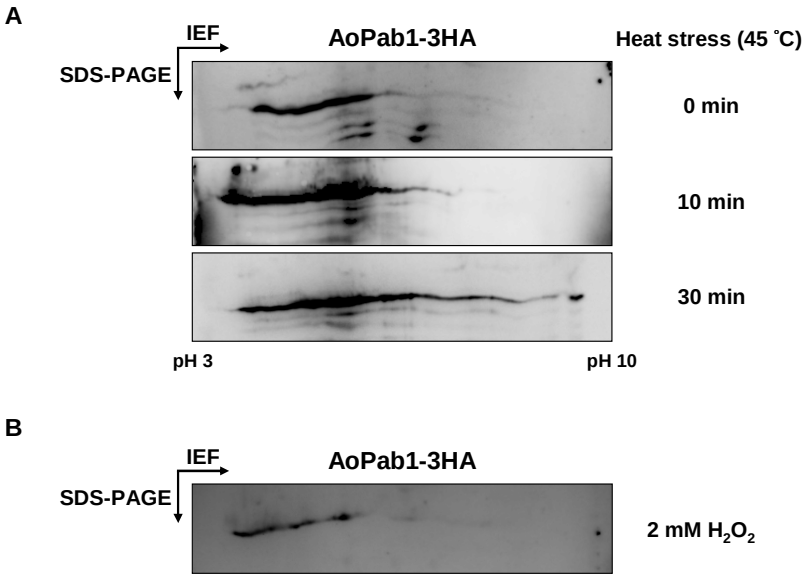

Figure 4-1. Two-dimensional gel electrophoresis/immunoblotting analysis of AoPab1.

(A) 20 μg of total cell extracts from AoPab1-3HA expressing cells exposed to heat stress for 0, 10 or 30 min were resolved in the first dimension using an IEF tip with pH 3-10 and a 10% SDS/PAGE for the second dimension. AoPab1 was revealed using anti-HA antibody. (B) Lysates from cells treated with 2 mM H_2O_2 for 30 min were analyzed as described in (A).

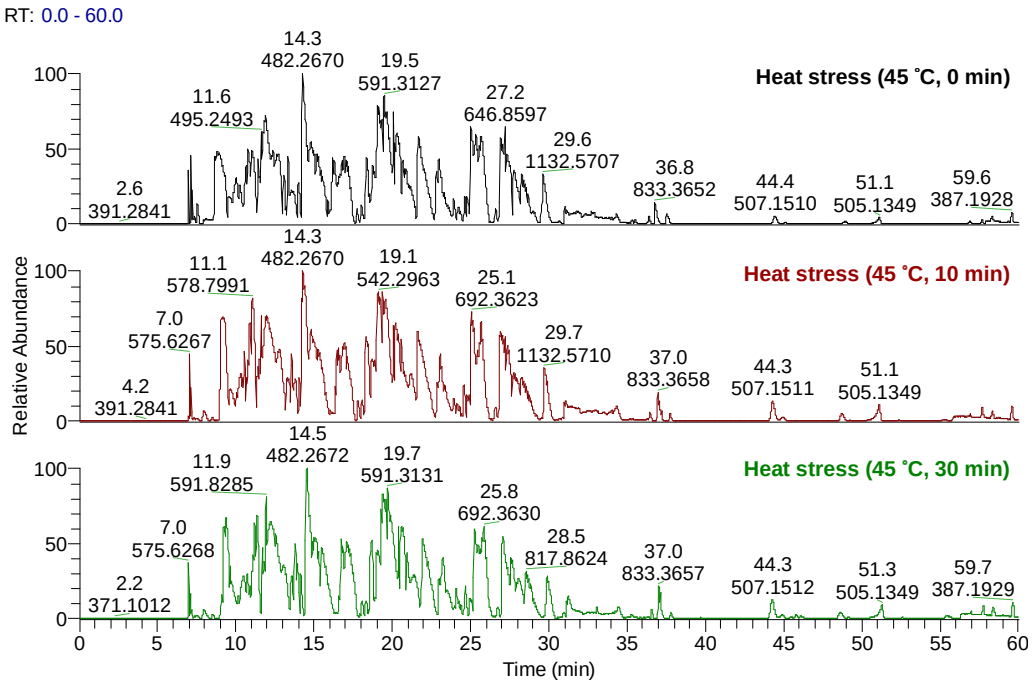

Figure 4-2 HPLC spectra of trypsinized AoPab1-3HA from cells exposed to heat stress for 0 (top), 10 (middle), and 30 (bottom) min.

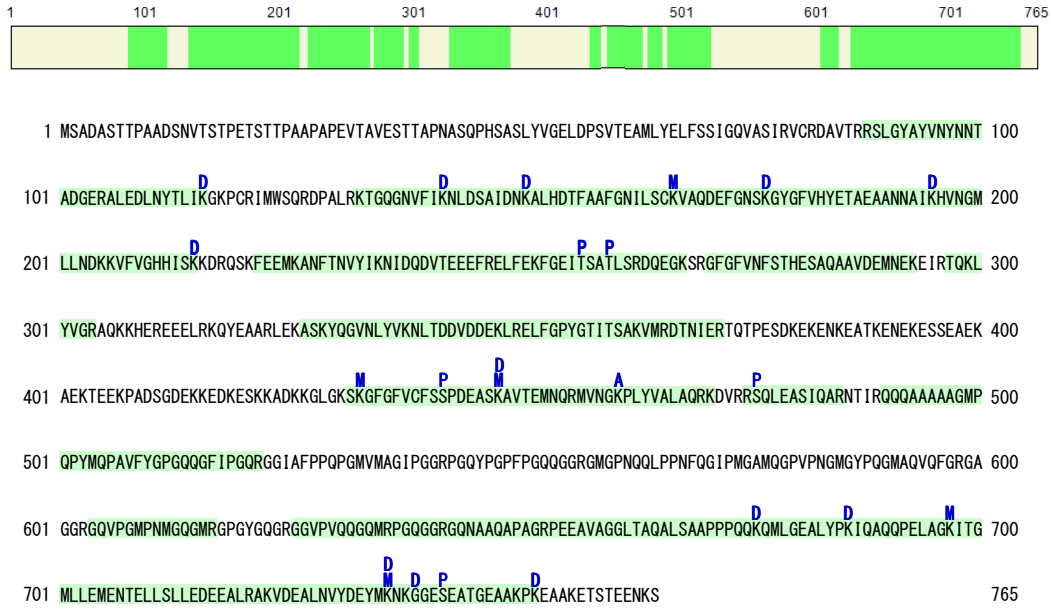

Figure 4-3. PTMs identified in AoPab1 form unstressed cells.

The upper panel represents the full sequence of AoPab1. The filled (green) sections show the relative portions of trypsinized peptides identified in LC-MS/MS analysis. Trypsinized peptides resulted in ~60% sequence coverage of AoPab1. A: Acetylation; D: Dimethylation; M: Methylation; P: Phosphorylation.

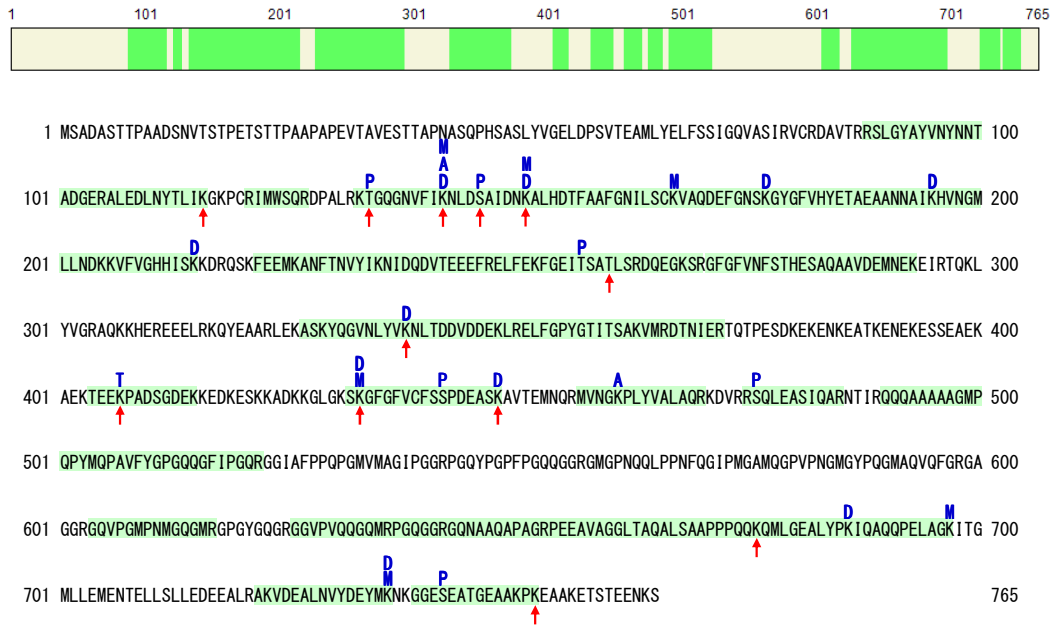

Figure 4-4. PTMs identified in AoPab1 form cells expose to heat stress for 10 min.

The upper panel represents the full sequence of AoPab1. The filled (green) sections show the relative portions of trypsinized peptides identified in LC-MS/MS analysis. Trypsinized peptides resulted in ~60% sequence coverage of AoPab1. A: Acetylation; D: Dimethylation; M: Methylation; P: Phosphorylation. Red arrows indicate amino acid sites where modifications are different from those in unstressed cells.

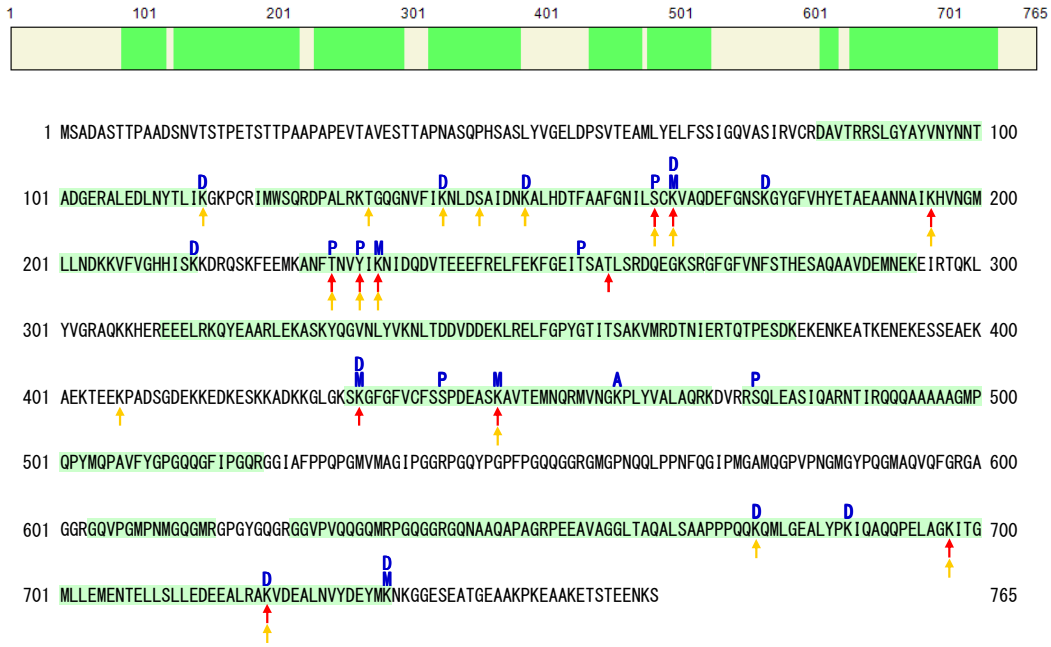

Figure 4-5. PTMs identified in AoPab1 form cells expose to heat stress for 30 min.

The upper panel represents the full sequence of AoPab1. The filled (green) sections show the relative portions of trypsinized peptides identified in LC-MS/MS analysis. Trypsinized peptides resulted in ~60% sequence coverage of AoPab1. A: Acetylation; D: Dimethylation; M: Methylation; P: Phosphorylation. Red and yellow arrows indicate amino acid sites where modifications are different from those in unstressed cells and cells expose to heat stress for 10 min, respectively.

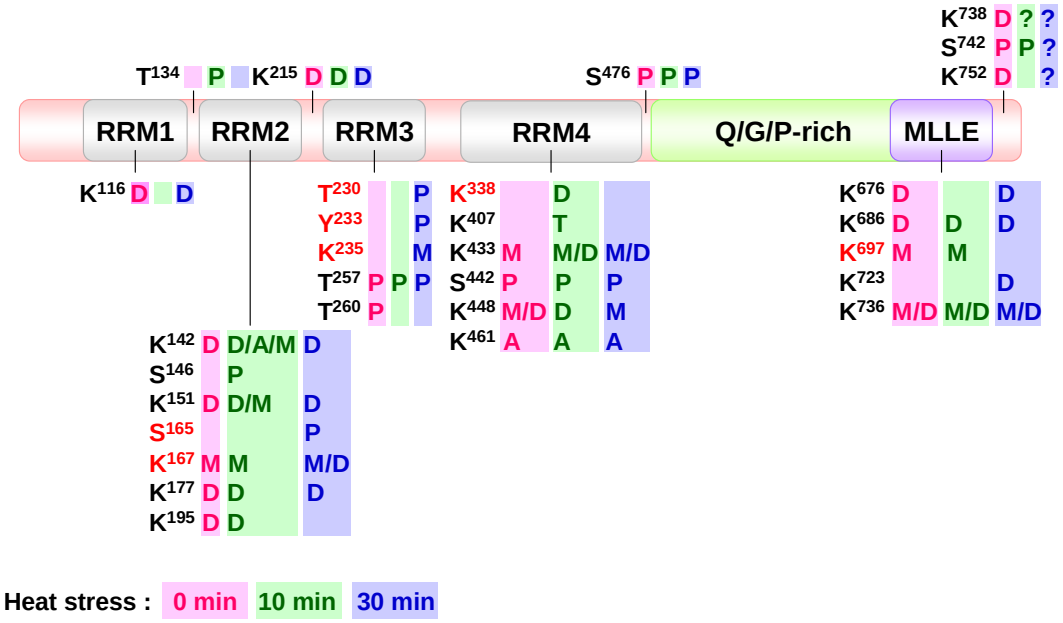

Figure 4-6. PTMs of AoPab1 identified in cells treated with heat stress for 0, 10, and 30 min.

Diagrammatic representation of the domain arrangement of AoPab1 is shown in middle. RRM1-4: RNA binding domains; Q/G/P-rich: Glutamine/Glycine/Proline-rich region; MLLE: mademoiselle domain. Amino acid residues that are conserved among Pab1 orthologs are emphasized using red color. PTMs identified in cells treated with heat stress for 0, 10, and 30 min are colored pink, green, and blue, respectively. A: Acetylation, D: Dimethylation, M: Methylation, P: Phosphorylation, T: Trimethylation.

A

B

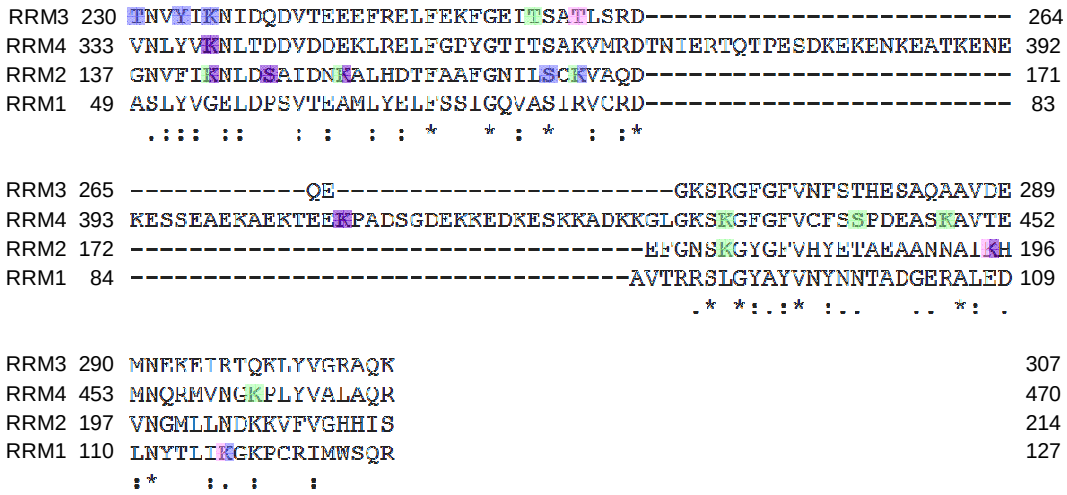

Figure 4-7. A sequence alignment of four RRMs of AoPab1 marked with identified PTMs.

(A) Diagrammatic representation of the domain arrangement of AoPab1. RRM1-4: RNA binding domains; Q/G/P-rich: Glutamine/Glycine/Proline-rich region; MLLE: mademoiselle domain. (B) A Sequence alignment of four RRMs of AoPab1. Pink, blue, and purple color indicate amino acids sites where specific moifications appear in unstressed cells, cells exposed to heat stress for 10 min, and for 30 min, respectively. Green color indicates amino acids sites where modifications appear in all three conditions.

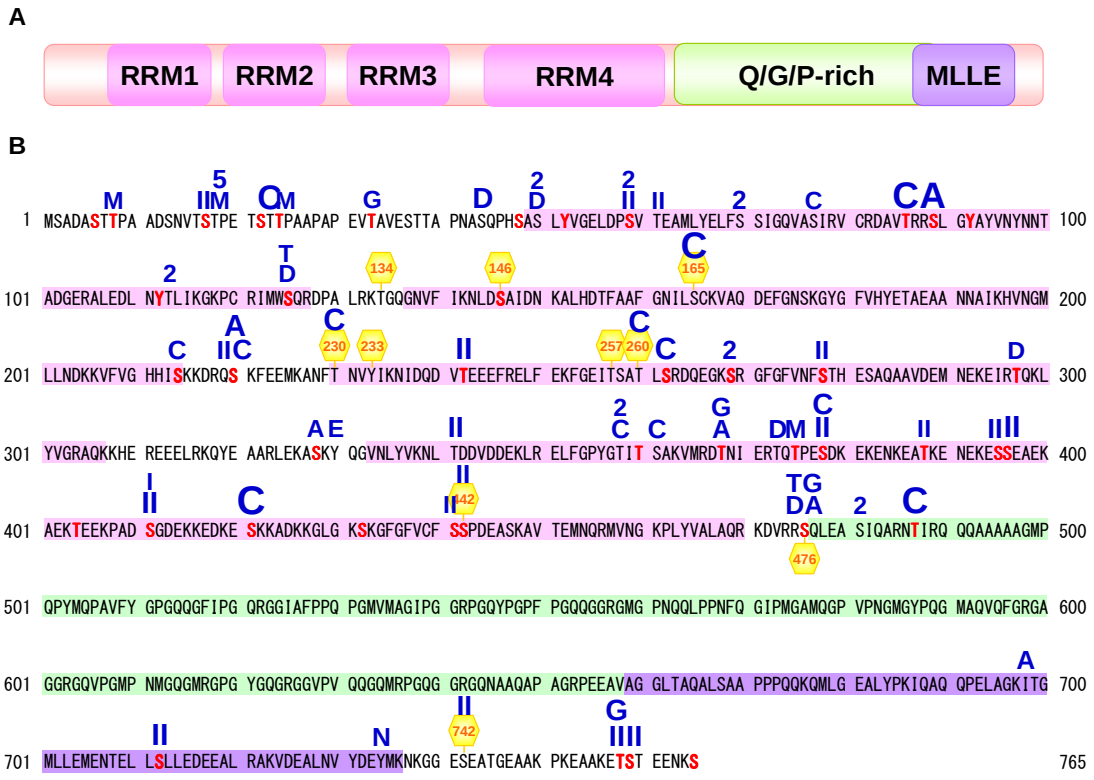

Figure 4-8. A sequence alignment of four RRMs of AoPab1 marked with identified PTMs.

(A) Diagrammatic representation of the domain arrangement of AoPab1. RRM1-4: RNA binding domains; Q/G/P-rich: Glutamine/Glycine/Proline-rich region; Mlle: mademoiselle domain. (B) An *in silico*-based prediction approach was used for the analysis of phosphorylation sites within the primary amino acid sequences of AoPab1. Red colored-letters indicate the phosphorylation sites predicted by the NetPhos program which evaluates serine, threonine and tyrosine (S/T/Y) phosphorylation sites in eukaryotic proteins by applying a neural network method that recognizes the amino acid patterns around the phosphorylated residue. Yellow color-coded diagram depicts experimentally determined S/T/Y phosphorylation sites. Blue colored-letters indicate putative kinases at each phosphorylation site using kinase-specific predictions from NetphosK. The size of blue colored-letters is correlated to a probability score for kinases at a given position. See Table 4-2 for a complete score listing. A: protein

kinase A (PKA), C: protein kinase C (PKC), G: protein kinase G (PKG), II: casein Kinase II (CKII), 2: cell division cycle 2 kinase (CDC2) , T: serine protein kinase Ataxia telangiectasia mutated (ATM), D: DNA-dependent protein kinase (DNA-PK), 5: cyclin-dependent kinase 5 (CDK5), M: mitogen-activated protein kinase p38 (p38MAPK), I: casein kinase I (CKI), N: insulin receptor kinase (INSR), E: epidermal growth factor receptor (EGFR).

Table 4-1. Predicted phosphorylation sites of AoPab1 with corresponding kinases using kinase-specific prediction.

Site	Kinases	Score	Site	Kinases	Score
Thr[8]	p38MAPK	0.5	Tyr[330]	EGFR	0.51
Ser[17]	CKII	0.57	Thr[341]	CKII	0.65
Thr[18]	p38MAPK	0.52	Thr[358]	PKC	0.55
	CDK5	0.55		CDC 2	0.51
Thr[23]	PKC	0.75	Ser[361]	PKC	0.54
Thr[24]	p38MAPK	0.51	Thr[368]	PKA	0.51
Thr[33]	PKG	0.55		PKG	0.54
Ser[44]	DNAPK	0.64	Thr[373]	DNAPK	0.55
Ser[50]	DNAPK	0.53	Thr[375]	p38MAPK	0.57
	CDC2	0.51	Ser[378]	CKII	0.64
Ser[59]	CKII	0.55		PKC	0.65
	CDC2	0.53	Thr[388]	CKII	0.52
Thr[61]	CKII	0.51	Ser[395]	CKII	0.61
Ser[70]	CDC 2	0.56	Ser[396]	CKII	0.71
Ser[77]	PKC	0.52	Ser[411]	CKII	0.7
Thr[86]	PKC	0.79		CKI	0.52
Ser[89]	PKA	0.8	Ser[421]	PKC	**0.89**
Thr[113]	CDC 2	0.51	Ser[441]	CKII	0.53
Ser[125]	DNAPK	0.52	Ser[442]	CKII	0.57
	ATM	0.52	Ser[476]	DNAPK	0.56
Ser[165]	PKC	0.79		ATM	0.51
Ser[214]	PKC	0.56		PKA	0.57
Ser[220]	CKII	0.57		PKG	0.52
	PKC	0.59	Ser[481]	CDC 2	0.51
	PKA	0.69	Thr[487]	PKC	0.83
Thr[230]	PKC	0.7	Thr[699]	PKA	0.56
Thr[242]	CKII	0.71	Ser[712]	CKII	0.72
Thr[260]	PKC	0.68	Tyr[734]	INSR	0.55
Ser[262]	PKC	0.68	Ser[742]	CKII	0.58
Ser[269]	CDC 2	0.57	Thr[758]	CKII	0.66
Ser[278]	CKII	0.56		PKG	0.56
Thr[297]	DNAPK	0.54	Ser[759]	CKII	0.57
Ser[328]	PKA	0.51			

Conclusion and Perspectives

In recent years, an emerging role of cytoplasmic mRNP granules on the post-transcriptional regulation of gene expression has recieved great attention. For a lack of such studies in filamentous fungi, this study was to characterize stress granules in filamentous fungus *A. oryzae* to provide an integrated perspective on eukaryotic stress response.

In the Chapter 1, to show formation of stress granules in response to stress is a general phenomenon in *A. oryzae*, I approached it from different aspects, including using different markers, targeting *egfp* gene at the genomic loci, and surveying with various stress conditions. Fluorescence microscopy observations indicate that the formation and polarized localization of stress granules at the phyphal tip is a general phenomenon in response to external stress in *A. oryzae*. The significance of this observation is that the post-transcriptional regulation of gene expression by remodeling mRNA between polysomes and mRNP granules during stress likely occurs in *A. oryzae*. In support with this suggestion, several mRNAs ecoding secreted proteins are redistributed from poysomes to monosomes during ER stress in *A. niger* (Guillemette *et al*., 2007). Stress granules are known as large cytoplasmic mRNA-protein complexes. To prove accumulation of mRNA with marker proteins simutaneously, I had tried to set up mRNA visualization system in *A. oryzae*, but it has not been successful yet.

In the Chapter 2, I have made a functional connection of AoSO to stress granules. AoSO is known to accumulate at the septal pore to prevent cells from cytoplasmic loss when cells are exposed to various stresses (Maruyama *et al*., 2010). In addition to septal pore localizaiton, subcellular localization analyses have shown that AoSO accumulates as cytoplasm foci (Figure 2-1A). Colocalization of AoSO-EGFP with

stress granule marker protein AoPab1-mDsRed, physical interaction between AoSO-EGFP and AoPab1-3HA, and the sensitivity of AoSO cytoplasmic foci to cycloheximide treatment suggest that AoSO is a novel component of stress granules (Figure 2-1). Furthermore, functional assay using *Aoso*-disruptant revealed that AoSO influences the formation and localization of stress granules. The composition of stress granules is species-specific and varies in different stress conditions (Hoyle *et al*., 2007; Buchen *et al*., 2008; Ohn *et al*., 2008). For example, in mammalian cells, stress granules typically contain eIF4F components (eIF4E, eIF4G and eIF4A), eIF3 and 40S ribosomal subunits, and their assembly is strongly dependent upon individual eIF3 subunits (Ohn *et al*., 2008). However, in *S. cerevisiae*, eIF3 or 40S ribosomal subunits are not found in glucose deprivation-induced stress granules (Hoyle *et al*., 2007; Buchan *et al*., 2008). Furthermore, TIA-1 and its yeast homolog Pub1p facilitate stress granule assembly in response to arsenite and glucose deprivation, respectively (Gilks *et al*. 2004; Buchan *et al*. 2008), but not in response to other stresses such as heat shock (López de Silanes *et al*., 2005; Grousl *et al*. 2009). Orthologs of the *so* gene have only been identified in the genomes of Pezizomycotina species (Fleißner *et al*., 2005), therefore I presume that AoSO, which influences formation and localization of stress granule, is a novel stress granule component specific to Pezizomycotina.

The fate of stress granules is perhaps the least understood part in their biogenesis and disassembly. During recovery from stress, stress granules could be disassembled by dissociation of the interactions creating the larger aggregate. mRNAs inside stress granules are targeted to P-bodies to be degraded (Sheth and Parker, 2003), or re-entry into polysomes to be translated (Brengues *et al*., 2005; Bhattacharyya *et al*., 2006). In the Chapter 3, I provided an additional fate for the mRNPs that accumulate

within stress granules during prolonged stress, where stress granule-associated mRNPs unable to return to translation might instead be targeted for vacuole/lysosome-based degradation through autophagy. Firstly, colocalization of autophagosome marker EGFP-AoAtg8 and stress granules labeled with AoPab1-mDsRed was observed in cells exposed to heat stress. Additionally, prolonged heat stress-induced decrease of AoPab1-3HA was greatly inhibited in an autophagy-defective strain, *Aoatg8* disruptant. I still need more evidence to confirm the hypothesis that stress granules are degraded through autophagy under sustained stress, such as an accumulation of stress granule marker protein in the vacuole during prolonged heat stress. A very recent microscope-based study in yeast supports this idea (Buchan and Parker, 2009); an increase in constitutive stress granules under normal growth condition is observed in autophagy-defective mutants. Additionally, disruption of *ATG15* results in the accumulation of Pab1p-GFP in an intravacuolar compartment (IVC).

The significance of stress granules as well as autophagy in the pathogenesis of neurodegenerative diseases has been revealed recently. However, these studies have been carried out independently. A pathological hallmark of many neurodegenerative diseases is the accumulation of mutant protein aggregates (Jucker and Walker, 2013; Takalo *et al*., 2013). Dysfunction of autophagy to remove these protein aggregates results in the pathogenesis of neurodegenerative disorders (Banerjee *et al*., 2010; Nixon, 2013). Aggregation of these pathological proteins might be proceeded through the stress granule pathway (Wolozin, 2012), or be advanced in stress granules (Buchan *et al*., 2013; Li *et al*., 2013). These observations suggest that accumulation of protein aggregates in cells may have deleterious impacts. Thus, clearance of stress granules, which are large mRNA-protein aggregate complexes, by autophagy may be crucial for cell viability under sustained stress.

The role of PABP in regulating mRNA translation and stability requires extensive protein-protein and protein-nucleic acid interactions. Posttranslational modification is an ideal mechanism to coordinate this complex interaction network during a stress. In the Chapter 4, some of PTMs of AoPab1 were identified. Firstly, 2D-SDS/PAGE analyses revealed that AoPab1 was extensively post-translationally modified under normal growth condition. Exposure to heat stress for short and prolonged time resulted in the changes in the dirstribution of PTM isoforms. Furthermore, precise identification of PTMs of AoPab1 using LC-MS/MS revealed that acetylation and mono/di/tri-methylation of lysine, and phosphorylation of serine/treonine/tyrosine were modified at several residues throughout all the functional domains of AoPab1, with an exception of Q/G/P-rich region. Recently, post-translational modification has been analyzed in mammalian and yeast PABPs (Brook *et al*., 2012; Low *et al*., 2013). Both of these studies have identified unusual glutamate methylation with unkown function. Glutamate methylation was not analyzed in this study, therefore it is unclear whether AoPab1 was modified by methylation at glutamate residues. Additional tyrosine phosphorylation and lysine trimethylation were identified in AoPab1, which are not found in mammalian and yeast PABPs. Functions of these PTMs are unknown, but they are considered to influence RNA and/or protein interactions, and therefore the function of AoPab1. Additionally, LC-MS/MS analyses and *in silico* prediction of AoPab1 phosphorylation sites suggest that PKC and its counteracting phosphatase may be involved in the post-translational regulation of AoPab1 in response to heat stress. The involvement of PKC in the suppression of apoptosis and in polarity establishment under heat stress has been reported in *A. nidulans* (Katayama *et al*., 2012). The role of PKC in AoPab1 during heat stress remains to be elucidated.

A. oryzae is an industrial important strain widely used in traditional fermentated food industry. Additionally, the natural ability of *A. oryzae* to secrete a variety of proteins in large quantities (Kitamoto, 2002) makes it a very useful host in industrial application. However, low yield is still a major bottleneck for heterologous protein production, even though many genetic approaches targeted at transcriptional control or post-translational control have been used to improve hetrologous protein production for industrial application, such as gene fusion with highly expressed genes as carrier proteins (Ward *et al*., 1990; Tsuchiya *et al*., 1994) and disruption of protease genes (Jin *et al*., 2007; Yoon *et al*., 2009; Yoon *et al*., 2011). The preliminary results in this study suggest the reprogramming mRNA during stress. Preventing mRNA from sequestration in the stress granules or degradation at P-bodies may benefit to the increase of heterologous protein production. Further studying and understanding of post-trancriptional regulation of gene expression on mRNA modulation may provide new insights for industrial application in the near future.

Filamentous fungi are well known for the highly polarized growth, which secretory vesicles, cytoskeletal elements, and related components are concentrated at the hyphal tip as a well-organized cluster that determines hyphal growth and polarity (Harris et al., 2005; Steinberg, 2007). Most interstingly, polarized localization of stress granules at hyphal tip were observated in *A. oryzae*, suggesting a spatial specificity of the posttranscriptional regulation of gene expression in *A. oryzae*. Based on these observations, I speculate that asymmetrical localization of mRNA at the hyphal tip results in the spatially restricted formation of stress granules or that mRNAs at the hyphal tip are preferentially routed into stress granules as an acute response to stress.

In recent years, studies of stress granules as well as autophagy attract great

attention in neurodegenerative diseases, because misregulation results in the pathogenesis. However, these studies have been carried out independently, and it was not known how to link them together in the disease process. Degradation of stress granules via autophagy pathway observed in *A. oryzae* provides the first insight into how their roles are coordinated in pathogenesis of neurodegenerative diseases. It requires more integrated studies of stress granules and autophagy in the future.

Posttranslational modification is an ideal mechanism to regulate protein-protein interactions and protein functions during stress, in which rapid and reversible protein modifications allow adaptation to stress without new protein synthesis. AoPab1 is dynamically regulated by post-translational modifications during stress, suggesting that mRNA-protein and/or protein-protein interactions of AoPab1 may be altered in response to stress. Understanding of mechanisms underlying mRNA-protein/protein-protein interaction and stress granule assembly/disassembly assists disease prevention, control, and therapy. Therefore, elucidating the key physiological targets of various modifications and the mechanisms underlying their effects will be an important future goal. Filamentous fungi are attractive organisms to study fundamental processes of the eukaryotic cell. One of the benefits of using microorganism instead of mammalian cells is that genetic engineering is easily manipulated in microorganism to study a gene function or the role of a specific region, and even a specific amino acid on the function of protein. For the highly conserved nature of stress granule formation and components, the advance in the research of stress granules using *A. oryzae* is expected to contribute to human pathological research.

Materials and Methods

1. Plasmid construction

For the ectopic expression of proteins and for the expression of disruption cassette, plasmids were constructed using the MultiSite Gateway system (Invitrogen, Carlsbad, CA, USA).

1.1 Plasmids for the expression of fluorescent fusion proteins

Plasmids for the expression of fluorescent fusion proteins were constructed using the MultiSite Gateway system (Invitrogen, Carlsbad, CA, USA). ORF regions of *Aopab1* (AO090003000927), *Aopub1* (AO090001000353), *Aodcp2* (AO090120000363), and *Aoedc3* (AO090120000481) genes were amplified by PCR using the genomic DNA of *A. oryzae* wild-type strain RIB40 as a template, and then cloned into pDONR221 by the BP clonase reaction, generating center entry clones pgEpab1, pgEpub1, pgEdcp2, and pgEedc3, respectively. The center entry clones were individually mixed with 5’ entry clone pg5'PaB, 3’ entry clone pg3'E, and destination vector pgDN for the LR clonase reaction, generating plasmids pgDPaPab1E, pgDPaPub1E, pgDPaDcp2E, and pgDPaEdc3E, respectively. For the expression of AoPab1-mDsRed, pgEpab1 was mixed with 5’ entry clone pg5'PaB, 3’ entry clone pg3'DRM-CF, and destination vector pgDSO for the LR clonase reaction, generating plasmid pgCPaPab1DR. For the expression of EGFP, 5’ entry clone pg5'PaB, center entry clone pgEEG, and 3’ entry clone pg3'Ta were mixed with destination vector pgDN for the LR clonase reaction, generating plasmid pgDPaE.

1.2 Plasmids for the expression of HA-tagged AoPab1

For the expression of AoPab1-3HA, pgEpab1 was mixed with 5’ entry clone pg5'PaB, 3’ entry clone pg3'HA3, and destination vector pgDSO for the LR clonase reaction, generating plasmid pgCPaPab13HA.

1.3 Plasmids for the expression of disruption cassette

To generate the DNA fragment for disruption of *Aopub1*, 1.3 kb of the 5'-flanking region and 1.5 kb of the 3'-flanking region of *Aopub1* were amplified by PCR using genomic DNA of wild-type strain RIB40 as a template, and introduced into plasmids pDONR P4-P1R and pDONR P2R-P3 by the BP clonase reaction, generating the 5' entry clone pg5Pub1up and 3' entry clone pg3Pub1dw, respectively. Plasmids pg5Pub1up and pg3Pub1dw were mixed with center entry clone pgEpG and destination vector pDEST R4-R3 for the LR clonase reaction to generate plasmid pgdPub1.

1.4 Plasmids for the expression of DNA fragment for targeting *egfp* at genomic loci

DNA fragments containing 3' terminal 1.5 kb of *Aopab1* or *Aodcp2* (stop codon was removed), *egfp, adeA* gene, and 1.5 kb of 3'-flanking regions of *Aopab1* or *Aodcp2* was generated using fusion PCR and cloned into TOPO vector (pCR4Blunt-TOPO) individually, generating plasmid pTPab1EaA and pTDcp2EaA, respectively.

2. *Escherichia coli* strain and transformation

2.1 *E.coli* strain

E.coli DH5α was used for DNA manipulations.

2.2 Growth conditions

For liquid culture, single colony of *E. coli* was inoculated into 10 ml of Luria-Bertani (LB) medium supplemented with appropriate antibiotics (100 μg/mL ampicillin or kanamycin) and cultured at 37°C for 12-16 h. For isolation of single

colony, an aliquot of *E. coli* culture was spreaded on a 1.5% LB agar plate supplemented with appropriate antibiotics and cultured at 37°C overnight.

2.3 Transformation of *E. coli* cells

Competent cells were taken out from -80^{o}C freezer and thawed on ice. After mixing gently, aliquots of cells were transferred into 1.5 ml Eppendorf tubes. For transformation of plasmid DNA or BP reaction mixtures, use 100 μl of competent cells. For transformation of LR reaction mixtures, use 200 μl of competent cells. 1 μl of plasmid DNA, 10.5 μl BP reaction mixtures, or 21 μl LR reaction mixtures were added into cells. After mixing gently, tubes were incubated on ice for 30 min. Heat shock was operated by placing tubes in 42^{o}C water bath for ~45 seconds. Tubes were replaced on ice for 2-5 minutes. 250 μl of pre-warmed (37°C) SOC medium was added into tubes and incubated at 37°C for 60 min with shacking. Cells were spreaded on LB plates supplemented with appropriate antibiotics.

3. Plasmid preparation

3.1 Plasmid isolation

Plasmids were extracted using alkaline-SDS lysis method. 10 ml of bacterial liquid culture was centrifuged at 3500 rpm, 4°C, for 5 min. Bacterial pellet was resuspended in 200 μl of ice-cooled Sol I and transferred into 1.5 ml tubes. 400 μl of freshly prepared Sol II was added into suspension, mixed thoroughly by repeated gentle inversion, and incubated on ice for 5 min. 300 μl of ice-cooled Sol III was added into cell lysates and mixed thoroughly by hand shacking. Tubes were incubated on ice for 5 min. 100 μl of ice-cooled CI solution (Chloroform:Isoamylalcohol =24:1, v/v) was added into tubes and mixed thoroughly by hand shacking. After centrifuge at 15000 rpm, 4°C, for 8 min, 800 μl of supernatant was recovered and added into 600 μl of

ice-cooled isopropanol in fresh 1.5 ml tubes and mixed thoroughly by vigorously vortex. After centrifuge at 15000 rpm, 4°C, for 8 min, supernatant was removed by aspirator and pellet was air-dried for about 10 min. The pellet was dissolved in 400 μl of TE buffer. After addition of 1 ul RNase A (10 mg/ml) the mixture was incubate at 64°C for 15 min (or 37°C for 30 min) to remove RNA. 400 μl of PCI solution (phenol:chloroform:isoamylalcohol=25:24:1, v/v/v) *was* added into mixtures and mixed thoroughly by vigorously vortex. After centrifuge at 15000 rpm, 4°C, for 5 min, supernatant was recovered and added into 400 μl of ice-cold CI solotion in fresh 1.5 ml tubes and mixed thoroughly by vigorously vortex. After centrifuge again, supernatant was recovered and added into 40 μl of 3M sodium acetate solution (pH 5.2) and l ml of ice-cooled 100% ethaol in fresh 1.5 ml tubes and mixed thoroughly by vigorously vortex. After centrifuge again, the pellet was washed with 200 μl of ice-cooled 70% ethanol and centrifuged at 15000 rpm, 4°C, for 5 min. The supernatant was removed by aspirator and the pellet was air-dried for about 10 min. The pellet was dissolved in 50-100 μl of TE buffer.

3.2 Characterization of purified plasmid

The identity of the purified plasmid was verified using restriction mapping. Briefly, appropriate restriction enzymes were selected for enzyme digestion. 1 μl of purified plasmid was mixed with 1 μl of selected restriction enzyme, 10x appropriate buffer, and distilled water to bring total volume to 20 μl. Mixtures were mixed gently and incubated at 37°C for 1 h. The sizes of the resulting fragments were determined by 0.8 % agarose gel electrophoresis.

3.3 Concentration estimation

To determine the concentration of purified plasmid, 1 μl of plasmid was digested

using one-cut restriction enzyme at 37°C for 1 h. 1 µl, 2 µl, 3 µl, and 5 µl of the linearized plasmid was applied on a 0.8% agarose gel along with λ DNA/*Hin*dIII markers as molecular standards of known concentration. The concentration of plasmid was calculated by comparison of band intensities with λ DNA/*Hin*dIII markers.

3.4 Insert sequencing

Insert sequences were determined by sequencing using appropriate primers.

4. *A. oryzae* strains and transformation

4.1 *A. oryzae* strains

The *A. oryzae* strains used in this study are listed in Appendix I.

4.2 Transformation

Transformation of *A. oryzae* was carried out according to the standard method (Kitamoto, 2002). Parent strains were cultured on agar plates at 30 ºC for 5 to 7 days. Mycelia and conidia were collected from the surface of colonies using a toothpick and freshly inoculated into 100 ml DPY medium. After cultivation at 30 ºC for 18-20 h, mycelia were filtered from the growth medium using a Miracloth placed on a funnel. Mycelia were rinsed with sterile distilled water and the remaining water from the mycelia was soaked out by spreading out the mycelia on the Miracloth. For protoplasts preparation, the proper amount of dried mycelia were then transferred into L-shaped glass test tubes containing 10 ml of the freshly prepared Yatalase enzyme solution (TF Solution I) and incubated at 30ºC for 3 h with constant shacking at 50 rpm. Hyphal debris was removed by filtration through a Miracloth placed on a funnel. The recovered protoplasts were added with 10 ml of TF Solution II and centrifuged at 2000 rpm, 4°C, for 8 min. The recovered protoplasts were washed twice by

suspending the pellet in 5 ml of TF Solution II and centrifuged again. Protoplast concentration was adjusted to 1-5 × 10^7 /ml in TF Solution II. 200 µl of this suspension was mixed with transforming DNA (5-10 µg/µl) and incubated on ice for 30 min. Polyethylene glycol (PEG) containing TF Solution III was added and gently mixed with the reaction mixture in three consecutive steps (250, 250, and 850 µl) and incubated at room temperature for 20 min. Protoplasts were recovered by adding 5 ml of TF Solution II to the transformation mixture and centrifuged at 2000 rpm, 4°C, for 8 min. The recovered protoplasts were resuspended in 500 µl of TF Solution II. This suspension was mixed with 5 ml of appropriate pre-warmed soft top agar (selective medium containing 1.2 M sorbitol and 0.8 % agar) and poured onto the same selective medium agar plate. After cultivation at 30°C for 3-5 days, transformants were transferred into selective medium agar plates. Homokaryotic transmormants were isolated after several times of subculture.

4.2.1 Generation of fluorescent fusion protein-expressing strains

To generate of EGFP fusion protein expressing strains, plasmids pgPaPab1E and pgPapub1E were introduced into strain NSRKu70-1-1A; while plasmid pgPaDcp2E was introduced into strain NS4. The resulting transformants were selected using Czapek-Dox (CD) medium supplemented with 0.15% methionine (CD + Met).

To generate a strain co-expressing AoDcp2-EGFP and AoPab1-mDsRed, plasmid pgCPaPab1DR was introduced into strain S-Dcp2E, and positive transformants were selected on CD medium. To generate a strain co-expressing AoSO-EGFP and AoPab1-mDsRed, plasmid pgCPaPab1DR was introduced into strain NSK-ASG1, and positive transformants were selected on CD medium. To generate a strain co-expressing EGFP-AoAtg8 and AoPab1-mDsRed, plasmid pgCPaPab1DR was introduced into strain S-EA8, and positive transformants were selected on CD

medium.

To express AoPab1-EGFP in an *Aoso* deletion background, plasmid pgDPaPab1E was introduced into Δ*Aoso* strain (NSK-SO11), and positive transformants were selected on CD+Met medium. To express AoPab1-EGFP in an *Aoatg8* deletion background, plasmid pgDPaPab1E was introduced into Δ*Aoatg8* strain, and positive transformants were selected on CD+Met medium.

4.2.2 Generation of *Aopub1* disruptant

To generate an *Aopub1* disruptant, a DNA fragment containing the 5'-flanking region of *Aopub1*, *pyrG* marker, and 3'-flanking region of *Aopub1*, was amplified by PCR from plasmid pgdPub1, purified and then introduced into *A. oryzae* strain NSPlD1.

4.2.3 Generation of HA-tagged AoPab1-expressing strains

To express AoPab1-3HA in the EGFP or AoSO-EGFP-expressing strain, plasmid pgCPaPab13HA was introduced into SK-E strain or NSK-ASG1, and positive transformants were selected on CD medium.

5. Conidia collection

Conidia were harvested from the surface of colonies after cultivation on agar plates at 30ºC for 5 to 7 days. The culture was stirred with 10 ml of 0.01% (v/v) Tween 80 aqueous solution using a pasteur pipette. After transferring to a 15 ml Falcon tube, conidia suspension was and mixed by vigorous vortex and filtered using Miracloth (Calbiochem, Darmstadt, Germany). The filtrate was centrifuged at 3000 rpm, 4ºC, for 5 min. For washing the pellet, the pellet was resuspended in 5 ml of 0.01% (v/v) Tween 80 aqueous solution and centrifuged again. Finally, conidia

suspension was obtained by adding 1 ml of distilled water to resuspend the pellet.

6. Glycerol stock

To make a glycerol stock, 700 μl of conidia suspension was added into 300 μl of 80% glycerol in a sterile screw cap microcentrifuge tube and stored at -80°C.

7. **Fluorescence microscopy**

For microscopic examination, approximately 10^4 conidia of cells were inoculated into 100 μl CD or CD medium supplemented with 1.5% methionine in a glass-bottom dish (Asahi Techno Glass, Chiba, Japan), and incubated at 30°C for 18 h before being exposed to stress conditions. For temperature stress, cells were shifted from 30 to 4°C for 30 min or to 45°C for 10 min. For glucose deprivation, cells were washed three times with CD medium without glucose, and further incubated for 10 min in CD medium without glucose. For ER, osmotic, and oxidative stresses, culture medium was removed and replaced by medium containing 10 mM DTT, 1.2 M sorbitol, or 2 mM H_2O_2, respectively, and cells were further incubated for 60, 30, and 30 min. Stressed cells were observed by confocal microscopy using an IX71 inverted microscope (Olympus, Tokyo, Japan) equipped with a 100× Neofluor objective lens (1.40 numerical aperture), 488-nm (Furukawa Electric, Tokyo, Japan) and 561-nm semiconductor lasers (Melles Griot, Carlsbad, CA, USA), GFP, DsRed, and DualView filters (Nippon Roper, Chiba, Japan), a CSU22 confocal scanning system (Yokogawa Electronics, Tokyo, Japan), and an Andor iXon cooled digital CCD camera (Andor Technology PLC, Belfast, UK). Images were analyzed with Andor iQ software (Andor Technology PLC) and representative images are shown.

8. Genomic DNA preparation

After cultivation on agar plates at 30ºC for 5 to 7 days, a proper amount of mycelia and conidia were collected from the surface of colonies using a toothpick and freshly inoculated into 20 ml DPY medium and incubated at 30ºC for 18-10 h. 0.2-0.3 g of mycelia were harvested by filtration, frozen in liquid nitrogen, and pulverized using a multibead shocker (Yasui kikai, Osaka, Japan). Total genomic DNA was extracted in 100 μl GE solution (See Appendix V) and incubated at 60ºC for 3 h with constant shacking at 50 rpm. Lysates were transferred into 1.5 ml tubes and added with the equal amount of PCI solution (phenol:chloroform:isoamylalcohol=25:24:1, v/v/v) (~700 μl). After mixing thoroughly by hand shacking, mixtures were centrifuged at 4ºC, 15000 rpm, for 10 min. The supernatant was recovered and added with an equal amount of PCI (~600 μl) and centrifuged at 4ºC, 15000 rpm, for 5 min. The supernatant was recovered and added with an equal amount of CI solution (Chloroform:Isoamylalcohol =24:1, v/v) (~500 μl) and centrifuged at 4ºC, 15000 rpm, for 5 min. The supernatant was recovered and DNA was precipitated by adding the supernatant into 900 μl of ice-cooled ethanol precipitation solution and mixed thoroughly by repeated gentle inversion. After centrifugation at 4ºC, 15000 rpm, for 10 min, supernatant was removed by aspirator and pellet was air-dried for about 10 min. The pellet was dissolved in 400 μl of TE buffer. After addition of 1 μl RNase A (10 mg/ml) the mixture was incubate at 64°C for 15 min (or 37°C for 30 min) to remove RNA. 400 μl of PCI was added into mixtures and mixed thoroughly by repeated gentle inversion. After centrifuge at 15000 rpm, 4°C, for 5 min, the supernatant was recovered and added into 350 μl of ice-cold CI solotion in fresh 1.5 ml tubes and mixed thoroughly by repeated gentle inversion. After centrifugation at 15000 rpm, 4°C, for 5 min, the supernatant was recovered and added into 1 ml of ice-cold ethanol precipitation solution in fresh 1.5 ml tubes and mixed thoroughly by repeated gentle inversion.

After centrifugation at 15000 rpm, 4°C, for 10 min, the pellet was rinsed with 200 μl of ice-cooled 70% ethanol and centrifuged at 15000 rpm, 4°C, for 5 min. After centrifuge again, the supernatant was removed by aspirator and the pellet was air-dried for about 10 min. Finally, the genomic DNA pellet was dissolved in 100 μl of TE buffer and stored at 4ºC.

9. Southern blotting

9.1 *egfp*-targeted at genomic loci of *Aopab1* and *Aodcp2*

To confirm whether *egfp* was targeted at the genomic locus of *Aopab1*, genomic DNA of the strain was digested with the restriction enzymes *Eco*T22I and *Hin*dIII (Takara, Otsu, Japan), and was separated in a 0.8% gel by electrophoresis. The DNA was then transferred onto a Hybond N+ membrane (GE Healthcare, Buckinghamshire, UK) and detected with specific probes using the ECL Detection kit (GE Healthcare) and a LAS-4000 miniEPUV luminescent image analyzer (Fujifilm, Tokyo, Japan). The 1.5-kb downstream flanking regions of *Aopab1* amplified from pTPab1EaA were used as probes.

To confirm whether *egfp* was targeted at the genomic locus of *Aodcp2*, *Eco*RI and *Hin*dIII (Takara, Otsu, Japan) were used. The 1.5-kb downstream flanking regions of *Aodcp2* amplified from pTDcp2EaA were used as probes.

9.2 *Aopub1* disruptant

Deletion of *Aopub1* was confirmed by Southern blotting analysis. Briefly, genomic DNA of the strain was digested with the restriction enzymes *Bgl*II and *Bam*HI (Takara, Otsu, Japan), and was separated in a 0.8% gel by electrophoresis. The DNA was then transferred onto a Hybond N+ membrane and detected with specific probes using the ECL Detection kit and a LAS-4000 miniEPUV luminescent image

analyzer. The 1.5-kb downstream flanking regions of *Aopub1* amplified from pgdPub1 were used as probes.

10. Protein extraction

Approximately 10^7 conidia of cells expressing were inoculated in 20 ml DPY medium, and cultured at 30°C for 10 h before being exposed to heat stress. 0.2-0.3 g of mycelia were harvested by filtration, frozen in liquid nitrogen, and pulverized using a multibead shocker (Yasui kikai, Osaka, Japan). Total proteins were extracted in phosphate buffer or lysis buffer for immunoblotting or immunoprecipitation, respectively (See Appendix V).

11. Protein assay

The concentration of the isolated proteins was determined by Bradford assay (Bradford, 1976). The method is a colorimetric analytic procedure, based on the proportional binding of the dye Coomassie Brilliant Blue G-250 to proteins. The protein concentration of a test sample is determined by comparison to that of a series of protein standards. A set of bovine serum albumin (BSA) standard was prepared by adding 0.1% BSA (Takara, Japan) with extraction buffer to make concentrations of 0, 2, 4, 8, 16 μg/ml in a total volume of 20 μl. 1 μl of each protein sample was mixed with 19 μl extraction buffer. 5x Bradford Reagent (BioRad, USA) was diluted with water. 1 ml of 1x dye reagent was added to each sample. Mixture was incubated at room temperature for at least 5 min. The absorbance of each sample was measure at 595 nm.

12. SDS-PAGE and immunoblotting

Proteins were extracted in phosphate buffer (140 mM NaCl, 2.7 mM KCl, 10 mM

Na_2HPO_4, and 1.8 mM KH_2PO_4, pH 7.4) with 1 mM PMSF, and 1x protease inhibitor cocktail (Sigma, St.Louis, MO, USA), and centrifuged at 15000 rpm, 4ºC, for 30 min to remove cell debris. Equal amount of proteins were separated by 10% SDS-PAGE under reducing condition and then electrophoretically transferred onto polyvinylidine difluoride (PVDF) membranes (Immobilon-P; Millipore, Bedford, MA). Membranes (Immobilon-P; Millipore, Bedford, MA) were either incubated with the anti-GFP (1:3,000 dilution; Funakoshi Co. Ltd., Tokyo, Japan), the anti-HA (1:1000 dilution) antibody, or anti-α-tubulin antibody (1:1,000 dilution; Sigma, St.Louis, MO, USA)). Anti-mouse immunoglobulin G labeled with peroxidase (1:1,000 dilution; Funakoshi Co. Ltd, Tokyo, Japan) was used as secondary antibody. Detection was performed using Super Signal West Pico Stable Peroxidase and Super Signal West Pico Luminol Enhancer solutions (Pierce, Rockford, IL, USA) and LAS-100plus luminescent image analyzer (Fuji Photo Film, Tokyo, Japan).

13. Immunoprecipitation

Proteins were extracted in lysis buffer (10 mM Tris-HCl [pH 7.5], 150 mM NaCl, 0.5% NP-40, 0.5 mM EDTA, 1 mM PMSF, and 1x protease inhibitor cocktail [Sigma, St.Louis, MO, USA]). After centrifugation at 5000 g, 4ºC, for 10 min, the supernatants were incubated with anti-HA-tag mAb-Magnetic Agarose beads (Medical & Biological Laboratories Co. Ltd., Nagoya, Japan) for 2 hr. Immune complexes were washed four times with wash buffer [10 mM Tris-HCl [pH 7.5], 300 mM NaCl, 0.5% NP-40, 0.5 mM EDTA, 1 mM PMSF), and subjected to immunoblotting.

14. Two dimensional polyacrylamide gel electrophoresis (2D-PAGE)

14.1 Sample preparation

All procedures were performed at 4°C. Protein samples were concentrated and desalted using acetone precipitation for the following 2D-PAGE. Briefly, eight volumes of ice-cooled 100% acetone was added to 20 μg of protein samples, and incubated at -20°C for at least 2 hr for protein precipitation. After precipitation, the solution was centrifuged at 14000 g, 4ºC, for 10 min. The protein pellet was air dried for 2-3 min, and resuspended in the rehydration buffer [8 M urea, 2 M thiourea, 4% (w/v) CHAPS, 0.5% (v/v) carrier ampholyte, and 20 mM DTT] in a concentration of 20 μg/ 10 μl for the downstream 2D-PAGE anaysis.

14.2 2D-PAGE

An isoelectric focusing (IEF) chip (pH 3 to 10; BM-113010, SHARP, Osaka, Japan) was used for the first dimensional separation, and a 10% SDS-PAGE (BM-12100, SHARP, Osaka, Japan) was used for the second dimensional separation. All procedures were performed using an automated 2D-Electrophoresis Device, Auto2D BM-100 (SHARP, Osaka, Japan) under the following conditions:

14.2.1 Rehydration

Samples were introduced into IEF chip at 20°C for 30 min. IEF chip was incubated in the rehydration buffer at 20°C for 5 min.

14.2.2 IEF (current limit: 100 μA; temperature: 20°C)

Step 1: held at 200 V for 5 min

Step 2: increased to 1000 V in 5 min

Step 3: held at 1000 V for 5 min

Step 4: increased to 7000 V in 20 min

Step 5: held at 7000 V for 5 min

14.2.3 Equilibration

IEF chip was incubated in the equilibration buffer [500 mM Tris-HCL (pH 6.6), 12.5% glycerol, 50 mM dithiothreitol (DTT), sodium dodecyl sulfate (SDS), and 0.1 % bromophenol blue (BPB)] at 20°C for 5 min.

14.2.4 SDS-PAGE (voltage limit: 300 V; temperature: 10°C)

Equilibrated IEF gel was loaded onto 10% SDS-PAGE. The upper running buffer contained 25 mM Tris, 192 mM Glysin, and 6.94 mN SDS, and the lower running buffer was 150 mM Tris-HCl (pH 8.8). Electrophoresis was run at constant current 20 mA for 40 min. SDS-PAGE was then electrophoretically transferred onto PVDF membranes and subjected to immunoblotting.

15. Polymerase Chain Reaction (*PCR*)

15.1 PrimeSTAR HS DNA Polymerase

For DNA cloning and amplification, PrimeSTAR HS DNA Polymerase (Takara Bio, Otsu, Japan) was used for high fidelity DNA amplification. All PCRs were performed in 50 μl reactions that contained 1 μl of template DNA, 0.24 μM each primer, dNTP mixture (2.5 mM each), 1 mM Mg^{2+} containing buffer, 1.25 U PrimeSTAR DNA polymerase, and distilled water to bring total volume to 50 μl. Thermocycling conditions of PCR were as follows: an initial denaturation of 5 min at 98°C, 25 cycles of 10 s at 98°C, 15 s at 58°C, and 1 kb/min at 72°C, and then a final extension of 7-9 min at 72°C. PCR products were held at 4°C until analysis by agarose gel electrophoresis.

15.2 *Ex Taq* DNA Polymerase

To quickly screen for plasmids containing a desired insert, *Ex Taq* DNA Polymerase (Takara Bio, Otsu, Japan) was used for bacterial colony PCR. All PCRs were prepared as follows: 0.4 μM each primer, dNTP mixture (2.5 mM each), 1x

buffer, 0.25 U *Ex Taq* DNA Polymerase, and distilled water to bring total volume to 20 µl. A single bacterial colony was picked up by touching with a plastic pipet tip. Another agar plate containing the appropriate antibiotics was streaked with the pipet tip and incubated at 37°C for 3-5 h. The pipet tip was then dipped into each reaction tube. Thermocycling conditions of PCR were as follows: an initial denaturation of 5 min at 98°C, 35 cycles of 10 s at 98°C, 30 s at 53°C, and 1 kb/min at 72°C, and then a final extension of 7-9 min at 72°C. PCR products were held at 4°C until analysis by agarose gel electrophoresis.

15.3 KOD FX Neo

To quickly screen for colonies containing a desired insertion or disruption of target gene after transformation, KOD FX Neo (Toyobo Life Science, Osaka, Japan) was used for fungal colony PCR. For crude sample preparation, a small amount of conidia were collected from the surface of colonies using a toothpick in 50 µl TE buffer. All PCRs were prepared as follows: 2 µl of crude samples, 0.2 µM each primer, dNTP mixture (0.4 mM each), 1x buffer, 0.4 U KOD FX Neo, and distilled water to bring total volume to 20 µl. Thermocycling conditions of PCR were as follows: an initial denaturation of 5 min at 94°C, 35 cycles of 10 s at 98°C, 30 s at 60°C, and 1 kb/min at 68°C, and then a final extension of 7-9 min at 68°C. PCR products were held at 4°C until analysis by agarose gel electrophoresis.

16. Liquid chromatography-mass spectrometry/ mass spectrometry (LC-MS/MS)

16.1 In-gel digestion

Immunoprecipitated AoPabl-3HA from unstressed cells or cells exposed to heat stress for 10 and 30 min was separated using 10% SDS-PAGE. Coomassie-Blue-stained protein bands of AoPab1-3HA were excised, cut into cubes

(ca. 1×1 mm), and transferred into a microcentrifuge tube. To remove acetic acid or other low-molecular weight, water-soluble molecules from gel pieces, gel pieces were washed with 500 µl of ddH_2O and incubated at 37°C for 30 s for 3 times. Gel pieces were de-stained by incubating with 100 µl of 50 mM NH_4HCO_3/50% CH_3CN (1:1, vol/vol) at 37°C for 10 min with occasional vortexing (incubation time is dependent on stain intensity). After removing de-stain solution, gel pieces were dehydrated by incubating with 50 µl of CH_3CN at 37°C for 15 min. Gel pieces were vacuum-dried in a desiccator. For reducing alkylation, gel pieces were first incubated with 50 µl of 0.01 M DDT/100 mM NH_4HCO_3 at 50°C for 15 min. After cooling down to room temperature, 2 µl of 0.25 M Iodoacetamide (IAA)/100 mM NH_4HCO_3 was added and incubated at room temperature for another 15 min in dark. After removing supernatant, gel pieces were washed with 50 µl of 100 mM NH_4HCO_3. After removing supernatant, gel pieces were washed again with 50 µl of 50 mM NH_4HCO_3/50% CH_3CN (1:1, v/v). Gel pieces were vacuum-dried in a desiccator. Dry gel pieces were saturated by incubating with 20 µl (or enough volume o cover the dry gel pieces) of trypsin solution (10 ng/µl) (Sigma, St.Louis, MO, USA) on ice for 15 min. After spinning down, gel containing tubes were wrapped in parafilm, and incubated at 37°C overnight. To extract peptide digestion products, 50 µl of 50% CH_3CN/1%TFA was added into each tube, and incubated at 37°C for 10 min. Supernatant was transferred into a new tube. This step was repeated again, and supernatant was combined together. 50 µl of 80% CH_3CN was added into each tube, and incubated at 37°C for 2 min, and supernatant was combined together. Obtained supernatant was vacuum-dried in a desiccator.

16.2 HPLC conditions

HPLC system	EASY-nLC 1000 (Thermo Fisher Scientific)
Column	NANO-HPLC capillary column, C18 (Nikkyo Technos) 0.075 x 150 mm
Mobile phase	A : 0.1% Formic acid B: Acetonitrile / 0.1% Formic acid
Gradient	Total time 60 min 0/5 - 48/35 - 60/65 (min/%B)
Flow rate	300 nl/min
Trap column	Acclaim® PepMap100 pre-column, 100 μm x 2 cm (Thermo Fisher Scientific)

16.3 Mass spectrometry

Mass spectrometer	Q Exactive (Thermo Fisher Scientific)
Mass range	m/z 350-1800
Sample inj. vol.	4/20 μl (2% Acetonitrile / 0.1%TFA)

16.4 Data search

Software	Proteome Discoverer (Ver.1.4) with the MASCOT search engine (Ver. 2.4.1)
Database	SwissProt 2013_10
Taxonomy	Other Fungi
Enzyme	Trypsin
Precursor mass tol.	6 ppm
Fragment mass tol.	20 mmu

17. *In silico* prediction of AoPab1 phosphorylation sites

FASTA formatted AoPab1 amino acid sequences were submitted to NetPhos 2.0 server (http:// www.cbs.dtu.dk/services/NetPhos/) to generate neural network

predictions for serine, threonine and tyrosine phosphorylation potential. A generic prediction score classification was applied to the data set for the phosphoresidue prediction: low, 0-0.499; high, 0.500-0.999. Kinase-specific protein phosphorylation site prediction employing ESS filtering (Evolutionary stable sites) on the NetPhosK 1.0 server (http://www.cbs.dtu.dk/services/NetPhosK/) was also performed (threshold =0.5) using the same sequence with a data set covering the following kinases: protein kinase A (PKA), protein kinase C (PKC), protein kinase G (PKG), casein Kinase II (CKII), cell division cycle 2 kinase (CDC2), calcium/ calmodulin-dependent protein kinase type II (CaMK-II), serineprotein kinase Ataxia telangiectasia mutated (ATM), DNAdependent protein kinase (DNAPK), cyclin-dependent kinase 5 (CDK5), mitogen-activated protein kinase p38 (p38MAPK), glycogen synthase kinase 3 (GSK3), casein kinase I (CKI), protein kinase B (PKB), ribosomal S6 kinase (S6K), insulin receptor kinase (INSR), epidermal growth factor receptor (EGFR) and Src tyrosine kinase (SRC) (Blom *et al*., 2004).

Appendixes

Appendix I. Strain list

Strain	Host	Genotype	Reference
RIB40		Wild-type	Machida et al., 2005
NSRKu70-1-1A	NSRKu-70-1-1	*niaD*⁻ *sC*⁻ *adeA*⁻ Δ*argB*::*adeA*⁻ Δ*ku70*::*argB adeA*	Escaño et al., 2009
NS4	niaD300	*niaD*⁻ *sC*⁻	Yamada et al., 1997
NSPlD1	NSlD	*niaD*⁻ *sC*⁻ *adeA*⁻ Δ*argB*::*adeA*⁻ Δ*ligD*::*argB* Δ*pyrG*::*adeA*	Maruyama and Kitamoto, 2008
NSlD1	NSPlD1	*niaD*⁻ *sC*⁻ *adeA*⁻ Δ*argB*::*adeA*⁻ Δ*ligD*::*argB* Δ*pyrG*::*adeA pyrG*	Maruyama and Kitamoto, 2008
NSR-ΔlD2	NSAR1	*niaD*⁻ *sC*⁻ *adeA*⁻ Δ*argB*::*adeA*⁻ Δ*ligD*::*argB*	Maruyama and Kitamoto, 2008
NSK-ASG1	NSK-ΔSO11	*niaD*⁻ *sC*⁻ *adeA*⁻ Δ*argB*::*adeA*⁻ Δ*ku70*::*argB* Δ*Aoso*::*adeA* pgPaBSG [P*amyB*::*Aoso-egfp*::T*amyB*::*niaD*]	Maruyama et al., 2010
SK-Pab1E	NSRKu70-1-1A	*niaD*⁻ sC⁻ *adeA*⁻ Δ*argB*::*adeA*⁻ Δ*ku70*::*argB adeA* pgDPaPab1E [P*amyB*::*Aopab1-egfp*::T*amyB*::*niaD*]	This study
SK-Pub1E	NSRKu70-1-1A	*niaD*⁻ sC⁻ *adeA*⁻ Δ*argB*::*adeA*⁻ Δ*ku70*::*argB adeA* pgDPaPub1E [P*amyB*::*Aopub1-egfp*::T*amyB*::*niaD*]	This study
SK-E	NSRKu70-1-1A	*niaD*⁻ *sC*⁻ *adeA*⁻ Δ*argB*::*adeA*⁻ Δ*ku70*::*argB adeA* pgPaE [P*amyB*:: *egfp*::T*amyB*::*niaD*]	This study
S-ΔlD2-Pab1E	NSR-ΔlD2	*niaD*⁻ *sC*⁻ *adeA*⁻ Δ*argB*::*adeA*⁻ Δ*ligD*::*argB Aopab1-egfp*::*adeA* pNR10 [*niaD*]	This study
S-ΔlD2-Dcp2E	NSR-ΔlD2	*niaD*⁻ *sC*⁻ *adeA*⁻ Δ*argB*::*adeA*⁻ Δ*ligD*::*argB Aodcp2-egfp*::*adeA* pNR10 [*niaD*]	This study
S-Dcp2E	NS4	*niaD*⁻ *sC*⁻ pgDPaDcp2E [P*amyB*::*Aodcp2-egfp*::T*amyB*::*niaD*]	This study
S-Edc3E	NS4	*niaD*⁻ *sC*⁻ pgDPaEdc3E [P*amyB*::*Aoedc3-egfp*::T*amyB*::*niaD*]	This study
SK-ΔSO11-Pab1E	NSK-ΔSO11	*niaD*⁻ *sC*⁻ *adeA*⁻ Δ*argB*::*adeA*⁻ Δ*ku70*::*argB* Δ*Aoso*::*adeA* pgDPaPab1E [P*amyB*::*Aopab1-egfp*::T*amyB*::*niaD*]	This study
Dcp2E-Pab1DR	S-Dcp2E	*niaD*⁻ *sC*⁻ pgDPaDcp2E (P*amyB*::*Aodcp2-egfp*::T*amyB*::*niaD*) pgCPaPab1DR [P*amyB*::*Aopab1-mDsRed*::T*amyB*::*sC*]	This study
K-ASG1-Pab1DR	NSK-ASG1	*niaD*⁻ *sC*⁻ *adeA*- Δ*argB*::*adeA*- Δ*ku70*::*argB* Δ*Aoso*::*adeA* pgPaBSG [P*amyB*::*Aoso-egfp*::T*amyB*::*niaD*] pgCPaPab1DR [P*amyB*::*Aopab1-mDsRed*::T*amyB*::*sC*]	This study

Appendix I. Strain list (continued)

Strain	Host	Genotype	Reference
K-ASG1-Pab13HA	NSK-ASG1	*niaD*⁻ *sC*⁻ *adeA*- Δ*argB*::*adeA*- Δ*ku70*::*argB* Δ*Aoso*::*adeA* pgPaBSG [P*amyB*::*Aoso-egfp*::T*amyB*::*niaD*]	This study
		pgCPaPab13HA [P*amyB*::*Aopab1-3HA*::T*amyB*::*sC*]	
K-EGFP-Pab13HA	SK-E	*niaD*⁻ *sC*⁻ *adeA*⁻ Δ*argB*::*adeA*⁻ Δ*ku70*::*argB adeA* pgPaE [P*amyB*:: *egfp*::T*amyB*::*niaD*]	This study
		pgCPab13HA [P*amyB*::*Aopab1-3HA*::T*amyB*::*sC*]	
NSlD-ΔPub1	NSPlD1	*niaD*⁻ *sC*⁻ *adeA*⁻Δ*argB*::*adeA*⁻ Δ*ligD*::*argB* Δ*pyrG*::*adeA* Δ*Aopub1*::*pyrG*	This study
K-EA8-Pab1DR	PA8GAtg8	*niaD*⁻ *sC*⁻ *adeA*⁻ Δ*argB*::*adeA*⁻ Δ*ku70*::*argB adeA* pgEGA8 [P*Aoatg8*:: *egfp*::*Aoatg8*::*niaD*]	This study
		pgCPaPab1DR [P*amyB*::*Aopab1-mDsRed*::T*amyB*::*sC*]	
ΔA8-Pab1E	Δ*Aoatg8*	*niaD*⁻ *sC*⁻ *adeA*⁻ Δ*argB*::*adeA*⁻ Δ*ku70*::*argB* Δ*Aoatg8*::*adeA* pgDPaPab1E [P*amyB*::*Aopab1-egfp*::T*amyB*::*niaD*]	This study
ΔA8-Pab13HA	Δ*Aoatg8*	*niaD*⁻ *sC*⁻ *adeA*⁻ Δ*argB*::*adeA*⁻ Δ*ku70*::*argB* Δ*Aoatg8*::*adeA* pgCPab13HA [P*amyB*::*Aopab1-3HA*::T*amyB*::*sC*]	This study

Appendix II. Plasmid list

Plasmid	**Vector**	**Description**
pgEGFPadeA		Generated by Dr. kimura
pgEPab1	pDONR221	Center entry clone containing coding region of *Aopab1*
pgEPub1	pDONR221	Center entry clone containing coding region of *Aopub1*
pgEDcp2	pDONR221	Center entry clone containing coding region of *Aodcp2*
pgEEdc3	pDONR221	Center entry clone containing coding region of *Aoedc3*
pgDPaPab1E	pgDN	AoPab1-EGFP expressing plasmid
pgDPaPub1E	pgDN	AoPub1-EGFP expressing plasmid
pgDPaDcp2E	pgDN	AoDcp2-EGFP expressing plasmid
pgDPaEdc3E	pgDN	AoEdc3-EGFP expressing plasmid
pgCPaPab1DR	pgDSO	AoPab1-mDsRed expressing plasmid
pgDPaE	pgDN	EGFP expressing plasmid
pgCPaPab13HA	pgDSO	AoPab1-3HA expressing plasmid
pg5Pub1up	pDONR P4-P1R	1.3 kb of the 5'- flanking region of *Aopub1*
pg3Pub1dw	pDONR P2R-P3	1.5 kb of the 3'- flanking region of *Aopub1*
pgdPub1	pDEST R4-R3	*Aopub1* disruption cassette
pTPab1EaA	pCR4Blunt-TOPO	Cassette for targeting *egfp* at *Aopab1* genomic locus
pTDcp2EaA	pCR4Blunt-TOPO	Cassette for targeting *egfp* at *Aodcp2* genomic locus

Appendix III. Primer list

Primer	Sequence (5'→3')	Target	Aim
attBE-Aopab1-F	GGGGACAAGTTTGTACAAAAAAGCAGGCTATGTCTGCCGACGCCTCTAC	AoPab1 ORF	To construct plasmid pgEPab1
attBE-Aopab1-R	GGGGACCACTTTGTACAAGAAAGCTGGGTCCGACTTGTTCTCTTCGGTAGAG	AoPab1 ORF	To construct plasmid pgEPab1
attBE-Aopub1-F	GGGGACAAGTTTGTACAAAAAAGCAGGCTATGGCTGATAACGTACCCGCC	AoPub1 ORF	To construct plasmid pgEPub1
attB-Aopub1-R	GGGGACCACTTTGTACAAGAAAGCTGGGTCCGCTTGGTAGCCTCCAAAG	AoPub1 ORF	To construct plasmid pgEPub1
attBE-Aodcp2-F	GGGGACAAGTTTGTACAAAAAAGCAGGCTATGACAGAAACAAAGATGCATTTAGAAGATTGTAAGT	AoDcp2 ORF	To construct plasmid pgEDcp2
attBE-Aodcp2-R	GGGGACCACTTTGTACAAGAAAGCTGGGTCCTTGTTCCCTTTGGCAACACC	AoDcp2 ORF	To construct plasmid pgEDcp2
attBE-Aoedc3-F	GGGGACAAGTTTGTACAAAAAAGCAGGCTATGGATCGCGCCCGCAAGAA	AoEdc3 ORF	To construct plasmid pgEEdc3
attBE-Aoedc3-R	GGGGACCACTTTGTACAAGAAAGCTGGGTCAGCAGAGGATGGCTGGTAG	AoEdc3 ORF	To construct plasmid pgEEdc3
Aopab1-922-F1	AAGCACGAGCGTGAGGAGGA	3’ terminal 1.5 kb of *Aopab1*	To construct plasmid pTPab1EaA
Aopab1-e-R1	tgctcaccatCGACTTGTTCTCTTCGGTAGAGG	3’ terminal 1.5 kb of *Aopab1*	To construct plasmid pTPab1EaA
Aopab1-E-aA-F2	GAACAAGTCGatggtgagcaagggcgagga	*egfp*-T*amyB*-a*deA*	To construct plasmid pTPab1EaA
E-aA-pab1dw-R2	gagacacaaaatCATGCCGTCATGTCCAGGAAGA	*egfp*-T*amyB*-a*deA*	To construct plasmid pTPab1EaA
aA-pab1dw1-F3	TGACGGCATGattttgtgtctcaatgtgtgatatccacgg	3’-flanking region of *Aopab1*	To construct plasmid pTPab1EaA
Aopab1-dw1500-R3	GGAGCCGCACGGGAAATC	3’-flanking region of *Aopab1*	To construct plasmid pTPab1EaA
Aodcp2-1126-F1	AACCCACAGACCCCGAGAAATG	3’ terminal 1.5 kb of *Aodcp2*	To construct plasmid pTDcp21EaA
Aodcp2-e-R1	tgctcaccatCTTGTTCCCTTTGGCAACACCTTG	3’ terminal 1.5 kb of *Aodcp2*	To construct plasmid pTDcp21EaA
Aodcp2-E-aA-F2	AGGGAACAAGatggtgagcaagggcgagga	*egfp*-T*amyB*-a*deA*	To construct plasmid pTDcp21EaA
E-aA-dcp2dw-R2	acaagcacgcCATGCCGTCATGTCCAGGAAG	*egfp*-T*amyB*-a*deA*	To construct plasmid pTDcp21EaA
aA-dcp2dw1-F3	TGACGGCATGgcgtgcttgtacctggcatttc	3’-flanking region of *Aodcp2*	To construct plasmid pTDcp21EaA

Appendix III. Primer list (continued)

Primer	Sequence (5'→3')	Target	Aim
Aodcp2-dw1500-R3	GCTTTAACTTTGACCTCTCCAGGC	3’-flanking region of *Aodcp2*	To construct plasmid pTDcp21EaA
attB5-Pub1-up-1300-F	GGGGACAACTTTGTATAGAAAAGTTGggatgttaccgtttgattgaccattgc	5’-flanking region of *Aopub1*	To construct plasmid pg5Pub1up
attB5-Pub1-up-1-R	GGGGACTGCTTTTTTGTACAAACTTGtgttgaaagatcacaagccgcaatatacaag	5’-flanking region of *Aopub1*	To construct plasmid pg5Pub1up
attB3-Pub1-dw-1-F	GGGGACAGCTTTCTTGTACAAAGTGGcctatcgtccagtatacttcgctg	3’-flanking region of *Aopub1*	To construct plasmid pg3Pub1dw
attB3-Pub1-dw-1500-R	GGGGACAACTTTGTATAATAAAGTTGccattgctctgcctcccc	3’-flanking region of *Aopub1*	To construct plasmid pg3Pub1dw

Underlines indicate *attB* sequences.

Appendix IV. Medium compositions

All media were sterilized at 120 ºC for 15 min.

Dextrin-peptone-yeast extract (DPY) medium

Component	Final concentration	Amount
Dextrin	2%	2 g
Polypeptone	1%	1 g
Yeast extract	0.5%	0.5 g
KH_2PO_4	0.5%	0.5 g
$MgSO_4 \cdot 7H_2O$	0.05%	0.05 g
ddH_2O		Fill up to 100 ml

Potato dextrose (PD) medium

Component	Amount
Potato dextrose agar	39 g
ddH_2O	Fill up to 1000 ml

Czapek-Dox (CD) medium

Component	Final concentration	Amount
$NaNO_3$	0.3%	0.3 g
KCl	0.2%	0.2 g
KH_2PO_4	0.1%	0.1 g
$MgSO_4 \cdot 7H_2O$	0.05%	0.05 g
2% $FeSO_4 \cdot 7H_2O$	0.002%	100 μl
Glucose	2%	2 g
(Agar)	(1.5%)	(1.5 g)
ddH_2O		fill up to 100 ml

Adjust pH to 5.5 with 0.4 N NaOH.

CD + Met medium

For selective medium, CD medium is supplemented with 0.0015% methionine. For culture for the microscopic examination, CD medium is supplemented with 0.15% methionine.

Minimal (M) medium

Component	Final concentration	Amount
NH_4Cl	0.2%	0.2 g
$(NH_4)2SO_4$	0.1%	0.1 g
KCl	0.05%	0.05 g
NaCl	0.05%	0.05 g
KH_2PO_4	0.1%	0.1 g
$MgSO_4 \cdot 7H_2O$	0.05%	0.05 g
2% $FeSO_4 \cdot 7H_2O$	0.002%	100 µl
Glucose	2%	2 g
(Agar)	(1.5%)	(1.5 g)
ddH_2O		fill up to 100 ml

Adjust pH to 5.5 with 0.4 N NaOH.

M+met medium

For selective medium, M medium is supplemented with 0.15% methionine.

Luria-Bertani (LB) medium

Component	Final concentration	Amount
Yeast Extract	0.5%	0.5 g
Bacto-tryptone	1%	1 g
NaCl	0.5%	0.5 g
(Agar)	(1.5%)	(1.5 g)
ddH_2O		Fill up to 100 ml

Add 100 µl ampicillin or kanamycin stock (100 mg/ml): to 100 mL LB-broth solution at room temperature after autoclaving.

Appendix V. Buffers and solutions

1. Reagents for plasmid isolation

Solution I

Component	Final concentration	Amount
Glucose	50 mM	0.9 g
1M Tris-HCl [pH 8.0]	25 mM	2.5 ml
0.5 M EDTA [pH 8.0)	10 mM	2 ml
ddH_2O		Fill up to 100 ml

Solution II (freshly prepared)

Component	Final concentration	Amount
0.4 M NaOH	0.2 N	1 ml
10% SDS	1%	200 µl
ddH2O		800 µl

Solution III

Component	Final concentration	Amount
5 M NaOAc	0.2 N	60 ml
Acetic acid	1%	11.5 ml
ddH2O		28.5 ml

TE buffer (Tris-EDTA buffer)

Component	Final concentration	Amount
1M Tris-HCl [pH 8.0]	10 mM	1 ml
0.5 M EDTA	1 mM	200 µl
ddH_2O		98.8 ml

2. Reagents for Southern blotting

Denaturation solution

Component	Final concentration	Amount
NaCl	1.5 M	4.4 g
NaOH	0.5 M	1 g
ddH_2O		Fill up to 50 ml

Neutralization solution

Component	Final concentration	Amount
1M Tris-HCl [pH7.5]	0.5 M	25 ml
NaCl	1.5 M	4.4 g
ddH_2O		25 ml

20x SCC

Component	Final concentration	Amount
NaCl	3 M	175.3 g
Na_3citrate · dihydrate	0.3 M	8.8 g
ddH_2O		Fill up to 1 L

Adjust to pH 7.0 with 5N NaOH. Dilute 1:10 with ddH2O to obtain the 2x concentration.

Prehybridization/hybridization buffer

Component	Amount
Blocking reagent	1.5 g
NaCl	0.86 g
Gold hybridization buffer	30 ml

Pre-warm at 42°C.

For hybridization, mix probe with 15 ml of buffer.

Probe preparation

Adjust probe DNA concentration to 100 ng/10 μl. Boil probe DNA for 5 min and keep on ice for 5 min. Add 10 μl of labeling reagent into probe DNA and mix it by pipetting. Add 10 μl of glutaraldehyde solution into the mixture and mix it by pipetting. After incubation at 37°C for 10 min, add the mixture into 15 ml of pre-warmed hybridization buffer.

Primary wash buffer

Component	Amount
Urea	18 g
10% SDS	2 ml
20x SCC	1.25 ml
ddH_2O	Fill up to 50 ml

3. Reagents for *A. oryzae* transformation

TF Solution 0

Component	Final concentration	Amount
Maleic acid	50 mM	1.16 g
ddH_2O		Fill up to 200 ml

Adjust to pH 5.5 with 5 N NaOH.

TF Solution 1 (freshly prepared)

Component	Final concentration	Amount
Yatalase	1%	0.1 g
$(NH_4)_2SO_4$	0.6 M	0.79 g
TF Solution 0		Fill up to 10 ml

Sterilize by filtration through a 0.45 μm filter.

TF Solution 2

Component	Final concentration	Amount
Sorbitol (Glucitol)	1.3 M	87.4 g
$CaCl_2 \cdot 2H_2O$	50 mM	2.94 g
NaCL	35 mM	0.82 g
1 M Tris-HCl [pH7.5]	10 mM	4 ml
ddH_2O		Fill up to 400 ml

TF Solution 3

Component	Final concentration	Amount
PEG 4000	60%	120 g
$CaCl_2 \cdot 2H_2O$	50 mM	1.47 g
1 M Tris-HCl [pH7.5]	10 mM	2 ml
ddH_2O		Fill up to 200 ml

4. Reagents for *A. oryzae* genomic DNA preparation

GE solution

Component	Final concentration	Amount
0.5 M EDTA	50 mM	5 ml
10% SDS	0.5%	2.5 ml
50 mg/ml Proteinase K	0.1 mg/ml	100 µl
ddH_2O		42.4 ml

Ethanol precipitation solution

Component	Amount
100% Ethanol	40 ml
3M NaOAc [pH 5.2]	1.6 ml

PCI solution

Phenol:Chloroform:Isoamylalcohol (25:24:1, v/v)

CI solution

Chloroform:Isoamylalcohol (24:1, v/v)

5. Reagents for immunoprecipitation

Lysis buffer

Component	Final concentration	Amount
1 M Tris-HCl [pH7.5]	10 mM	100 µl
5 M NaCl	150 mM	300 µl
NP-40	0.5%	0.05 g
0.5 M EDTA	0.5 mM	10 µl
100 mM PMSF	1 mM	100 µl
Protease inhibitor cocktail	1x	100 µl
ddH_2O		9.8 ml

Washing buffer

Component	Final concentration	Amount
1 M Tris-HCl [pH 7.5]	10 mM	100 µl
5 M NaCl	300 mM	600 µl
NP-40	0.5%	0.05 g
0.5 M EDTA	0.5 mM	10 µl
ddH_2O		9.8 ml

6. Protein extraction buffer

Component	Final concentration	Amount
50 mM Tris-HCl [pH 7.5]	49 mM	9.8 ml
100 mM PMSF	1 mM	100 µl
Protease inhibitor cocktail	1x	100 µl

7. Reagents for SDS-PAGE

4% Stacking gel preparation:

Component	Amount
30% Acrylamide/Bis-acrylamide	2 ml
2x Tris-SDS [pH 6.8]	6 ml
ddH_2O	4 ml
10 % APS	100 µl
0.5 M EDTA	10 µl

10% Separating gel preparation

Component	Amount
30% Acrylamide/Bis-acrylamide	10 ml
2x Tris-SDS [pH 8.8]	15 ml
ddH_2O	5 ml
10% APS	300 µl
0.5 M EDTA	30 µl

2x Tris-SDS [pH 6.8]

Component	Final concentration	Amount
Tris	247.64 mM	15 g
SDS	0.2%	1 g
ddH_2O		Fill up to 10 ml

Adjust to pH 6.8 with concentrated HCl

2x Tris-SDS [pH 8.8]

Component	Final concentration	Amount
Tris	750 mM	45.43 g
SDS	0.2%	1 g
ddH_2O		Fill up to 500 ml

Adjust to pH 8.8 with concentrated HCl

1x Laemmli running buffer

Component	Final concentration	Amount
Tris	25 mM	3.03 g
SDS	0.1%	1 g
Glycine	188 mM	14.1 g
ddH_2O		Fill up to 1 L

5x Laemmli sample buffer

Component	Final concentration	Amount
2x Tris-SDS [pH 6.8]	165 mM	6.66 ml
SDS	7.5%	0.075 g
β-mercapto-ethanol	5%	0.5 ml
Glycerol	50%	5 ml
BPB	0.0125%	1.25 mg
ddH_2O		Fill up to 10 ml

8. Reagents for immunoblotting

5x Transfer buffer

Component	Final concentration	Amount
Tris	240 mM	29 g
SDS	0.185%	1.85 g
Glycine	193 mM	14.5 g
Methanol	10%	100 ml
ddH_2O		Fill up to 1 L

0.1% Tween tris-buffered saline (TTBS)

Component	Final concentration	Amount
Tris	20 mM	2.42 g
NaCl	500 mM	29.22 g
Tween 20	0.1%	1 g
ddH_2O		Fill up to 1 L

Adjust to pH 7.5 with concentrated HCl

9. Reagents for in-gel digestion (for one sample)

50 mM NH_4HCO_3/50% CH_3CN

Component	Final concentration	Amount
100 mM NH_4HCO_3	50 mM	1250 µl
CH_3CN	50%	1250 µl

50% CH_3CN/ 1% TFA

Component	Final concentration	Amount
CH_3CN	50%	500 µl
TFA	1%	10 µl
ddH_2O		490 µl

80% CH_3CN

Component	Final concentration	Amount
CH_3CN	80%	400 µl
ddH_2O		190 µl

Trypsin solution

Component	Final concentration	Amount
Trpsin	10 ng/µl	20 µg
Resuspension buffer		2 ml

Heat at 30°C for 15 min before use.

References

1. **Abe K, Gomi K, Hasegawa F and Machida M.** Impact of *Aspergillus oryzae* genomics on industrial production of metabolites. *Mycopathologia* 162: 3: 143-153, 2006.

2. **Albrecht M and Lengauer T.** Survey on the PABC recognition motif PAM2. *Biochem.Biophys.Res.Commun.* 316: 1: 129-138, 2004.

3. **Alers S, Loffler AS, Wesselborg S and Stork B.** Role of AMPK-mTOR-Ulk1/2 in the regulation of autophagy: cross talk, shortcuts, and feedbacks. *Mol.Cell.Biol.* 32: 1: 2-11, 2012.

4. **Anderson P and Kedersha N.** RNA granules: post-transcriptional and epigenetic modulators of gene expression. *Nat.Rev.Mol.Cell Biol.* 10: 6: 430-436, 2009a.

5. **Anderson P and Kedersha N.** Stress granules. *Curr.Biol.* 19: 10: R397-8, 2009b.

6. **Anderson P and Kedersha N.** Stressful initiations. *J.Cell.Sci.* 115: Pt 16: 3227-3234, 2002.

7. **Arimoto K, Fukuda H, Imajoh-Ohmi S, Saito H and Takekawa M.** Formation of stress granules inhibits apoptosis by suppressing stress-responsive MAPK pathways. *Nat.Cell Biol.* 10: 11: 1324-1332, 2008.

8. **Aylmore RC, Wakley GE and Todd NK.** Septal Sealing in the Basidiomycete Coriolus-Versicolor. *J.Gen.Microbiol.* 130: NOV: 2975-2982, 1984.

9. **Banerjee R, Beal MF and Thomas B.** Autophagy in neurodegenerative disorders: pathogenic roles and therapeutic implications. *Trends Neurosci.* 33: 12: 541-549, 2010.

10. **Bennett JW.** Aspergillus: a primer for the novice. *Med.Mycol.* 47 Suppl 1: S5-12, 2009.

11. **Bhattacharyya SN, Habermacher R, Martine U, Closs EI and Filipowicz W.** Relief of microRNA-mediated translational repression in human cells subjected to stress. *Cell* 125: 6: 1111-1124, 2006.

12. **Birney E, Kumar S and Krainer AR.** Analysis of the RNA-recognition motif and RS and RGG domains: conservation in metazoan pre-mRNA splicing factors. *Nucleic Acids Res.* 21: 25: 5803-5816, 1993.

13. **Black JC, Van Rechem C and Whetstine JR.** Histone lysine methylation dynamics: establishment, regulation, and biological impact. *Mol.Cell* 48: 4: 491-507, 2012.

14. **Blom N, Gammeltoft S and Brunak S.** Sequence and structure-based prediction of eukaryotic protein phosphorylation sites. *J.Mol.Biol.* 294: 5: 1351-1362, 1999.

15. **Blom N, Sicheritz-Ponten T, Gupta R, Gammeltoft S and Brunak S.** Prediction of post-translational glycosylation and phosphorylation of proteins from the amino acid sequence. *Proteomics* 4: 6: 1633-1649, 2004.

16. **Bollig F, Winzen R, Kracht M, Ghebremedhin B, Ritter B, Wilhelm A, Resch K and Holtmann H.** Evidence for general stabilization of mRNAs in response to UV light. *Eur.J.Biochem.* 269: 23: 5830-5839, 2002.

17. **Bosco DA, Lemay N, Ko HK, Zhou H, Burke C, Kwiatkowski TJ,Jr, Sapp P, McKenna-Yasek D, Brown RH,Jr and Hayward LJ.** Mutant FUS proteins that cause amyotrophic lateral sclerosis incorporate into stress granules. *Hum.Mol.Genet.* 19: 21: 4160-4175, 2010.

18. **Brengues M and Parker R.** Accumulation of polyadenylated mRNA, Pab1p, eIF4E, and eIF4G with P-bodies in *Saccharomyces cerevisiae*. *Mol.Biol.Cell* 18: 7: 2592-2602, 2007.

19. **Brengues M, Teixeira D and Parker R.** Movement of eukaryotic mRNAs between polysomes and cytoplasmic processing bodies. *Science* 310: 5747: 486-489, 2005.

20. **Brook M, McCracken L, Reddington JP, Lu ZL, Morrice NA and Gray NK.** The multifunctional poly(A)-binding protein (PABP) 1 is subject to extensive dynamic post-translational modification, which molecular modelling suggests

plays an important role in co-ordinating its activities. *Biochem.J.* 441: 3: 803-812, 2012.

21. **Brook M, Smith JW and Gray NK.** The DAZL and PABP families: RNA-binding proteins with interrelated roles in translational control in oocytes. *Reproduction* 137: 4: 595-617, 2009.

22. **Buchan JR, Capaldi AP and Parker R.** TOR-tured yeast find a new way to stand the heat. *Mol.Cell* 47: 2: 155-157, 2012.

23. **Buchan JR, Kolaitis RM, Taylor JP and Parker R.** Eukaryotic stress granules are cleared by autophagy and Cdc48/VCP function. *Cell* 153: 7: 1461-1474, 2013.

24. **Buchan JR, Muhlrad D and Parker R.** P bodies promote stress granule assembly in *Saccharomyces cerevisiae*. *J.Cell Biol.* 183: 3: 441-455, 2008.

25. **Buchan JR, Nissan T and Parker R.** Analyzing P-bodies and stress granules in *Saccharomyces cerevisiae*. *Methods Enzymol.* 470: 619-640, 2010.

26. **Buchan JR and Parker R.** Eukaryotic stress granules: the ins and outs of translation. *Mol.Cell* 36: 6: 932-941, 2009.

27. **Buchan JR, Yoon JH and Parker R.** Stress-specific composition, assembly and kinetics of stress granules in *Saccharomyces cerevisiae*. *J.Cell.Sci.* 124: Pt 2: 228-239, 2011.

28. **Burd CG, Matunis EL and Dreyfuss G.** The multiple RNA-binding domains of the mRNA poly(A)-binding protein have different RNA-binding activities. *Mol.Cell.Biol.* 11: 7: 3419-3424, 1991.

29. **Burgess HM and Gray NK.** mRNA-specific regulation of translation by poly(A)-binding proteins. *Biochem.Soc.Trans.* 38: 6: 1517-1522, 2010.

30. Christensen, Tove, Woeldike ,Helle, Boel ,Esper, Mortensen S,B., Hjortshoej ,Kirsten, Thim ,Lars and Hansen M,T. High level expression of recombinant genes in *Aspergillus oryzae*. Bio/Technology 6: 1419-1422, 1988.

31. **Ciosk R, DePalma M and Priess JR.** ATX-2, the *C. elegans* ortholog of ataxin 2, functions in translational regulation in the germline. *Development* 131: 19: 4831-4841, 2004.

32. **Clarke SG.** Protein methylation at the surface and buried deep: thinking outside the histone box. *Trends Biochem.Sci.* 38: 5: 243-252, 2013.

33. **Clarke SG and Tamanoi F** eds. The Enzymes Volume 24: Protein Methyltransferases, Academic Press, (Amsterdam), pp. 3-570, 2006.

34. **Coller J and Parker R.** General translational repression by activators of mRNA decapping. *Cell* 122: 6: 875-886, 2005.

35. **De Virgilio C and Loewith R.** Cell growth control: little eukaryotes make big contributions. *Oncogene* 25: 48: 6392-6415, 2006.

36. **Decker CJ and Parker R.** P-bodies and stress granules: possible roles in the control of translation and mRNA degradation. *Cold Spring Harb Perspect.Biol.* 4: 9: a012286, 2012.

37. **Decker CJ, Teixeira D and Parker R.** Edc3p and a glutamine/asparagine-rich domain of Lsm4p function in processing body assembly in *Saccharomyces cerevisiae*. *J.Cell Biol.* 179: 3: 437-449, 2007.

38. **Deo RC, Sonenberg N and Burley SK.** X-ray structure of the human hyperplastic discs protein: an ortholog of the C-terminal domain of poly(A)-binding protein. *Proc.Natl.Acad.Sci.U.S.A.* 98: 8: 4414-4419, 2001.

39. **Dewey CM, Cenik B, Sephton CF, Johnson BA, Herz J and Yu G.** TDP-43 aggregation in neurodegeneration: are stress granules the key? *Brain Res.* 1462: 16-25, 2012.

40. **Drawbridge J, Grainger JL and Winkler MM.** Identification and characterization of the poly(A)-binding proteins from the sea urchin: a quantitative analysis. *Mol.Cell.Biol.* 10: 8: 3994-4006, 1990.

41. **Duncan R, Milburn SC and Hershey JW.** Regulated phosphorylation and low abundance of HeLa cell initiation factor eIF-4F suggest a role in translational control. Heat shock effects on eIF-4F. *J.Biol.Chem.* 262: 1: 380-388, 1987.

42. **Duncan RF and Hershey JW.** Protein synthesis and protein phosphorylation during heat stress, recovery, and adaptation. *J.Cell Biol.* 109: 4 Pt 1: 1467-1481, 1989.

43. **Elden AC, Kim HJ, Hart MP, Chen-Plotkin AS, Johnson BS, Fang X, Armakola M, Geser F, Greene R, Lu MM, Padmanabhan A, Clay-Falcone D, McCluskey L, Elman L, Juhr D, Gruber PJ, Rub U, Auburger G, Trojanowski JQ, Lee VM, Van Deerlin VM, Bonini NM and Gitler AD.** Ataxin-2 intermediate-length polyglutamine expansions are associated with increased risk for ALS. *Nature* 466: 7310: 1069-1075, 2010.

44. **Engh I, Wurtz C, Witzel-Schlomp K, Zhang HY, Hoff B, Nowrousian M, Rottensteiner H and Kuck U.** The WW domain protein PRO40 is required for fungal fertility and associates with Woronin bodies. *Eukaryot.Cell.* 6: 5: 831-843, 2007.

45. **Erickson SL and Lykke-Andersen J.** Cytoplasmic mRNP granules at a glance. *J.Cell.Sci.* 124: Pt 3: 293-297, 2011.

46. **Eulalio A, Behm-Ansmant I and Izaurralde E.** P bodies: at the crossroads of post-transcriptional pathways. *Nat.Rev.Mol.Cell Biol.* 8: 1: 9-22, 2007.

47. **Fabian MR, Mathonnet G, Sundermeier T, Mathys H, Zipprich JT, Svitkin YV, Rivas F, Jinek M, Wohlschlegel J, Doudna JA, Chen CY, Shyu AB,**

Yates JR,3rd, Hannon GJ, Filipowicz W, Duchaine TF and Sonenberg N. Mammalian miRNA RISC recruits CAF1 and PABP to affect PABP-dependent deadenylation. *Mol.Cell* 35: 6: 868-880, 2009.

48. **Fabian MR, Sonenberg N and Filipowicz W.** Regulation of mRNA translation and stability by microRNAs. *Annu.Rev.Biochem.* 79: 351-379, 2010.

49. **FAO_WHO.** Committee on Food Additives 31. World Health Organization Technical Report Series: Geneva, 1987.

50. **Feng D, Liu L, Zhu Y and Chen Q.** Molecular signaling toward mitophagy and its physiological significance. *Exp.Cell Res.* 319: 12: 1697-1705, 2013.

51. **Fleissner A and Dersch P.** Expression and export: recombinant protein production systems for *Aspergillus*. *Appl.Microbiol.Biotechnol.* 87: 4: 1255-1270, 2010.

52. **Fleißner A and Glass NL.** SO, a protein involved in hyphal fusion in *Neurospora crassa*, localizes to septal plugs. *Eukaryot.Cell.* 6: 1: 84-94, 2007.

53. **Fleißner A, Leeder AC, Roca MG, Read ND and Glass NL.** Oscillatory recruitment of signaling proteins to cell tips promotes coordinated behavior during cell fusion. *Proc.Natl.Acad.Sci.U.S.A.* 106: 46: 19387-19392, 2009.

54. **Fleißner A, Sarkar S, Jacobson DJ, Roca MG, Read ND and Glass NL.** The so locus is required for vegetative cell fusion and postfertilization events in *Neurospora crassa*. *Eukaryot.Cell.* 4: 5: 920-930, 2005.

55. **Franks TM and Lykke-Andersen J.** The control of mRNA decapping and P-body formation. *Mol.Cell* 32: 5: 605-615, 2008.

56. **Funakoshi Y, Doi Y, Hosoda N, Uchida N, Osawa M, Shimada I, Tsujimoto M, Suzuki T, Katada T and Hoshino S.** Mechanism of mRNA deadenylation: evidence for a molecular interplay between translation termination factor eRF3 and mRNA deadenylases. *Genes Dev.* 21: 23: 3135-3148, 2007.

57. **Gallie DR, Le H, Caldwell C, Tanguay RL, Hoang NX and Browning KS.** The phosphorylation state of translation initiation factors is regulated developmentally and following heat shock in wheat. *J.Biol.Chem.* 272: 2: 1046-1053, 1997.

58. **Gallie DR and Tanguay R.** Poly(A) binds to initiation factors and increases cap-dependent translation in vitro. *J.Biol.Chem.* 269: 25: 17166-17173, 1994.

59. **Garneau NL, Wilusz J and Wilusz CJ.** The highways and byways of mRNA decay. *Nat.Rev.Mol.Cell Biol.* 8: 2: 113-126, 2007.

60. **Gilks N, Kedersha N, Ayodele M, Shen L, Stoecklin G, Dember LM and Anderson P.** Stress granule assembly is mediated by prion-like aggregation of TIA-1. *Mol.Biol.Cell* 15: 12: 5383-5398, 2004.

61. **Ginsberg SD, Galvin JE, Chiu TS, Lee VM, Masliah E and Trojanowski JQ.** RNA sequestration to pathological lesions of neurodegenerative diseases. *Acta Neuropathol.* 96: 5: 487-494, 1998.

62. **Glozak MA, Sengupta N, Zhang X and Seto E.** Acetylation and deacetylation of non-histone proteins. *Gene* 363: 15-23, 2005.

63. **Grousl T, Ivanov P, Frydlova I, Vasicova P, Janda F, Vojtova J, Malinska K, Malcova I, Novakova L, Janoskova D, Valasek L and Hasek J.** Robust heat shock induces eIF2alpha-phosphorylation-independent assembly of stress granules containing eIF3 and 40S ribosomal subunits in budding yeast, *Saccharomyces cerevisiae*. *J.Cell.Sci.* 122: Pt 12: 2078-2088, 2009.

64. **Guillemette T, van Peij N, Goosen T, Lanthaler K, Robson GD, van den Hondel CA, Stam H and Archer DB.** Genomic analysis of the secretion stress response in the enzyme-producing cell factory *Aspergillus niger*. *BMC Genomics* 8: 158, 2007.

65. **Harding HP, Zhang Y, Bertolotti A, Zeng H and Ron D.** Perk is essential for translational regulation and cell survival during the unfolded protein response. *Mol.Cell* 5: 5: 897-904, 2000.

66. **Harris SD, Read ND, Roberson RW, Shaw B, Seiler S, Plamann M and Momany M.** Polarisome meets spitzenkorper: microscopy, genetics, and genomics converge. *Eukaryot.Cell.* 4: 2: 225-229, 2005.

67. **Herrmann M, Sprote P and Brakhage AA.** Protein kinase C (PkcA) of *Aspergillus nidulans* is involved in penicillin production. *Appl.Environ.Microbiol.* 72: 4: 2957-2970, 2006.

68. **Hinnebusch AG.** Translational regulation of GCN4 and the general amino acid control of yeast. *Annu.Rev.Microbiol.* 59: 407-450, 2005.

69. **Holcik M and Sonenberg N.** Translational control in stress and apoptosis. *Nat.Rev.Mol.Cell Biol.* 6: 4: 318-327, 2005.

70. **Hoshino S, Imai M, Kobayashi T, Uchida N and Katada T.** The eukaryotic polypeptide chain releasing factor (eRF3/GSPT) carrying the translation termination signal to the 3'-Poly(A) tail of mRNA. Direct association of erf3/GSPT with polyadenylate-binding protein. *J.Biol.Chem.* 274: 24: 16677-16680, 1999.

71. **Howard RJ.** Ultrastructural analysis of hyphal tip cell growth in fungi: Spitzenkorper, cytoskeleton and endomembranes after freeze-substitution. *J.Cell.Sci.* 48: 89-103, 1981.

72. **Hoyle NP, Castelli LM, Campbell SG, Holmes LE and Ashe MP.** Stress-dependent relocalization of translationally primed mRNPs to cytoplasmic granules that are kinetically and spatially distinct from P-bodies. *J.Cell Biol.* 179: 1: 65-74, 2007.

73. **Huang J and Klionsky DJ.** Autophagy and human disease. *Cell.Cycle* 6: 15: 1837-1849, 2007.

74. **Ikematsu N, Yoshida Y, Kawamura-Tsuzuku J, Ohsugi M, Onda M, Hirai M, Fujimoto J and Yamamoto T.** Tob2, a novel anti-proliferative Tob/BTG1 family member, associates with a component of the CCR4 transcriptional regulatory complex capable of binding cyclin-dependent kinases. *Oncogene* 18: 52: 7432-7441, 1999.

75. **Inoue Y and Klionsky DJ.** Regulation of macroautophagy in *Saccharomyces cerevisiae*. *Semin.Cell Dev.Biol.* 21: 7: 664-670, 2010.

76. **Ito D and Suzuki N.** Conjoint pathologic cascades mediated by ALS/FTLD-U linked RNA-binding proteins TDP-43 and FUS. *Neurology* 77: 17: 1636-1643, 2011.

77. **Jackson RJ, Hellen CU and Pestova TV.** The mechanism of eukaryotic translation initiation and principles of its regulation. *Nat.Rev.Mol.Cell Biol.* 11: 2: 113-127, 2010.

78. **Jedd G and Pieuchot L.** Multiple modes for gatekeeping at fungal cell-to-cell channels. *Mol.Microbiol.* 2012.

79. **Jin FJ, Watanabe T, Juvvadi PR, Maruyama J, Arioka M and Kitamoto K.** Double disruption of the proteinase genes, tppA and pepE, increases the production level of human lysozyme by *Aspergillus oryzae*. *Appl.Microbiol.Biotechnol.* 76: 5: 1059-1068, 2007.

80. **Johnson BS, Snead D, Lee JJ, McCaffery JM, Shorter J and Gitler AD.** TDP-43 is intrinsically aggregation-prone, and amyotrophic lateral sclerosis-linked mutations accelerate aggregation and increase toxicity. *J.Biol.Chem.* 284: 30: 20329-20339, 2009.

81. **Jucker M and Walker LC.** Self-propagation of pathogenic protein aggregates in neurodegenerative diseases. *Nature* 501: 7465: 45-51, 2013.

82. **Jung JH and Kim J.** Accumulation of P-bodies in *Candida albicans* under different stress and filamentous growth conditions. *Fungal Genet.Biol.* 48: 12: 1116-1123, 2011.

83. **Juvvadi PR, Maruyama J and Kitamoto K.** Phosphorylation of the *Aspergillus oryzae* Woronin body protein, AoHex1, by protein kinase C: evidence for its role in the multimerization and proper localization of the Woronin body protein. *Biochem.J.* 405: 3: 533-540, 2007.

84. **Katayama T, Uchida H, Ohta A and Horiuchi H.** Involvement of protein kinase C in the suppression of apoptosis and in polarity establishment in *Aspergillus nidulans* under conditions of heat stress. *PLoS One* 7: 11: e50503, 2012.

85. **Kaushik S and Cuervo AM.** Chaperone-mediated autophagy: a unique way to enter the lysosome world. *Trends Cell Biol.* 22: 8: 407-417, 2012.

86. **Kedersha N, Cho MR, Li W, Yacono PW, Chen S, Gilks N, Golan DE and Anderson P.** Dynamic shuttling of TIA-1 accompanies the recruitment of mRNA to mammalian stress granules. *J.Cell Biol.* 151: 6: 1257-1268, 2000.

87. **Kedersha N, Stoecklin G, Ayodele M, Yacono P, Lykke-Andersen J, Fritzler MJ, Scheuner D, Kaufman RJ, Golan DE and Anderson P.** Stress granules and processing bodies are dynamically linked sites of mRNP remodeling. *J.Cell Biol.* 169: 6: 871-884, 2005.

88. **Kedersha NL, Gupta M, Li W, Miller I and Anderson P.** RNA-binding proteins TIA-1 and TIAR link the phosphorylation of eIF-2 alpha to the assembly of mammalian stress granules. *J.Cell Biol.* 147: 7: 1431-1442, 1999.

89. **Khaleghpour K, Kahvejian A, De Crescenzo G, Roy G, Svitkin YV, Imataka H, O'Connor-McCourt M and Sonenberg N.** Dual interactions of the translational repressor Paip2 with poly(A) binding protein. *Mol.Cell.Biol.* 21: 15: 5200-5213, 2001.

90. **Khan IA, Lu JP, Liu XH, Rehman A and Lin FC.** Multifunction of autophagy-related genes in filamentous fungi. *Microbiol.Res.* 167: 6: 339-345, 2012.

91. **Kikuma T and Kitamoto K.** Analysis of autophagy in *Aspergillus oryzae* by disruption of Aoatg13, Aoatg4, and Aoatg15 genes. *FEMS Microbiol.Lett.* 316: 1: 61-69, 2011.

92. **Kikuma T, Ohneda M, Arioka M and Kitamoto K.** Functional analysis of the ATG8 homologue Aoatg8 and role of autophagy in differentiation and germination in *Aspergillus oryzae*. *Eukaryot.Cell.* 5: 8: 1328-1336, 2006.

93. **Kitamoto K.** Molecular biology of the Koji molds. *Adv.Appl.Microbiol.* 51: 129-153, 2002.

94. **Klann E and Dever TE.** Biochemical mechanisms for translational regulation in synaptic plasticity. *Nat.Rev.Neurosci.* 5: 12: 931-942, 2004.

95. **Kobayashi T, Abe K, Asai K, Gomi K, Juvvadi PR, Kato M, Kitamoto K, Takeuchi M and Machida M.** Genomics of *Aspergillus oryzae*. *Biosci.Biotechnol.Biochem.* 71: 3: 646-670, 2007.

96. **König J, Baumann S, Koepke J, Pohlmann T, Zarnack K and Feldbrugge M.** The fungal RNA-binding protein Rrm4 mediates long-distance transport of ubi1 and rho3 mRNAs. *EMBO J.* 28: 13: 1855-1866, 2009.

97. **Kozlov G, Safaee N, Rosenauer A and Gehring K.** Structural basis of binding of P-body-associated proteins GW182 and ataxin-2 by the Mlle domain of poly(A)-binding protein. *J.Biol.Chem.* 285: 18: 13599-13606, 2010.

98. **Kozlov G, Trempe JF, Khaleghpour K, Kahvejian A, Ekiel I and Gehring K.** Structure and function of the C-terminal PABC domain of human poly(A)-binding protein. *Proc.Natl.Acad.Sci.U.S.A.* 98: 8: 4409-4413, 2001.

99. **Kraft C, Peter M and Hofmann K.** Selective autophagy: ubiquitin-mediated recognition and beyond. *Nat.Cell Biol.* 12: 9: 836-841, 2010.

100. **Krick R, Bremer S, Welter E, Schlotterhose P, Muehe Y, Eskelinen EL and Thumm M.** Cdc48/p97 and Shp1/p47 regulate autophagosome biogenesis in concert with ubiquitin-like Atg8. *J.Cell Biol.* 190: 6: 965-973, 2010.

101. **Kroemer G, Marino G and Levine B.** Autophagy and the integrated stress response. *Mol.Cell* 40: 2: 280-293, 2010.

102. **Kunz JB, Schwarz H and Mayer A.** Determination of four sequential stages during microautophagy in vitro. *J.Biol.Chem.* 279: 11: 9987-9996, 2004.

103. **LaGrandeur T and Parker R.** The cis acting sequences responsible for the differential decay of the unstable MFA2 and stable PGK1 transcripts in yeast include the context of the translational start codon. *RNA* 5: 3: 420-433, 1999.

104. **Lai J, Koh CH, Tjota M, Pieuchot L, Raman V, Chandrababu KB, Yang D, Wong L and Jedd G.** Intrinsically disordered proteins aggregate at fungal cell-to-cell channels and regulate intercellular connectivity. *Proc.Natl.Acad.Sci.U.S.A.* 109: 39: 15781-15786, 2012.

105. **Lamphear BJ and Panniers R.** Heat shock impairs the interaction of cap-binding protein complex with 5' mRNA cap. *J.Biol.Chem.* 266: 5: 2789-2794, 1991.

106. **Lamphear BJ and Panniers R.** Cap binding protein complex that restores protein synthesis in heat-shocked Ehrlich cell lysates contains highly phosphorylated eIF-4E. *J.Biol.Chem.* 265: 10: 5333-5336, 1990.

107. **Laroia G, Cuesta R, Brewer G and Schneider RJ.** Control of mRNA decay by heat shock-ubiquitin-proteasome pathway. *Science* 284: 5413: 499-502, 1999.

108. **Le H, Browning KS and Gallie DR.** The phosphorylation state of the wheat translation initiation factors eIF4B, eIF4A, and eIF2 is differentially regulated during seed development and germination. *J.Biol.Chem.* 273: 32: 20084-20089, 1998.

109. **Le H, Browning KS and Gallie DR.** The phosphorylation state of poly(A)-binding protein specifies its binding to poly(A) RNA and its interaction with eukaryotic initiation factor (eIF) 4F, eIFiso4F, and eIF4B. *J.Biol.Chem.* 275: 23: 17452-17462, 2000.

110. **Le H, Tanguay RL, Balasta ML, Wei CC, Browning KS, Metz AM, Goss DJ and Gallie DR.** Translation initiation factors eIF-iso4G and eIF-4B interact with the poly(A)-binding protein and increase its RNA binding activity. *J.Biol.Chem.* 272: 26: 16247-16255, 1997.

111. **Levin DE.** Regulation of cell wall biogenesis in *Saccharomyces cerevisiae*: the cell wall integrity signaling pathway. *Genetics* 189: 4: 1145-1175, 2011.

112. **Li YR, King OD, Shorter J and Gitler AD.** Stress granules as crucibles of ALS pathogenesis. *J.Cell Biol.* 201: 3: 361-372, 2013.

113. **Lim NS, Kozlov G, Chang TC, Groover O, Siddiqui N, Volpon L, De Crescenzo G, Shyu AB and Gehring K.** Comparative peptide binding studies of the PABC domains from the ubiquitin-protein isopeptide ligase HYD and

poly(A)-binding protein. Implications for HYD function. *J.Biol.Chem.* 281: 20: 14376-14382, 2006.

114. **Liu-Yesucevitz L, Bilgutay A, Zhang YJ, Vanderweyde T, Citro A, Mehta T, Zaarur N, McKee A, Bowser R, Sherman M, Petrucelli L and Wolozin B.** Tar DNA binding protein-43 (TDP-43) associates with stress granules: analysis of cultured cells and pathological brain tissue. *PLoS One* 5: 10: e13250, 2010.

115. **Livingstone M, Atas E, Meller A and Sonenberg N.** Mechanisms governing the control of mRNA translation. *Phys.Biol.* 7: 2: 021001-3975/7/2/021001, 2010.

116. **López de Silanes I, Galban S, Martindale JL, Yang X, Mazan-Mamczarz K, Indig FE, Falco G, Zhan M and Gorospe M.** Identification and functional outcome of mRNAs associated with RNA-binding protein TIA-1. *Mol.Cell.Biol.* 25: 21: 9520-9531, 2005.

117. **Low JK, Hart-Smith G, Erce MA and Wilkins MR.** The *Saccharomyces cerevisiae* poly(A)-binding protein is subject to multiple post-translational modifications, including the methylation of glutamic acid. *Biochem.Biophys.Res.Commun.* 2013.

118. **Lu X, de la Pena L, Barker C, Camphausen K and Tofilon PJ.** Radiation-induced changes in gene expression involve recruitment of existing

messenger RNAs to and away from polysomes. *Cancer Res.* 66: 2: 1052-1061, 2006.

119. **Ma S, Musa T and Bag J.** Reduced stability of mitogen-activated protein kinase kinase-2 mRNA and phosphorylation of poly(A)-binding protein (PABP) in cells overexpressing PABP. *J.Biol.Chem.* 281: 6: 3145-3156, 2006.

120. **Machida M, Asai K, Sano M, Tanaka T, Kumagai T, Terai G, Kusumoto K, Arima T, Akita O, Kashiwagi Y, Abe K, Gomi K, Horiuchi H, Kitamoto K, Kobayashi T, Takeuchi M, Denning DW, Galagan JE, Nierman WC, Yu J, Archer DB, Bennett JW, Bhatnagar D, Cleveland TE, Fedorova ND, Gotoh O, Horikawa H, Hosoyama A, Ichinomiya M, Igarashi R, Iwashita K, Juvvadi PR, Kato M, Kato Y, Kin T, Kokubun A, Maeda H, Maeyama N, Maruyama J, Nagasaki H, Nakajima T, Oda K, Okada K, Paulsen I, Sakamoto K, Sawano T, Takahashi M, Takase K, Terabayashi Y, Wortman JR, Yamada O, Yamagata Y, Anazawa H, Hata Y, Koide Y, Komori T, Koyama Y, Minetoki T, Suharnan S, Tanaka A, Isono K, Kuhara S, Ogasawara N and Kikuchi H.** Genome sequencing and analysis of *Aspergillus oryzae*. *Nature* 438: 7071: 1157-1161, 2005.

121. **Machida M, Yamada O and Gomi K.** Genomics of *Aspergillus oryzae*: learning from the history of Koji mold and exploration of its future. *DNA Res.* 15: 4: 173-183, 2008.

122. **Manjithaya R, Nazarko TY, Farre JC and Subramani S.** Molecular mechanism and physiological role of pexophagy. *FEBS Lett.* 584: 7: 1367-1373, 2010.

123. **Markham P.** Occlusions of Septal Pores in Filamentous Fungi. *Mycol.Res.* 98: 1089-1106, 1994.

124. **Maruyama J, Escaño CS and Kitamoto K.** AoSO protein accumulates at the septal pore in response to various stresses in the filamentous fungus *Aspergillus oryzae*. *Biochem.Biophys.Res.Commun.* 391: 1: 868-873, 2010.

125. **Matthias P, Yoshida M and Khochbin S.** HDAC6 a new cellular stress surveillance factor. *Cell.Cycle* 7: 1: 7-10, 2008.

126. **Mauxion F, Chen CY, Seraphin B and Shyu AB.** BTG/TOB factors impact deadenylases. *Trends Biochem.Sci.* 34: 12: 640-647, 2009.

127. **Michelitsch MD and Weissman JS.** A census of glutamine/asparagine-rich regions: implications for their conserved function and the prediction of novel prions. *Proc.Natl.Acad.Sci.U.S.A.* 97: 22: 11910-11915, 2000.

128. **Mizushima N, Yoshimori T and Ohsumi Y.** The role of Atg proteins in autophagosome formation. *Annu.Rev.Cell Dev.Biol.* 27: 107-132, 2011.

129. **Mizutani O, Nojima A, Yamamoto M, Furukawa K, Fujioka T, Yamagata Y, Abe K and Nakajima T.** Disordered cell integrity signaling caused by disruption of the kexB gene in *Aspergillus oryzae*. *Eukaryot.Cell.* 3: 4: 1036-1048, 2004.

130. **Mochly-Rosen D, Das K and Grimes KV.** Protein kinase C, an elusive therapeutic target? *Nat.Rev.Drug Discov.* 11: 12: 937-957, 2012.

131. **Mollet S, Cougot N, Wilczynska A, Dautry F, Kress M, Bertrand E and Weil D.** Translationally repressed mRNA transiently cycles through stress granules during stress. *Mol.Biol.Cell* 19: 10: 4469-4479, 2008.

132. **Morano KA, Grant CM and Moye-Rowley WS.** The response to heat shock and oxidative stress in *Saccharomyces cerevisiae*. *Genetics* 190: 4: 1157-1195, 2012.

133. **Morawetz R, Lendenfeld T, Mischak H, Muhlbauer M, Gruber F, Goodnight J, de Graaff LH, Visser J, Mushinski JF and Kubicek CP.** Cloning and characterisation of genes (pkc1 and pkcA) encoding protein kinase C homologues from *Trichoderma reesei* and *Aspergillus niger*. *Mol.Gen.Genet.* 250: 1: 17-28, 1996.

134. **Moreno JA, Radford H, Peretti D, Steinert JR, Verity N, Martin MG, Halliday M, Morgan J, Dinsdale D, Ortori CA, Barrett DA, Tsaytler P, Bertolotti A, Willis AE, Bushell M and Mallucci GR.** Sustained translational repression by eIF2alpha-P mediates prion neurodegeneration. *Nature* 485: 7399: 507-511, 2012.

135. **Fumiaki M, Watanabe Y, Miki Y, Tanji K, Odagiri S, Eto K and Wakabayashi K.** Ubiquitin-negative, eosinophilic neuronal cytoplasmic inclusions associated with stress granules and autophagy: An immunohistochemical investigation of two cases. Neuropathology doi: 10.1111/neup.12075, 2013.

136. **Morozov IY, Jones MG, Spiller DG, Rigden DJ, Dattenbock C, Novotny R, Strauss J and Caddick MX.** Distinct roles for Caf1, Ccr4, Edc3 and CutA in the co-ordination of transcript deadenylation, decapping and P-body formation in *Aspergillus nidulans*. *Mol.Microbiol.* 76: 2: 503-516, 2010.

137. **Muckenthaler M, Gunkel N, Stripecke R and Hentze MW.** Regulated poly(A) tail shortening in somatic cells mediated by cap-proximal translational repressor proteins and ribosome association. *RNA* 3: 9: 983-995, 1997.

138. **Muhlrad D, Decker CJ and Parker R.** Turnover mechanisms of the stable yeast PGK1 mRNA. *Mol.Cell.Biol.* 15: 4: 2145-2156, 1995.

139. **Murrow L and Debnath J.** Autophagy as a stress-response and quality-control mechanism: implications for cell injury and human disease. *Annu.Rev.Pathol.* 8: 105-137, 2013.

140. **Newton AC.** Regulation of protein kinase C. *Curr.Opin.Cell Biol.* 9: 2: 161-167, 1997.

141. **Nilsson D and Sunnerhagen P.** Cellular stress induces cytoplasmic RNA granules in fission yeast. *RNA* 17: 1: 120-133, 2011.

142. **Nissan T, Rajyaguru P, She M, Song H and Parker R.** Decapping activators in *Saccharomyces cerevisiae* act by multiple mechanisms. *Mol.Cell* 39: 5: 773-783, 2010.

143. **Nixon R,A.** The role of autophagy in neurodegenerative disease. *Nat. Med.* 19: 8: 983-997, 2013.

144. **Nonhoff U, Ralser M, Welzel F, Piccini I, Balzereit D, Yaspo ML, Lehrach H and Krobitsch S.** Ataxin-2 interacts with the DEAD/H-box RNA helicase DDX6 and interferes with P-bodies and stress granules. *Mol.Biol.Cell* 18: 4: 1385-1396, 2007.

145. **Norbury C,J.** Cytoplasmic RNA: a case of the tail wagging the dog. *Nat. Rev. Mol. Cell Biol.* 14: 10: 643-653, 2013.

146. **Okochi K, Suzuki T, Inoue J, Matsuda S and Yamamoto T.** Interaction of anti-proliferative protein Tob with poly(A)-binding protein and inducible poly(A)-binding protein: implication of Tob in translational control. *Genes Cells* 10: 2: 151-163, 2005.

147. **Ohn T, Kedersha N, Hickman T, Tisdale S and Anderson P.** A functional RNAi screen links O-GlcNAc modification of ribosomal proteins to stress granule and processing body assembly. *Nat.Cell Biol.* 10: 10: 1224-1231, 2008.

148. **Parker R.** RNA degradation in Saccharomyces cerevisae. *Genetics* 191: 3: 671-702, 2012.

149. **Parker R and Sheth U.** P bodies and the control of mRNA translation and degradation. *Mol.Cell* 25: 5: 635-646, 2007.

150. **Parker R and Song H.** The enzymes and control of eukaryotic mRNA turnover. *Nat.Struct.Mol.Biol.* 11: 2: 121-127, 2004.

151. **Pickart CM.** Mechanisms underlying ubiquitination. *Annu.Rev.Biochem.* 70: 503-533, 2001.

152. **Pollack JK, Harris SD and Marten MR.** Autophagy in filamentous fungi. *Fungal Genet.Biol.* 46: 1: 1-8, 2009.

153. **Pollack JK, Li ZJ and Marten MR.** Fungal mycelia show lag time before re-growth on endogenous carbon. *Biotechnol.Bioeng.* 100: 3: 458-465, 2008.

154. **Powley IR, Kondrashov A, Young LA, Dobbyn HC, Hill K, Cannell IG, Stoneley M, Kong YW, Cotes JA, Smith GC, Wek R, Hayes C, Gant TW, Spriggs KA, Bushell M and Willis AE.** Translational reprogramming following UVB irradiation is mediated by DNA-PKcs and allows selective recruitment to the polysomes of mRNAs encoding DNA repair enzymes. *Genes Dev.* 23: 10: 1207-1220, 2009.

155. **Reggiori F and Klionsky DJ.** Autophagic processes in yeast: mechanism, machinery and regulation. *Genetics* 194: 2: 341-361, 2013.

156. **Reijns MA, Alexander RD, Spiller MP and Beggs JD.** A role for Q/N-rich aggregation-prone regions in P-body localization. *J.Cell.Sci.* 121: Pt 15: 2463-2472, 2008.

157. **Rice JC, Nishioka K, Sarma K, Steward R, Reinberg D and Allis CD.** Mitotic-specific methylation of histone H4 Lys 20 follows increased PR-Set7 expression and its localization to mitotic chromosomes. *Genes Dev.* 16: 17: 2225-2230, 2002.

158. **Rødland GE, Tvegard T, Boye E and Grallert B.** Crosstalk between the Tor and Gcn2 pathways in response to different stresses. *Cell.Cycle* 13: 3: 2013.

159. **Roux PP and Blenis J.** ERK and p38 MAPK-activated protein kinases: a family of protein kinases with diverse biological functions. *Microbiol.Mol.Biol.Rev.* 68: 2: 320-344, 2004.

160. **Roy G, De Crescenzo G, Khaleghpour K, Kahvejian A, O'Connor-McCourt M and Sonenberg N.** Paip1 interacts with poly(A) binding protein through two independent binding motifs. *Mol.Cell.Biol.* 22: 11: 3769-3782, 2002.

161. **Rubinsztein DC, Shpilka T and Elazar Z.** Mechanisms of autophagosome biogenesis. *Curr.Biol.* 22: 1: R29-34, 2012.

162. **Saibil H.** Chaperone machines for protein folding, unfolding and disaggregation. *Nat.Rev.Mol.Cell Biol.* 14: 10: 630-642, 2013.

163. **Scheper GC, Morrice NA, Kleijn M and Proud CG.** The mitogen-activated protein kinase signal-integrating kinase Mnk2 is a eukaryotic initiation factor 4E kinase with high levels of basal activity in mammalian cells. *Mol.Cell.Biol.* 21: 3: 743-754, 2001.

164. **Schwartz DC and Parker R.** Mutations in translation initiation factors lead to increased rates of deadenylation and decapping of mRNAs in *Saccharomyces cerevisiae*. *Mol.Cell.Biol.* 19: 8: 5247-5256, 1999.

165. **Shah KH, Zhang B, Ramachandran V and Herman PK.** Processing body and stress granule assembly occur by independent and differentially regulated pathways in *Saccharomyces cerevisiae*. *Genetics* 193: 1: 109-123, 2013.

166. **She M, Decker CJ, Chen N, Tumati S, Parker R and Song H.** Crystal structure and functional analysis of Dcp2p from *Schizosaccharomyces pombe*. *Nat.Struct.Mol.Biol.* 13: 1: 63-70, 2006.

167. **Shepherd VA, Orlovich DA and Ashford AE.** Cell-to-cell transport via motile tubules in growing hyphae of a fungus. *J.Cell.Sci.* 105: Pt 4: 1173-1178, 1993.

168. **Sheth U and Parker R.** Decapping and decay of messenger RNA occur in cytoplasmic processing bodies. *Science* 300: 5620: 805-808, 2003.

169. **Shpilka T, Weidberg H, Pietrokovski S and Elazar Z.** Atg8: an autophagy-related ubiquitin-like protein family. *Genome Biol.* 12: 7: 226, 2011.

170. **Siddiqui N, Mangus DA, Chang TC, Palermino JM, Shyu AB and Gehring K.** Poly(A) nuclease interacts with the C-terminal domain of polyadenylate-binding protein domain from poly(A)-binding protein. *J.Biol.Chem.* 282: 34: 25067-25075, 2007.

171. **Sonenberg N and Hinnebusch AG.** Regulation of translation initiation in eukaryotes: mechanisms and biological targets. *Cell* 136: 4: 731-745, 2009.

172. **Stanley RE, Ragusa MJ and Hurley JH.** The beginning of the end: how scaffolds nucleate autophagosome biogenesis. *Trends Cell Biol.* 2013.

173. **Steinberg G.** Hyphal growth: a tale of motors, lipids, and the Spitzenkörper. *Eukaryot.Cell.* 6: 3: 351-360, 2007.

174. **Swanlund JM, Kregel KC and Oberley TD.** Autophagy following heat stress: the role of aging and protein nitration. *Autophagy* 4: 7: 936-939, 2008.

175. **Swisher KD and Parker R.** Localization to, and effects of Pbp1, Pbp4, Lsm12, Dhh1, and Pab1 on stress granules in *Saccharomyces cerevisiae*. *PLoS One* 5: 4: e10006, 2010.

176. **Takahara T and Maeda T.** Transient sequestration of TORC1 into stress granules during heat stress. *Mol.Cell* 47: 2: 242-252, 2012.

177. **Takahashi S, Sakurai K, Ebihara A, Kajiho H, Saito K, Kontani K, Nishina H and Katada T.** RhoA activation participates in rearrangement of processing bodies and release of nucleated AU-rich mRNAs. *Nucleic Acids Res.* 39: 8: 3446-3457, 2011.

178. **Takalo M, Salminen A, Soininen H, Hiltunen M and Haapasalo A.** Protein aggregation and degradation mechanisms in neurodegenerative diseases. *Am.J.Neurodegener Dis.* 2: 1: 1-14, 2013.

179. **Taylor MJ and Richardson T.** Applications of microbial enzymes in food systems and in biotechnology. *Adv.Appl.Microbiol.* 25: 7-35, 1979.

180. **Teixeira D, Sheth U, Valencia-Sanchez MA, Brengues M and Parker R.** Processing bodies require RNA for assembly and contain nontranslating mRNAs. *RNA* 11: 4: 371-382, 2005.

181. **Teter SA, Eggerton KP, Scott SV, Kim J, Fischer AM and Klionsky DJ.** Degradation of lipid vesicles in the yeast vacuole requires function of Cvt17, a putative lipase. *J.Biol.Chem.* 276: 3: 2083-2087, 2001.

182. **Tsuchiya K, Nagashima T, Yamamoto Y, Gomi K, Kitamoto K, Kumagai C and Tamura G.** High level secretion of calf chymosin using a glucoamylase-prochymosin fusion gene in *Aspergillus oryzae*. *Biosci.Biotechnol.Biochem.* 58: 5: 895-899, 1994.

183. **Uchida N, Hoshino S and Katada T.** Identification of a human cytoplasmic poly(A) nuclease complex stimulated by poly(A)-binding protein. *J.Biol.Chem.* 279: 2: 1383-1391, 2004.

184. **Uttenweiler A and Mayer A.** Microautophagy in the yeast *Saccharomyces cerevisiae*. *Methods Mol.Biol.* 445: 245-259, 2008.

185. **Valbuena N, Rozalen AE and Moreno S.** Fission yeast TORC1 prevents eIF2alpha phosphorylation in response to nitrogen and amino acids via Gcn2 kinase. *J.Cell.Sci.* 125: Pt 24: 5955-5959, 2012.

186. **van Dijk E, Cougot N, Meyer S, Babajko S, Wahle E and Seraphin B.** Human Dcp2: a catalytically active mRNA decapping enzyme located in specific cytoplasmic structures. *EMBO J.* 21: 24: 6915-6924, 2002.

187. **van Peer AF, Muller WH, Boekhout T, Lugones LG and Wosten HA.** Cytoplasmic continuity revisited: closure of septa of the filamentous fungus Schizophyllum commune in response to environmental conditions. *PLoS One* 4: 6: e5977, 2009.

188. **Velichko AK, Markova EN, Petrova NV, Razin SV and Kantidze OL.** Mechanisms of heat shock response in mammals. *Cell Mol.Life Sci.* 70: 22: 4229-4241, 2013.

189. **Verghese J, Abrams J, Wang Y and Morano KA.** Biology of the heat shock response and protein chaperones: budding yeast (*Saccharomyces cerevisiae*) as a model system. *Microbiol.Mol.Biol.Rev.* 76: 2: 115-158, 2012.

190. **Voigt O and Pöggeler S.** Self-eating to grow and kill: autophagy in filamentous ascomycetes. *Appl.Microbiol.Biotechnol.* 97: 21: 9277-9290, 2013.

191. **Ward M, Wilson LJ, Kodama KH, Rey MW and Berka RM.** Improved production of chymosin in Aspergillus by expression as a glucoamylase-chymosin fusion. *Biotechnology (N.Y)* 8: 5: 435-440, 1990.

192. **Wei CC, Balasta ML, Ren J and Goss DJ.** Wheat germ poly(A) binding protein enhances the binding affinity of eukaryotic initiation factor 4F and (iso)4F for cap analogues. *Biochemistry* 37: 7: 1910-1916, 1998.

193. **Wek RC, Jiang HY and Anthony TG.** Coping with stress: eIF2 kinases and translational control. *Biochem.Soc.Trans.* 34: Pt 1: 7-11, 2006.

194. **Wilczynska A, Aigueperse C, Kress M, Dautry F and Weil D.** The translational regulator CPEB1 provides a link between dcp1 bodies and stress granules. *J.Cell.Sci.* 118: Pt 5: 981-992, 2005.

195. **Wilusz CJ, Gao M, Jones CL, Wilusz J and Peltz SW.** Poly(A)-binding proteins regulate both mRNA deadenylation and decapping in yeast cytoplasmic extracts. *RNA* 7: 10: 1416-1424, 2001.

196. **Wolozin B.** Regulated protein aggregation: stress granules and neurodegeneration. *Mol.Neurodegener* 7: 56-1326-7-56, 2012.

197. **Wullschleger S, Loewith R and Hall MN.** TOR signaling in growth and metabolism. *Cell* 124: 3: 471-484, 2006.

198. **Yan G, Lai Y and Jiang Y.** The TOR complex 1 is a direct target of Rho1 GTPase. *Mol.Cell* 45: 6: 743-753, 2012.

199. **Yao G, Chiang YC, Zhang C, Lee DJ, Laue TM and Denis CL.** PAB1 self-association precludes its binding to poly(A), thereby accelerating CCR4 deadenylation in vivo. *Mol.Cell.Biol.* 27: 17: 6243-6253, 2007.

200. **Yang XJ and Seto E.** Lysine acetylation: codified crosstalk with other posttranslational modifications. *Mol.Cell* 31: 4: 449-461, 2008.

201. **Yoon J, Kimura S, Maruyama J and Kitamoto K.** Construction of quintuple protease gene disruptant for heterologous protein production in *Aspergillus oryzae*. *Appl.Microbiol.Biotechnol.* 82: 4: 691-701, 2009.

202. **Yoon J, Maruyama J and Kitamoto K.** Disruption of ten protease genes in the filamentous fungus *Aspergillus oryzae* highly improves production of heterologous proteins. *Appl.Microbiol.Biotechnol.* 89: 3: 747-759, 2011.

203. **Zachara NE, O'Donnell N, Cheung WD, Mercer JJ, Marth JD and Hart GW.** Dynamic O-GlcNAc modification of nucleocytoplasmic proteins in response to stress. A survival response of mammalian cells. *J.Biol.Chem.* 279: 29: 30133-30142, 2004.

204. **Zekri L, Kuzuoglu-Ozturk D and Izaurralde E.** GW182 proteins cause PABP dissociation from silenced miRNA targets in the absence of deadenylation. *EMBO J.* 32: 7: 1052-1065, 2013.

205. **Zhang X, Wen H and Shi X.** Lysine methylation: beyond histones. *Acta Biochim.Biophys.Sin.(Shanghai)* 44: 1: 14-27, 2012.

206. **Zhang Y and Calderwood SK.** Autophagy, protein aggregation and hyperthermia: a mini-review. *Int.J.Hyperthermia* 27: 5: 409-414, 2011.

Acknowledgements

I would like to thank all those people who have made this dissertation possible.

First of all, I would like to express the deepest appreciation to all Japanese people. This dissertation would not have been accomplished without four-year full scholarship support received from the Interchange Association, Japan (公益財団法人交流協会). That is to say, my life has been financially supported by all Japanese taxpayers. I expect myself to be able to repay your favor in a certain way in the future.

I would like to gratefully and sincerely thank my supervisor Professor Katsuhiko Kitamoto for accepting me as a PhD student, because these four years have been a truly life-changing experience for me. I am very thankful for that he has given to me much freedom about my research, and a chance to attend to the international conference. He led me to come out of Taiwan to Japan, and then to the world. I also very appreciate for his enthusiasm to share Japanese culture and, especially, things about *A. oryzae*, with international students. To meet *A. oryzae* will definitely be the most important memory to me.

I am particularly grateful for constructive comments and suggestions given by Associate Professor Manabu Arioka.

I would like to thank Assistant Professor Jun-ichi Maruyama for his valuable advices, as well as his painstaking effort in proof reading the drafts. And the most importantly, I am extremely grateful for his support so that I could do experiments that I really wanted to do. Without his introducing, I would never have the data of 2D-SDS/PAGE and LC-MS/MS analyzes.

I would like to say a heartfelt thank you to Project Researcher Takashi Kikuma. His encouragement and friendliness mean a lot to me, especially when I was weary.

Thank all members, former and present, at the Laboratory of Microbiology for giving me friendship and laughs and making my PhD life delight and joyful. People say Japanese are cold and unfriendly, but I will tell them that it is not true.

I would like to extend my appreciation to my family and friends in Taiwan, Japan, and other countries. Especially to the Yu's family, I wouldn't have been in Japan without you. Distance never becomes our problem. Your support and encouragement are always my great strength. I have made it accomplished, because I do not want to fail to meet your expectations on me.

I would like to acknowledge people who have contributed to this dissertation:
Dr. Takuya Miyakawa and the Tanokura Laboratory (The University of Tokyo, Japan) for providing reagents and the machine for 2D-SDS/PAGE analysis;
Professor Yukishige Ito (Synthetic Cellular Chemistry Laboratory, RIKEN, Japan) and the Mass Spectrometry Service at RIKEN Brain Science Institute for conducting LC-MS/MS analysis;
Dr. Mirai Tanigawa and Professor Tatsuya Maeda (The University of Tokyo, Japan) for generously sharing their immunoprecipitation methods.

Lastly but the most importantly, I want to praise God for all You have given to me. From an anti-Christian to become a believer is the most incredible life-changing event happened in these four years. All glory and honor belong to God.

論文内容の要旨

応用生命工学　専攻
平成 23 年度博士課程　入学
氏　　名　黄　湘婷
指導教員名　北本　勝ひこ

論文題目

Studies on Stress Granules in *Aspergillus oryzae*
（麹菌 *Aspergillus oryzae* におけるストレス顆粒に関する研究）

Introduction

Microorganisms are constantly challenged by ever-changing variables in their environment. The ability to sense environmental stimuli, including stress, activate signal transduction, and mount appropriate acute and adaptive responses is crucial for eukaryotic cell survival. Adaptation requires physiological and metabolic changes, and is ultimately achieved through the regulation of gene expression. Traditionally, transcriptional regulation has been regarded as the major determinant of gene expression. However, accumulating evidence indicates that posttranscriptional modulation of mRNA stability and translation plays a key role in the control of gene expression and provides greater plasticity, allowing cells to immediately adjust protein synthesis in response to changes in the environment. Recent studies have demonstrated that one aspect of this modulation involves the remodeling of mRNAs translated from polysomes into non-translating messenger ribonucleoproteins (mRNPs), which accumulate in discrete cytoplasmic foci known as stress granules and processing bodies (P-bodies).

The common feature of environmental stress response in eukaryotic cells is the global translation inhibition, in which cells shut down protein synthesis to conserve anabolic energy and initiate a reconfiguration of gene expression. The stalled preinitiation complexes, together with their associated mRNAs, are routed into stress granules. However, a subset of mRNAs required for cell survival under stress conditions are not delivered to stress granules but stabilized and preferentially translated in the cytoplasm. The function of stress granules is not fully understood; however, they have been implicated in the posttranscriptional regulation processes, such as translational repression, mRNA storage, and cellular signal transduction.

Stress granules are conserved in eukaryotes and have been studied extensively in yeast and mammalian cells. However, stress granules in filamentous fungi, including *Aspergillus oryzae*, have not yet to be defined. For this reason, the present work was to study stress granules in *A. oryzae*.

Chapter 1. Cytoplasmic mRNP granules in *A. oryzae*

The poly(A)-binding protein Pab1p, which is involved in the translational regulation and stability of mRNAs, is one of the most reliable and easily visualized components of stress granules in the yeast *Saccharomyces cerevisiae*. A homolog of the *S. cerevisiae PAB1* gene was found in the *A. oryzae* genome database and designated as *Aopab1* (AO090003000927). To monitor stress granules by fluorescence microscopy, an AoPab1-EGFP fusion protein was expressed in *A. oryzae* under control of the *amyB* promoter as a stress granule marker. Global translational arrest is a common environmental stress response in eukaryotes, and the inhibition of translation initiation leads to the formation of stress granules. As a first step in characterizing stress granules in *A. oryzae*, several external stimuli were used to assess the induction of stress granules in cells. Under normal growth conditions, AoPab1-EGFP was dispersed throughout the cytoplasm. Exposing cells to stress, including heat stress (45°C, 10 min), cold stress (4°C, 30 min), glucose deprivation (10 min), ER stress (10 mM DTT, 60 min), osmotic stress (1.2 M sorbitol, 30 min), and oxidative stress (2 mM H_2O_2, 30 min), led to an induction of stress granules, as judged by the accumulation of AoPab1-EGFP as cytoplasmic foci. In eukaryotic cells, non-translating mRNAs also accumulate in P-bodies, which contain a conserved core of proteins involved in translational repression and mRNA degradation. To elucidate the spatial and functional links of stress granules and P-bodies, a strain co-expressing the P-bodies marker AoDcp2-EGFP and AoPab1-mDsRed was examined after being exposed to 45°C for 10 min. Under heat stress, stress granules were found to colocalize with P-bodies in *A. oryzae*. Finally, to investigate the functional importance of stress granule formation on cell survival against stress, an *A. oryzae* homolog of a well-known stress granule marker important for stress granule formation, *Aopub1*, was disrupted and cultured on PD plates containing 10 mM DTT, 2 mM H_2O_2, or 1.2 M sorbitol. The phenotype of the *Aopub1* disruptant was characterized by a slower growth rate, and a severe impairment in conidia formation. The growth retardation of the *Aopub1* disruptant was more severe under all examined stress conditions. Taken together, these results indicate that the formation of stress granules is a general phenomenon in response to external stress, which occurs also in *A. oryzae*.

Chapter 2. Identification of AoSO as a novel component of stress granules upon heat stress in *A. oryzae*

The mycelia of filamentous fungi consist of a network of interconnected hyphae, which are compartmentalized by septa. Septa contain a central pore that allows the movement of cytoplasm and organelles between adjacent hyphae for direct communication and coordination. However, in response to hyphal damage and stressful environmental conditions, cells defend against cytoplasmic loss by the rapid

occlusion of septal pores. It has been shown previously that an *A. oryzae* homolog of *Neurospora crassa* SO (SOFT) protein AoSO accumulates at the septal pore when cells are exposed to various stresses. The stress-induced accumulation behavior of AoSO suggests that it may interact with stress granules. To investigate this possibility, a strain co-expressing AoSO-EGFP and AoPab1-mDsRed was used to examine the relative localizations of AoSO and stress granules in cells exposed to heat stress. AoPab1-mDsRed did not accumulate at the septal pore in cells exposed to heat stress. However, in cells exposed to heat stress, AoSO-EGFP also accumulated as cytoplasmic foci, which colocalized with stress granules labeled with AoPab1-mDsRed at the hyphal tip. The physical interaction between AoSO-EGFP and AoPab1-3HA was confirmed by co-immunoprecipitation, although the association between AoSO-EGFP and AoPab1-3HA was not induced or increased after exposure to heat stress. To clarify if the aggregation of AoSO requires the presence of non-translating mRNAs, cycloheximide, which blocks translational elongation and traps mRNAs in polysomes, was used to deplete the pool of non-translating mRNAs. The heat stress-induced formation of cytoplasmic AoSO foci at the hyphal tip was greatly impaired by cycloheximide, suggesting that cytoplasmic AoSO foci require a pool of free mRNAs for their aggregation. However, cycloheximide did not affect the accumulation of AoSO at the septal pore. To gain a better understanding of the role of AoSO in stress granules, the effect of *Aoso* deletion on stress granule formation was examined. Heat stress-induced formation of stress granules was slightly impaired in the *Aoso*-deletion strain. The effect of *Aoso* deletion on stress granules was further evaluated by measuring the distance between the hyphal tip and stress granules. The distribution of the largest stress granules labeled with AoPab1-EGFP was less concentrated and more distant from the hyphal tip in the *Aoso*-deletion strain. Taken together, the results suggest that AoSO is a novel component of mRNP granules in *A. oryzae*, which influences the formation and localization of stress granules in cells exposed to heat stress.

Chapter 3. Participation of autophagy in the clearance of stress granules under sustained heat stress

The formation of stress granules in response to stress is a conserved phenomenon in eukaryotes, but little is known about the fate of stress granules. Autophagy is a conserved and tightly regulated process in eukaryotic cells for the bulk degradation of cytoplasmic components in the vacuole or lysosome to maintain cellular homeostasis. In *A. oryzae*, stress granules were often found to dock with vacuoles, suggesting a possibility that under sustained stress condition, stress granules are degraded by autophagy. To clarify it, a strain co-expressing the autophagosome marker EGFP-AoAtg8 and AoPab1-mDsRed was used to examine their relative

localizations, and the fusion proteins were colocalized in cells exposed to heat stress. Additionally, after exposure to heat stress, protein amount of stress granule component AoPab1-3HA was decreased in a time-dependent manner. However, in an autophagy-defective strain, *Aoatg8* disruptant, the degradation of AoPab1-3HA induced by heat stress was greatly inhibited. These results indicate that under sustained heat stress, the degradation of stress granule component is at least partially mediated through autophagy.

Chapter 4. The posttranslational modification of stress granule component AoPab1 in response to heat stress

Poly(A)-binding protein is a central regulator of mRNA translation and stability and is a core component of stress granules, suggesting that complex modulations are required to coordinate its multi-functions and rapid response to stress. Post-translational modification (PTM) is a crucial mechanism to regulate the functions of many eukaryotic proteins. To elucidate whether AoPab1 was post-translationally modified, lysates from unstressed cells or cells exposed to heat stress for 10 or 30 min were analyzed by two-dimensional SDS/PAGE. AoPab1-3HA was detected as a continuing band, indicating multiple PTM isoforms. In addition to a portion of isoforms with higher pI (basic isoforms), highly acidic isoforms appeared in cells exposed to heat stress for 10 min, and were not observed after exposure of heat stress for 30 min. Exposure to heat stress for 30 min induced a broad distribution of AoPab1 isoforms from pH 3-10 with highly basic species. To identify the PTMs in AoPabl, AoPabl-3HA was immunoprecipitated and analyzed using LC-MS/MS. Methylation, acetylation, and phosphorylation were identified at several residues throughout all the functional domains of AoPab1, with an exception of Q/G/P-rich region. Exposure to heat stress resulted in changes in PTMs of AoPab1. These results indicate that AoPab1 is subject to extensively post-translationaly modified and regulated dynamically in response to heat stress.

Conclusion

A. oryzae is an industrially important species for hetrogenous protein production. However, low yield is still a major bottleneck for hetrologous protein production, even many genetic approaches have been used to improve the productivity. The present study provides an integrated perspective on eukaryotic stress response. Understanding of post-trancriptional regulation of gene expression on mRNA modulation may provide new insights for industrial application in the near future.

Reference

H-T Huang, J Maruyama, and K Kitamoto. *Aspergillus oryzae* AoSO is a novel component of stress granules upon heat stress in filamentous fungi. PLOS ONE 8(8): e72209, 2013.